ABSTRACT

Title of Dissertation: **TOPOLOGICAL ANALYSIS AND FUNCTIONAL CHARACTERIZATION OF VACCINIA VIRUS MORPHOGENESIS PROTEINS**

Seong-In Hyun, Doctor of Philosophy, 2017

Dissertation directed by: Dr. Bernard Moss, Adjunct Professor, National Institutes of Health and Dr. Jeffrey DeStefano, Professor, Department of Cell Biology and Molecular Genetics

Poxviruses are large, enveloped, double-stranded DNA viruses that replicate in the cytoplasm of host cells and are responsible for diseases of humans and other animals. Vaccinia virus (VACV), the most extensively studied member in the family, encodes approximately 200 proteins, of which 100 are conserved in all members of the vertebrate subfamily of poxviruses and have roles in gene expression, DNA replication, morphogenesis and cell entry. Previous studies have shown that several vaccinia virus proteins localize to the endoplasmic reticulum (ER), suggesting that it serves as the source of viral membranes. Determining the topology of these viral proteins can provide information about protein function and viral membrane formation. My first project involved using an asymmetric self-associating split-GFP system to determine the topology of the transmembrane viral proteins L2 and A30.5 that localize in the endoplasmic reticulum. This split-GFP system uses large (215 aa)

and small (16 aa) fragments of GFP that fluoresce only upon complementation. Our results showed that a short GFP fragment can be used to tag small transmembrane viral proteins to determine their localization and topology in vivo. The second project focuses on a protein called I2, which I showed is required for later stage virion morphogenesis. I deleted the I2 gene from the VACV genome by homologous recombination. The I2-deletion mutant was unable to replicate in control cells demonstrating that the protein has an essential role in VACV replication. Transmission electron microscopy revealed a striking defect in virus morphogenesis. During normal VACV morphogenesis, spherical immature particles shed the viral D13 scaffold protein and assume the brick shape of mature infectious particles. However, this transition did not occur in cells infected with the I2-deletion mutant and dense spherical particles accumulated. Furthermore, the scaffold protein was retained on the defective particles. In addition, the levels of membrane proteins comprising the entry/fusion complex were greatly diminished in these particles although most other proteins were present at normal levels. Based on these data, I2 is important for removal of the scaffold protein from immature virus particles, which is necessary for subsequent steps in morphogenesis including the incorporation of the entry/fusion proteins into the viral membrane.

TOPOLOGICAL ANALYSIS AND FUNCTIONAL CHARACTERIZATION OF VACCINIA VIRUS MORPHOGENESIS PROTEINS

by

Seong-In Hyun

Dissertation submitted to the Faculty of the Graduate School of the
University of Maryland, College Park, in partial fulfillment
of the requirements for the degree of
Doctor of Philosophy
2017

Advisory Committee:
Dr. Jeffrey DeStefano, Chair
Dr. Bernard Moss, Co-chair
Dr. George Belov
Dr. James Culver
Dr. Eric Freed
Dr. Alison McBride

Dedication

I dedicate this dissertation to my family.

Acknowledgements

I would like to express my deep gratitude to my mentor Bernie Moss for his awesome mentorship and support. His lab was a perfect environment for me to grow as a person and a scientist. I also thank my co-advisor, Jeff DeStefano, for his continuous assistance and great teaching throughout my training. I would also like to thank other members of my advisory committee, George Belov, James Culver, Eric Freed, and Alison McBride, for all their time and guidance.

I would like to say thank you to the entire Moss lab members for their friendship and support. Special thanks to Liliana Maruri-Avidal for her great mentorship, Gilad Sivan for countless discussions, and my fellow graduate students Sara Reynolds and Carey Stuart for their companionship. I would also like to thank Paul Kennedy, the LVD office at NIH, and the BISI office at University of Maryland for administrative support.

Finally, I am greatly thankful to my parents, family, and friends for all their support throughout my years in graduate school.

Table of Contents

List of Tables

List of Figures

List of Abbreviations

AraC	cytosine arabinoside
bp	base pair
CFP	cyan fluorescent protein
CPXV	cowpox virus
Da	Dalton(s)
DAPI	4’,6-diamidino-2-phenylindole
DNA	deoxyribonucleic acid
dsDNA	double-stranded DNA
dsRNA	double-stranded RNA
EFC	entry/fusion complex
EM	electron microscopy
ER	endoplasmic reticulum
ERGIC	ER-Golgi intermediate complex
EV	enveloped virion
GAPDH	glyceraldehyde-3-phosphate dehydrogenase
GFP	green fluorescent protein
HA	hemagglutinin
HIV	human immunodeficiency virus
hpi	hours post-infection
h, hr	hour(s)
IP	immunoprecipitation

IPTG	isopropyl β-D-1-thiogalactopyranoside
ITR	inverted terminal repetition
IV	immature virion
MAb	monoclonal antibody
min	minute(s)
MOCV	molluscum contagiosum virus
MPXV	monkeypox virus
MV	mature virion
NCLDV	nucleo-cytoplasmic large DNA viruses
NPH I	nucleotide phosphohydrolase I
NTPase	nucleoside triphosphatase
OAS	2’5’-oligoadenylate synthetase
OPXV	orthopoxvirus
ORF	open reading frame
PAb	polyclonal antibody
PBS	phosphate-buffered saline
PCR	polymerase chain reaction
PDI	protein disulfide isomerase
PFU	plaque forming unit
PKR	protein kinase R
RAP94	RNA polymerase-associated protein of 94 kDa
RNA	ribonucleic acid
siRNA	small (or short) interfering RNA

TBS	Tris-buffered saline
TGN	trans-Golgi network
TM	transmembrane
ts	temperature-sensitive
VACV	vaccinia virus
VARV	variola virus
VETF	vaccinia early transcription factor
VITF	vaccinia intermediate transcription factor
VLTF	vaccinia late transcription factor
VMAP	viral membrane assembly protein
WR	Western Reserve
WV	wrapped virion
YFP	yellow fluorescent protein

Chapter 1: Introduction

The family *Poxviridae* is a group of large DNA viruses with many distinctive features that replicate in the cytoplasm (1). Among the family, variola virus (VARV) and molluscum contagiosum virus (MOCV) are obligate human pathogens. Other members such as monkeypox virus (MPXV) can also infect humans by transmission from other animal hosts. Smallpox, one of the most devastating diseases in world history, is caused by VARV. Beginning in 1967, the World Health Organization led an intensive smallpox eradication program and was able to declare eradication of the disease in May 1980 (2).

Despite the eradication of smallpox, poxviruses continue to be studied for multiple reasons. Their threat as infectious agents is ever-present due to the cessation of smallpox vaccination, which has left newer generations vulnerable to bioterrorism involving smallpox (3). Ongoing epidemics and endemics of other poxvirus members are also of concern. Recently, rising numbers of MPXV infections are being reported in Central Africa (4). The need for continuing poxvirus research goes beyond merely establishing defensive measures against these threats. In 1982, the use of poxviruses as expression vectors was first described, and since then they have been widely used throughout research (5). Moreover, the development for their uses in medical applications as vaccines (5) or oncolytic viruses (6, 7) is actively underway.

The fascinating characteristics of poxvirus are another reason for their continued research. Likewise, the principle goal of this dissertation is to reveal the unique nature of poxvirus morphogenesis. Vaccinia virus (VACV), a prototype in poxvirus research, is the most extensively studied member of the family. As an animal virus, it was the first to be propagated in cell culture, physically purified, accurately titered, chemically analyzed, and observed microscopically (1). Decades of extensive VACV research have produced many enlightening discoveries, which also gave inspirations to building concepts in virus-host interactions and molecular biology in general. However, morphogenesis still remains one of the most poorly understood areas of the poxviral replication cycle (8). This dissertation focuses on studying proteins required for VACV morphogenesis in an effort to add another stepping-stone towards a solid understanding of this complicated topic.

Chapter 3 describes the use of split-green fluorescent protein (GFP) to determine membrane topology of proteins associated with the endoplasmic reticulum (ER). Obtaining topological information can provide promising insights into protein interaction studies (9). Evidence suggests that ER is the source of viral membranes, and that multiple vaccinia proteins interact with the ER (8, 10, 11). To study how these proteins are oriented on the ER membrane, we adapted the split-GFP system to develop a simple and rapid method of determining topology. VACV morphogenesis proteins L2 and A30.5, previously with unknown topology, were analyzed with this method. Furthermore, we showed that our method can be used for non-viral (cellular) proteins as well. This work was published in the journal *Traffic* (12).

Chapter 4 covers a reverse genetics study on VACV protein I2, which turned out to have a crucial role in morphogenesis. Construction of an I2 knockout virus has led to striking observations including mislocalization of VACV entry/fusion proteins and retention of scaffold proteins on the virion surface. A large portion of this chapter is included in a manuscript being prepared for submission. While proteins discussed in chapter 3 are necessary for the early stages of morphogenesis, I2 plays a part in later stages of morphogenesis. Therefore, the virus morphogenesis section in literature review (chapter 2) will include VACV morphogenesis from early membrane formation stage to the later virion maturation stage, in addition to comparing each stage with those of other virus families. This work will be submitted to the *Journal of Virology*.

Chapter 2: Literature Review

2.1 Poxviridae

2.1.1 Classification

The family *Poxviridae* is a group of large enveloped double-stranded DNA (dsDNA) viruses, distinguished by its replication in the cytoplasm of host cells and its large complex virion containing a dsDNA genome of 130 to 300 kilobase pairs (kbp) with a hairpin loop at each end (1). Based on host range, the family is divided into two subfamilies *Chordopoxvirinae* and *Entomopoxvirinae* (Table 2.1). The subfamilies are subdivided into genera, which are classified by similarities in morphology and host range, as well as genetic and antigenic relatedness (1).

The *Chordopoxvirinae* infect vertebrates including various species of mammals, birds, and reptiles (13). According to the latest virus taxonomy release from the International Committee on Taxonomy of Viruses (14), the *Chordopoxvirinae* are comprised of 10 genera: *Avipoxvirus, Capripoxvirus, Cervidpoxvirus, Crocodylidpoxvirus, Leporipoxvirus, Molluscipoxvirus, Orthopoxvirus, Parapoxvirus, Suipoxvirus,* and *Yatapoxvirus* (Table 2.1). Novel poxviruses are constantly being discovered (15-20), adding more diversity to the family. Recently identified species such as squirrelpox virus (15, 17) and salmon gill

poxvirus (18) are yet to be assigned within a genus in the *Chordopoxvirinae* subfamily (Table 2.1). The *Entomopoxvirinae* infect insect hosts, and are further divided into three genera: *Alphaentomopoxvirus, Betaentomopoxvirus, Gammaentomopoxvirus,* and an unassigned group of two species (Table 2.1).

Poxviruses are also grouped as one of the nucleo-cytoplasmic large DNA viruses (NCLDV), with DNA sequencing and bioinformatics suggesting distant relationship with *Phycodnaviridae, Asfarviridae, Ascoviridae, Iridoviridae, Mimiviridae* and *Marseillevirus* (21). Additional relatives that have joined the NCLDV group are megaviruses (22), pandoraviruses (23), and pithoviruses (24), which were all recently discovered.

Table 2.1 Taxonomy of the *Poxviridae* family

Subfamily	Genus	Species
Chordopoxvirinae	*Avipoxvirus*	*Canarypox virus*
		Fowlpox virus
		Juncopox virus
		Mynahpox virus
		Pigeonpox virus
		Psittacinepox virus
		Quailpox virus
		Sparrowpox virus
		Starlingpox virus
		Turkeypox virus
	Capripoxvirus	*Goatpox virus*
		Lumpy skin disease virus
		Sheeppox virus
	Cervidpoxvirus	*Mule deerpox virus*
	Crocodylidpoxvirus	*Nile crocodilepox virus*
	Leporipoxvirus	*Hare fibroma virus*
		Myxoma virus
		Rabbit fibroma virus
		Squirrel fibroma virus
	Molluscipoxvirus	*Molluscum contagiosum virus*
	Orthopoxvirus	*Camelpox virus*
		Cowpox virus
		Ectromelia virus
		Monkeypox virus
		Raccoonpox virus
		Skunkpox virus
		Taterapox virus
		Vaccinia virus
		Variola virus
		Volepox virus
	Parapoxvirus	*Bovine papular stomatitis virus*
		Orf virus
		Parapoxvirus of red deer in New Zealand
		Pseudocowpox virus
	Suipoxvirus	*Swinepox virus*
	Unassigned	*Squirrelpox virus*
	Yatapoxvirus	*Tanapox virus*
		Yaba monkey tumor virus

Entomopoxvirinae	*Alphaentomopoxvirus*	*Anomala cuprea entomopoxvirus* *Aphodius tasmaniae entomopoxvirus* *Demodema bonariensis entomopoxvirus* *Dermolepida albohirtum entomopoxvirus* *Figulus sublaevis entomopoxvirus* *Geotrupes sylvaticus entomopoxvirus* *Melolontha melolontha entomopoxvirus*
	Betaentomopoxvirus	*Acrobasis zelleri entomopoxvirus*
		Adoxophyes honmai entomopoxvirus *Amsacta moorei entomopoxvirus* *Arphia conspersa entomopoxvirus* *Choristoneura biennis entomopoxvirus* *Choristoneura conflicta entomopoxvirus* *Choristoneura diversuma entomopoxvirus* *Choristoneura fumiferana entomopoxvirus* *Choristoneura rosaceana entomopoxvirus* *Chorizagrotis auxiliaris entomopoxvirus* *Heliothis armigera entomopoxvirus* *Locusta migratoria entomopoxvirus* *Mythimna separata entomopoxvirus* *Oedaleus senegalensis entomopoxvirus* *Operophtera brumata entomopoxvirus* *Schistocerca gregaria entomopoxvirus*
	Gammaentomopoxvirus	*Aedes aegypti entomopoxvirus* *Camptochironomus tentans entomopoxvirus* *Chironomus attenuatus entomopoxvirus* *Chironomus luridus entomopoxvirus* *Chironomus plumosus entomopoxvirus* *Goeldichironomus holoprasinus entomopoxvirus*
	Unassigned	*Diachasmimorpha entomopoxvirus* *Melanoplus sanguinipes entomopoxvirus 'O'*

Table created from data in Virus Taxonomy: 2015 Release (14), Copyright © 2017, International Committee on Taxonomy of Viruses (ICTV).

2.1.2 Orthopoxviruses

The orthopoxviruses (OPXVs) are the most extensively studied genus within the poxvirus family. The *Orthopoxvirus* genus is made up of 10 species: camelpox virus, cowpox virus (CPXV), ectromelia virus, MPXV, raccoonpox virus, skunkpox virus, taterapox virus, VACV, VARV, and volepox virus (Table 2.1). The names of these virus species do not necessarily indicate their natural reservoir. Most of the names were given based on the host where the virus was initially isolated. For example, the natural reservoirs of CPXV and MPXV are rodents, but they were first isolated in cows and monkeys, respectively, hence their names (1).

VARV the most infamous member of the OPXVs, is the causative agent of the smallpox disease, which made its mark as one of the most lethal diseases in human history (2). It is thought that for over three thousand years, smallpox spread across the world as human populations started to get well established and grew in numbers (25). Smallpox was universally feared for its high fatality rate, which was about 30% overall (26). The rate reached to 50% or more in very young individuals or in those over 40 years of age (27). In some places within Asia and Europe where old records exist, an average of 10% of all deaths were caused by smallpox each year (25). The concept of vaccines had not yet been developed, but continuous efforts were made throughout history to cure or prevent this threatening disease. From a historical perspective, these efforts became the foundation for the birth of vaccines and immunology (28). Prophylactic cutaneous or intranasal inoculations of smallpox scab material gave mild infection symptoms but ultimately prevented future lethal infections. This procedure was referred as the term ‘variolation’, and helped

significantly to alleviate the lethality of the disease (29). In 1798, Edward Jenner published a safer alternative process by describing that infection with material obtained from the non-lethal cowpox virus infection of a dairymaid protected against subsequent infection with smallpox (30). The Latin word for cow is *vacca* and for cowpox is *vaccinia*, which led Jenner to call this process *vaccination*. Jenner initially used CPXV as vaccines against smallpox, but live VACV became the main vaccine used during the smallpox eradication program (29).

VACV is very closely related to CPXV, and historically they have often been considered the same (31). The exact origin of VACV is unknown, with decades of laboratory passaging making it more difficult to trace back towards its origin (32). In addition to its role as the active constituent of the smallpox vaccine, VACV is the most extensively studied member of the poxvirus family. Its research continued despite the eradication of smallpox and has revealed countless characteristics of OPXV as a whole.

2.1.3 Virion structure

The virions of poxviruses are brick- or barrel- shaped with a membrane envelope around its complex structure (Figure 2.1). Unlike many other well-characterized viruses, poxvirus virions are large in size and lack symmetry. The size of the virion reaches about 360 X 270 X 250 nm in dimensions, big enough to barely see under a light microscope, but electron microscopy (EM) is used in most cases to

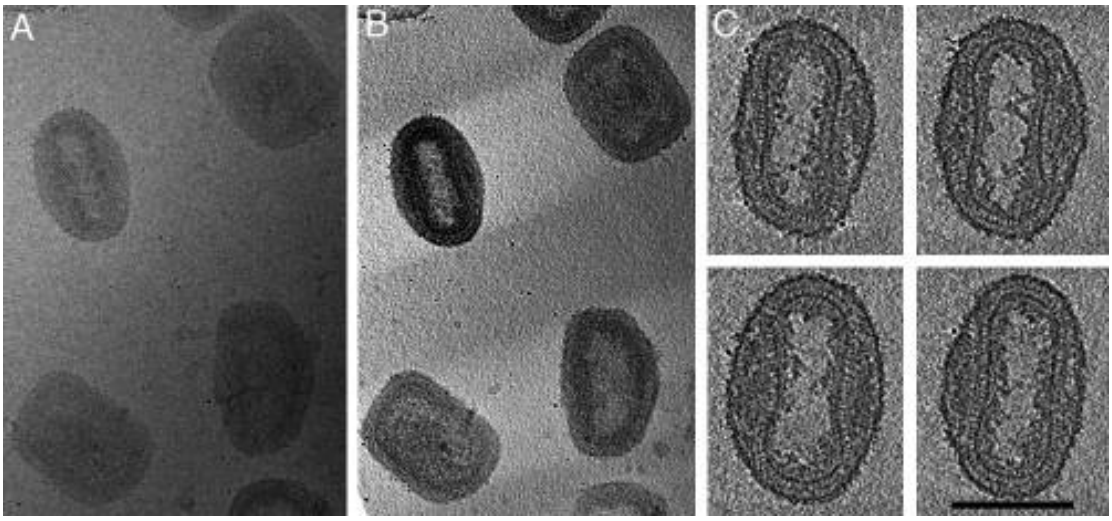

Figure 2.1 Isolated vaccinia virus particles (MV) preserved by rapid freezing and viewed by cryo-EM

(A) Cryo-electron micrograph showing an image of several particles in a typical projection. (B) Section taken from the tomographic reconstruction of the same area as in panel A. (C) Four sections of a particle taken subsequently. Each section is 24 nm thick and 24 nm apart from each other. Scale bar measures 200 nm. Figure reprinted from Cryklaff et al. (33) with permission, copyright (2005) National Academy of Sciences, U.S.A.

reveal greater detail under higher magnification (34, 35). There are several forms of infectious virions that vary mainly by the number of outer membrane layers, and they will be discussed in more detail later. The basic infectious form is the mature virion (MV), and it is the most abundant form produced during replication. MVs bear a single outer lipid membrane bilayer that is 5-6 nm thick (33), containing a dumbbell-shaped core and two lateral bodies within the cavities (1). Current techniques including EM and cryoelectron tomography are not sufficient to fully resolve the complex core structure, but suggest that the core wall has two layers surrounding the nucleoprotein (33). VACV MV is primarily composed of protein (90%), lipid (5%), and DNA (3.2%) by dry weight (36), with a overall mass of 5-10 femtogram (37, 38). Additionally, other components such as spermine, spermidine, and signs of RNA presence have been found in VACV MV (39, 40).

2.1.4 Genome organization

Poxviruses have large, linear dsDNA genomes that range from 130 to 300 kbp (1). The large size of the genome gives these viruses the capacity to encode numerous genes, with VACV containing more than 200 open reading frames (ORFs) in its ~195 kbp genome (41). At the ends of poxvirus genome there are regions called inverted terminal repetitions (ITRs), which are identical sequences but oriented in opposite directions at each end (Figure 2.2)(42). ITRs contain hairpin loops that connect the dsDNA at the very end of the genome, these loops are A/T rich and incompletely base-paired (43). They also include concatemer resolution sequences

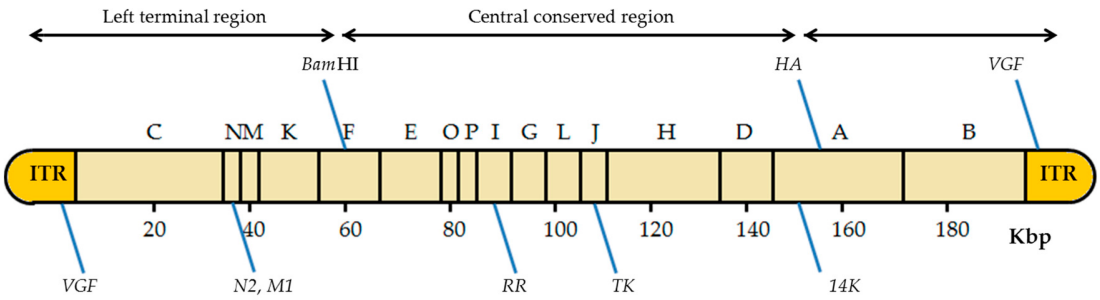

Figure 2.2 Diagram of vaccinia virus genome with *Hind*III restriction sites (44)

The VACV genome has various insertions sites, annotated with blue lines, where foreign genes can be inserted. ITRs: inverted terminal repeats; VGF: VACV growth factor gene; N2, M1: N2 and M1 genes; RR: ribonucleotide reductase gene; TK: thymidine kinase gene; 14K: A27 gene encoding 14 kDa fusion protein. Reprinted with permission from Ali et al (45).

(46) and sets of short tandemly repeated sequences (47). Variations such as duplications, deletions, and transpositions can alter the size of ITRs (48-50).

While variable genes involved in host interactions are located near the ends of the genome, the central region of the genome contains many of the highly conserved genes that are essential for viral replication (1). Almost 50 genes are conserved among all poxviruses including entomopoxviruses (Table 2.2), and about 50 additional genes are conserved in just chordopoxviruses (Table 2.3)(51). Most of the genes do not overlap and each is regulated by an early, intermediate or late promoter that is recognized by their respective transcription factors.

2.1.5 Gene nomenclature

The convention for naming VACV ORFs originated before whole genome sequencing was available (1). Poxvirus genomes can be digested with *Hind*III restriction endonuclease, generating fragments that could be separated as a ladder using agarose gel electrophoresis (Figure 2.3). A letter was assigned to each fragment from largest fragment 'A' to smallest fragment 'O' in alphabetic order (52). The ORFs contained within each *Hind*III fragment were assigned a number starting from 1, in accordance to their position in the genome from left to right, and the letter L or R to indicate the gene orientation. Each ORF name therefore consisted of the fragment letter, the ORF number, and its transcriptional direction L or R (this is dropped in polypeptide names) (1). For example, L2R gene is the 2nd ORF in the *Hind*III L fragment and is transcribed from left to right (R). The protein encoded by L2R is L2. Different nomenclature numbering ORFs from one end of the genome to

the other end is available, but the traditional letter names are still used widely in literature for consistency (1).

Table 2.2 Completely conserved gene families of *Poxviridae*

VV-Cop ORF	Family names of 49 poxvirus conserved genes	Family identification no.	Function[a]
A1L	Late transcription factor 2 (VLTF-2)	1153	T
A2L	Late transcription factor 3 (VLTF-3)	1228	T
A3L	P4b precursor	1072	M
A5R	RNA polymerase subunit 19 (RPO19)	1225	T
A7L	Early transcription factor—large (VETF-l)	914	T
A9L	Late virion membrane protein (MP), essential	1218	M
A10L	P4a precursor	1750	M
A11R	Unknown	1217	U
A16L	Unknown soluble-myristylated	887	U
A18R	DNA helicase, transcription	896	T
A21L	Unknown	1202	U
A22R	Holliday junction resolvase	1201	R
A23R	Intermediate transcription factor 3—large (VITF-3)	946	T
A24R	RNA polymerase subunit 132 (RPO132)	880	T
A28L	Unknown predicted signal peptide	1099	U
A29L	RNA polymerase subunit 35 (RPO35)	1197	T
A32L	ATPase-DNA packaging protein	1192	M
D1R	mRNA capping enzyme large subunit	1109	T
D4R	Uracil-DNA glycosylase	1130	R
D5R	NTPase, DNA replication	950	R
D6R	Early transcription factor—small (VETF-s), morphogenesis	1027	T, M
D7R	RNA polymerase subunit 18 (RPO18)	1141	T
D10R	Nucleophosphohydrolase-pyrophosphohydrolase downregulator	1143	T
D11L	Nucleophosphohydrolase I (NPH-I), virion	1093	T, M
D12L	mRNA capping enzyme small subunit, VITF	1151	T
D13L	Rifampin resistance MP, morphogenesis	883	M
E1L	Poly(A) polymerase large subunit	939	T
E6R	Unknown	1253	U
E9L	DNA polymerase	910	R
E10R	Redox-EVR-1, morphogenesis	900	M
F9L	Unknown predicted MP	1001	U
F10L	Serine-threonine kinase, morphogenesis	1065	M
G1L	Protease morphogenesis	1275	M
G5R	Unknown	1017	U
G6R	Unknown	1131	U
G9R	Myristylated protein	957	U
H2R	Unknown	1116	U

VV-Cop ORF	Family names of 49 poxvirus conserved genes	Family identification no.	Function[a]
H3L	Intracellular mature virus morphogenesis viral protein (VP55)	1269	M
H4L	RNA polymerase-associated protein (RAP94)	1695	T
H6R	Topoisomerase type I	908	R
I7L	Virion core protease	1015	M
I8R	RNA helicase, NPH-II	1104	T
J3R	Poly(A) polymerase small subunit VP39	895	T
J5L	Late MP, essential	1777	M
J6R	RNA polymerase subunit 147 (RPO147)	1040	T
L1R	Myrisylated MP virion	1044	M
L3L	Unknown	1285	U
L4R	Core packaging transcription	1283	T, M
L5R	Unknown predicted MP	1511	U

[a] T, transcription; M, morphogenesis; U, unknown; R, replication. Table reprinted from Upton et al. (51) with permission.

Table 2.3 Conserved gene families in *Chordopoxvirinae*

VV-Cop ORF	Family names of 41 chordopoxvirus conserved genes	Family identification no.	Function[a]
A2.5L	Thioredoxin-like protein	1552	M
A4L	Core protein	1580	M
A8R	Intermediate transcription factor 3—small (VITF-3)	1758	T
A6L	Unknown	1224	U
A12L	Structural protein	1216	M
A13L	Virion membrane protein (MP)	1575	M
A14L	Intracellular mature virus (IMV) phosphorylated MP	1323	M
A14.5L	IMV MP, virulence factor	1547	M
A15L	Unknown	1546	U
A17L	IMV phosphorylated MP	1206	M
A19L	Unknown	1545	U
A20R	DNA polymerase processivity factor	1203	R
A30L	Virion morphogenesis	1561	M
A34R	Extracellular enveloped virion glycoprotein	1540	M
D2L	Structural protein	1351	M
D3R	Structural protein	1350	M
D9R	*mutT* motif, nucleoside triphosphate pyrophosphohydrolase	1142	U
E2L	Unknown	1251	U
E4L	RNA polymerase subunit 30 (RPO30), VITF-1	1252	T
E8R	Endoplasmic reticulum-localized MP	1254	U
F12L	Actin tail, microtubule	1145	M
F13L	Phospholipase extracellular enveloped virion	1146	M
F15L	Unknown	1148	U
F17R	DNA-binding phosphoprotein	1150	R
G2R	Late transcription factor (VLTF)	1277	T
G3L	Unknown	1521	U
G4L	Glutaredoxin 2	1279	M
G5.5R	RNA polymerase subunit 7 (RPO7)	1133	T
G7L	Structural protein	1776	M
G8R	Late transcription factor 1 (VLTF-1)	1287	T
H1L	Tyrosine-serine phosphatase	1270	M
H5R	Late transcription factor 4 (VLTF-4)	1353	T
H7R	Unknown	1260	U
I1L	DNA-binding protein	1263	R
I2L	Unknown	1598	U
I3L	DNA-binding phosphoprotein	1265	R

VV-Cop ORF	Family names of 41 chordopoxvirus conserved genes	Family identification no.	Function[a]
I5L	Unknown VP13	1367	U
I6L	Unknown	1268	U
J1R	Virion	1273	M
J4R	RNA polymerase subunit 22 (RPO22)	1272	T
L2R	Unknown	1584	U

[a] T, transcription; M, morphogenesis; U, unknown; R, replication. Table reprinted from Upton et al. (51) with permission.

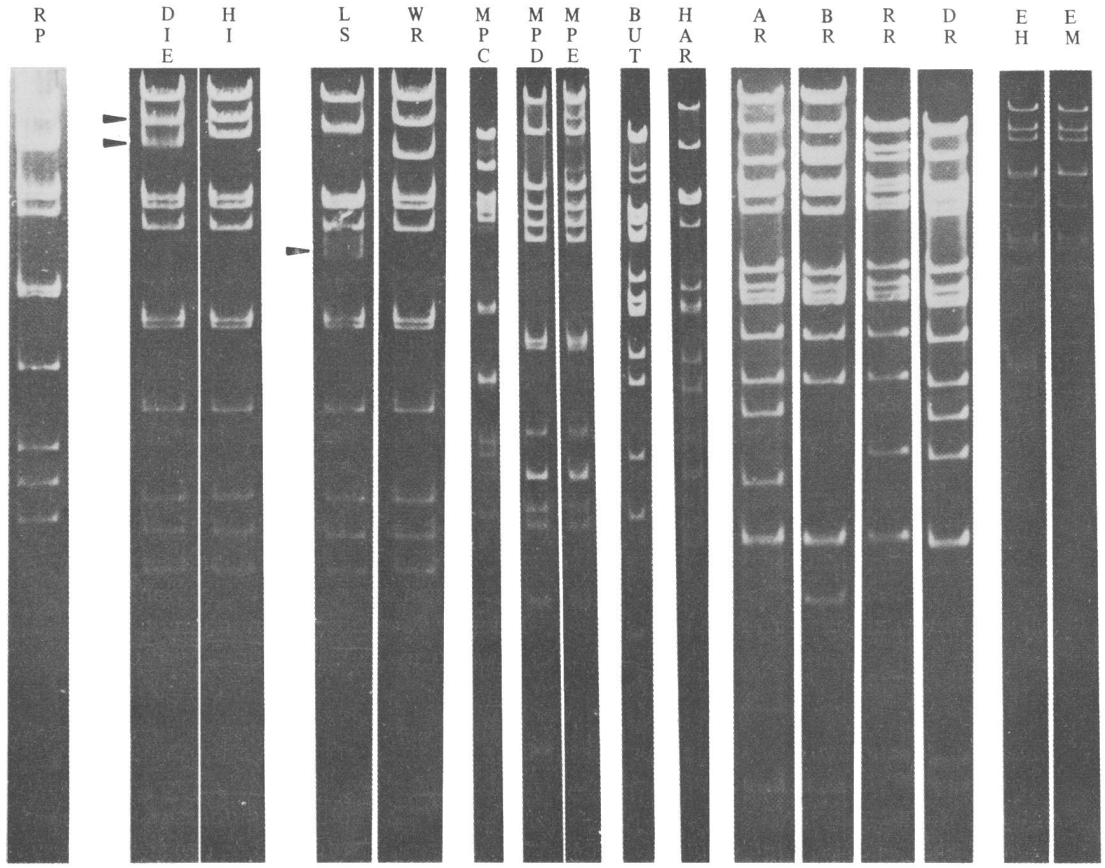

Figure 2.3 *Hind*III restriction fragments of poxvirus genomes

DNA fragments generated from rabbitpox strain Utrecht (RP); vaccinia strain DIE, Hall Institute (HI), Lister (LS), or Western Reserve (WR); monkeypox strain Congo (MPC), Denmark (MPD), or España (MPE); variola strain Butler (BUT) or Harvey (HAR); cowpox red strain Austria (AR), Brighton (BR), Ruthin (RR), or Daisy (DR); and ectromelia strain Hampstead (EH) or Moscow (EM). Fragments were separated by agarose slab gel electrophoresis. Arrows show size heterogeneity of fragment B,C, and G of indicated strains. Figure reprinted from Mackett et al. (53) with permission.

2.2 Poxvirus Replication

2.2.1 Attachment and entry

VACV cell attachment and entry is the crucial first step in initiating the entire viral replication cycle (Figure 2.4). VACV can enter into many different types of mammalian cells. The entry mechanisms vary based on the type of infectious virion forms (1). Two infectious forms exist, with MVs being more common than enveloped virions (EVs). MVs have a single outer membrane, but EVs have an additional membrane layer surrounding the MV form (Figure 2.5)(54). The additional membrane has at least six different proteins not present on the MV outer membrane, and this extra layer may provide additional resistance to antibody neutralization (55). MVs are believed to be important for animal-to-animal spread, while EVs are important for cell-to-cell spread (1).

Once the MV attaches to the cell, the virus core can enter by either direct fusion with the plasma membrane or following endocytosis (1). Entry via the endocytic route is promoted by low pH through endosomal acidification. Unlike many other enveloped viruses that encode merely one or two proteins for attachment and fusion, VACV encodes at least four attachment and 11 entry/fusion proteins (Table 2.4). A26, A27, D8, and H3 mediate attachment by binding cell surface glycosaminoglycans and laminin (1). A26 binds laminin, A27 and H3 bind heparin sulfate, and D8 binds chondroitin sulfate (56-59). Among the four attachment proteins, only D8 and H3 have transmembrane domains, while A26 and A27 are held on the membrane by forming a complex with another transmembrane protein A17 (60).

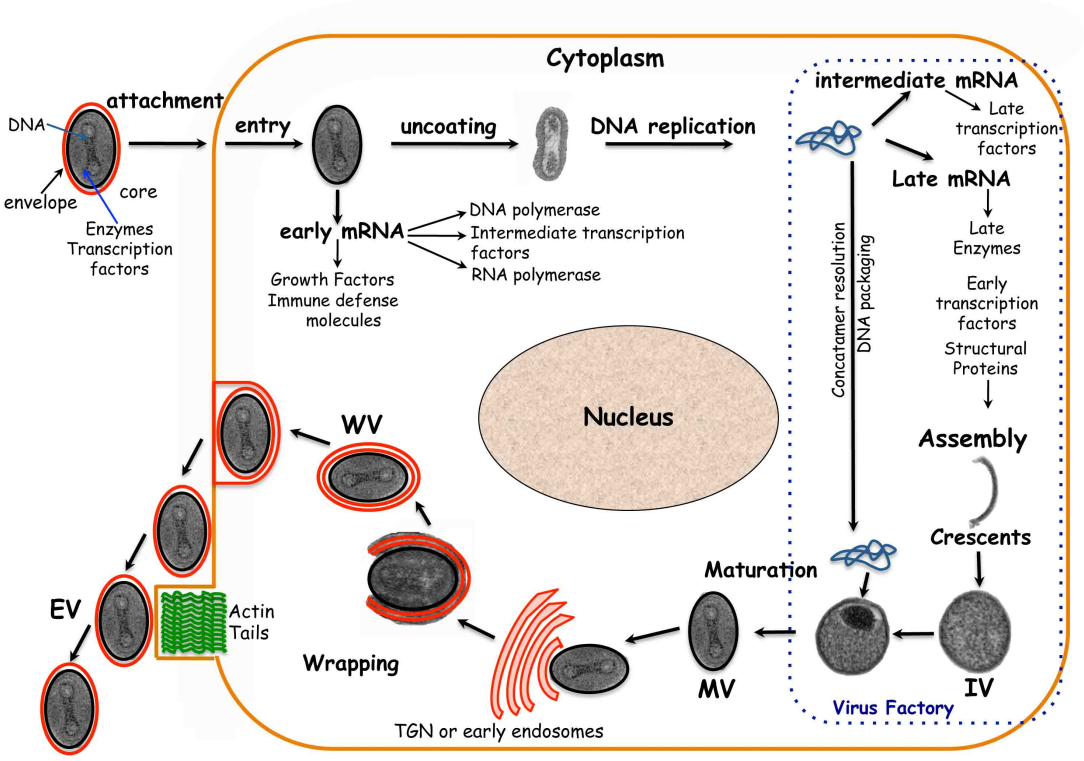

Figure 2.4 Replication cycle of orthopoxviruses

Infection cycle is initiated when an infectious form of the virion, such as MV or EV, attaches and enters the cell. As soon as entry occurs the early mRNAs are released and translated to produce proteins necessary for host immune defense, DNA replication, intermediate transcription, etc. Once DNA is replicated, intermediate gene expression can occur, followed by late gene expression. Proteins produced post-replication include structural and morphogenesis proteins that assemble viral membranes into immature virions (IVs). IVs go through maturation and MVs, the first infectious form, are produced. The MVs can further acquire an additional double membrane to become wrapped virions (WV) through wrapping of trans-Golgi network (TGN) or endosomal membranes. The WV outer membrane fuses with the plasma membrane as the virion leaves the cell in EV form. Illustration kindly provided by Liliana Maruri-Avidal.

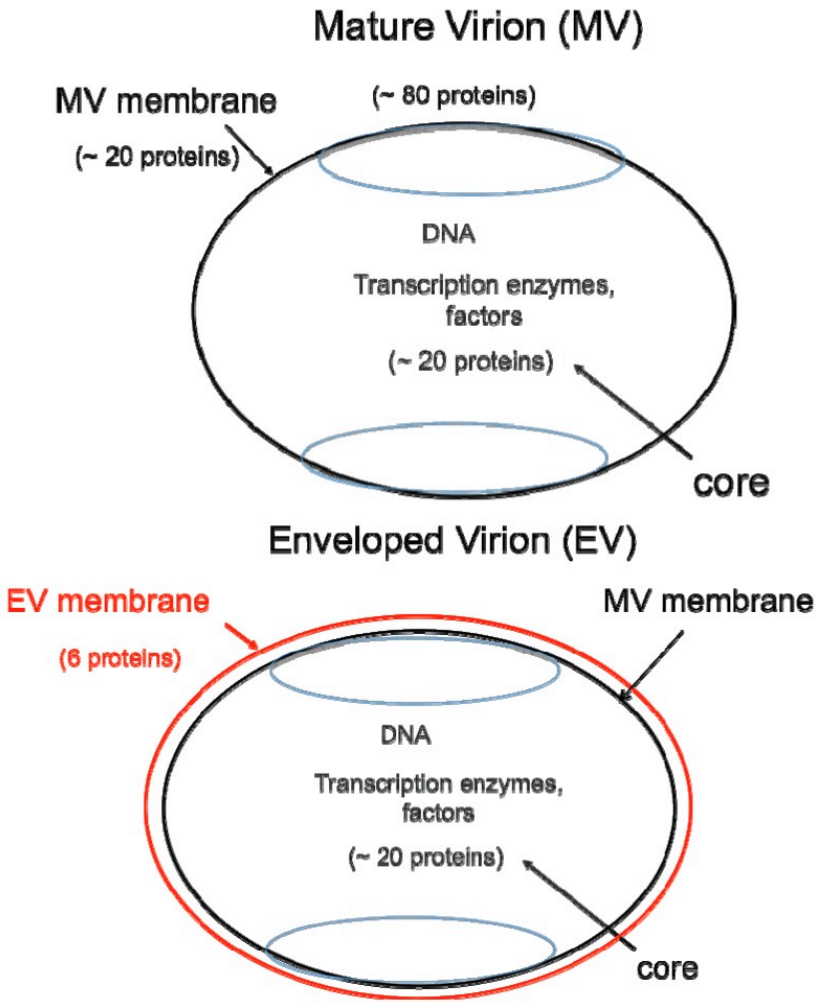

Figure 2.5 Two major forms of infectious vaccinia virions

The major difference between MVs and EVs is the presence of an additional outer membrane (red) on EVs. This additional membrane, annotated as EV membrane, contains six distinct proteins. The MV membrane, present in both MVs and EVs, contains about 20 proteins, including EFC proteins that mediate attachment and entry. Figure reprinted with permission from Moss, 2012 (61).

Fusion and core entry of VACV require a set of transmembrane proteins that form a complex known as the entry/fusion complex (EFC) on the MV membrane (Figure 2.5). The EFC is composed of 11 proteins: A16, A21, A28, F9, G3, G9, H2, J5, L1, L5, and O3 (54, 55, 61-75). Properties of each protein are listed in Table 2.4. Every member of the EFC is essential for entry and conserved in poxviruses, suggesting a common entry mechanism is used across the family (61). Repression of each entry/fusion protein does not affect assembly of virions, which appear normal by EM, but the virions are not able to enter new cells (1). With the exception of L1 and F9, absence of a single member in the EFC can cause the whole complex to breakdown. Thus, L1 and F9 are occasionally referred to as EFC-associated proteins. Protein I2 had also been implicated as a potential entry/fusion protein for the past few years, but it will be discussed later in chapter 4 that I2 is rather a viral morphogenesis protein.

Understanding the entry mechanism has faced many hurdles due to a lack of information including detailed structures and protein-protein interactions of entry/fusion proteins. Nevertheless, fusion of the MV membrane with the plasma membrane has been demonstrated (76, 77) and a few protein-protein interactions of entry proteins have been identified (74, 78, 79). EVs enter cells in a similar fashion to MVs. EVs shed their outermost membrane as they attach to the cell, so that the subsequent membrane (MV membrane) may undergo fusion with the plasma membrane. They may also enter by macropinocytosis (80), a regulated form of endocytosis with non-selective uptake.

Table 2.4 Vaccinia virus attachment and entry/fusion proteins

Protein	kDa	TM[a]	S-S[b]	Conserved[c]	Properties
Attachment proteins					
A26	58	–	–	–	Binds laminin; associates with A27; interacts with A16 and G9; fusion suppressor
A27	13	–	–	–	Binds heparan; associates with A26 and A17 membrane protein; Nt[d]
D8	35	N	–	–	Binds chondroitin; Nt
H3	38	C	–	P	Binds heparan; Nt
Entry-fusion complex					
A16	43	C	+	P	Homolog G9 and J5; interacts with G9 and A26; complex with G9 interacts with A56:K2 complex
A21	14	N	+	P	
A28	16	N	+	P	Interacts with H2; Nt
F9	24	C	+	P	
G3	13	N		P	Interacts with L5
G9	39	C	+	P	Homolog A16 and J5; interacts with A16 and A26; complex with A16 interacts with A56:K2 complex; Myr[e]
H2	22	N	+	P	Interacts with A28
J5	15	C	+	P	Homolog A16 and G9; Myr
L1	27	C	+	P	Myr; Nt
L5	15	C	+	P	Interacts with G3
O3	4	N		C	Smallest VACV protein

[a] TM, N- or C-terminal transmembrane domain. [b] S-S, intramolecular disulfide bond(s). [c] Conserved in all poxviruses (P) or all chordopoxviruses (C). [d] Nt, target of neutralizing antibody. [e] Myr, myristoylated. Table reprinted with permission from Moss 2016 (55).

2.2.2 Viral gene expression

VACV genes can be classified as early, intermediate, or late based on their temporal regulation (1). Expression stages within the replication cycle are annotated in Figure 2.4. Early transcripts are synthesized from a single entering genome prior to viral DNA (genome) replication. It is only after DNA replication that intermediate and late genes can be transcribed, thus often getting grouped together and referred to as post-replicative genes. Deep sequencing of the VACV transcriptome has detected RNAs of 118 ORFs before viral DNA replication and 93 ORFs post-replication (81). Cytosine arabinoside (AraC), a DNA replication inhibitor drug, is commonly used in poxviral studies to limit viral expression to early genes.

The virus encodes stage-specific transcription factors that function with the conserved early, intermediate, or late promoter sequences (82-84). Generally, early transcripts encode factors and enzymes for DNA replication, intermediate stage transcription, and host defense inhibition. Intermediate and late transcripts encode factors necessary for later steps of replication, such as virion assembly. Additionally, intermediate mRNAs encode factors for late gene expression, and late mRNAs encode early transcription machinery to be packaged into newly formed virions (1).

The early transcription factors and RNA polymerase are packaged in progeny virions along with other enzymes (85), which allows for immediate synthesis of early mRNA. Virus cores are transported to transcription sites on microtubules (86, 87) and start production of mRNAs within minutes after entry. Capped, polyadenylated and methylated mRNAs are produced by this early transcription system (88-91). The mRNA synthesis and modification system includes VACV early transcription factor

(VETF), DNA-dependent RNA polymerase, RNA polymerase-associated protein of 94-kDa (RAP94), poly(A) polymerase, nucleotide phosphohydrolase I (NPH I), topoisomerase, and enzymes for capping and methylation (1). VETF is a heterodimer of 82 and 74 kDa subunits, respectively encoded by late genes A7L and D6R (92-94). VETF interacts with RAP94, another late protein encoded by H4L gene (85). RAP94 is associated with RNA polymerase and confers promoter specificity for early gene transcription (95-97). There are eight subunits in the VACV RNA polymerase with seven of them being homologs of cellular RNA polymerase (98-108). Unlike VETF or RAP94, subunits of RNA polymerase are encoded by early genes as they are also needed for intermediate and late mRNA synthesis. VETF, RAP94, RNA polymerase, NPH I, and capping enzyme form a complex for accurate transcription and termination of early genes (109, 110).

Intermediate transcription requires RNA polymerase along with three VACV intermediate transcription factors: VITF-1, VITF-2, and VITF-3 (1). The E4 gene encodes VITF-1, which also serves as a subunit for RNA polymerase (107). VITF-2 is a cellular factor (111), and transcripts from A8R and A23R genes encode the components of VITF-3 (112). The list of intermediate gene products has been recently expanded to 53 genes (113), including three of four VACV late transcription factors (VLTFs) G8R, A1L, and A2L respectively encoding VLTF-1, VLTF-2, and VLTF-3 (114). Additionally, the H5R gene product VLTF-4 was shown to have a role in late transcription and to interact with other VLTFs (115, 116). 38 genes have been identified as late stage genes, including many of the MV membrane and morphogenesis proteins (113).

VACV temporal regulation of transcription is not solely dependent on sequential synthesis of mRNA. Transcripts from each stage decline rapidly, usually with half-lives of 30 min or less, which may ensure apparent distinction between the expression stages (117-120). Decapping enzymes encoded by D9R and D10R genes promote degradation of viral mRNAs, as decapped mRNAs are vulnerable to cellular 5' exonuclease digestion (1, 121-124). D9 and D10's activity is not limited to viral mRNAs but includes cellular mRNAs (125), possibly contributing to shutoff of host protein translation. Unlike early transcription, the intermediate and late transcription systems lack accurate termination, often generating variable lengths of 3' end on their mRNAs (126). Overextended mRNAs are subject to overlapping with transcripts from other ORFs, increasing the possibility of generating double-stranded RNAs (dsRNAs). Host innate defense proteins such as protein kinase R (PKR) or 2'5'-oligoadenylate synthetase (OAS) can be stimulated by dsRNAs to trigger antiviral responses (127-129). Mutations in catalytic sites of both D9 and D10 lead to accumulation of dsRNA, stressing the importance of decapping during VACV infection (130).

2.2.3 Viral genome replication

Poxviruses are distinguished from most DNA viruses as they replicate their dsDNA genome in the cytoplasm (Figure 2.4). DNA replication foci, often called viral factories (Figure 2.6), are detectable in the cytoplasm using microscopy (131-133). Multiple VACV proteins involved in DNA replication have been found with temperature-sensitive (ts) mutants: E9L encodes DNA polymerase (134-136), D5R

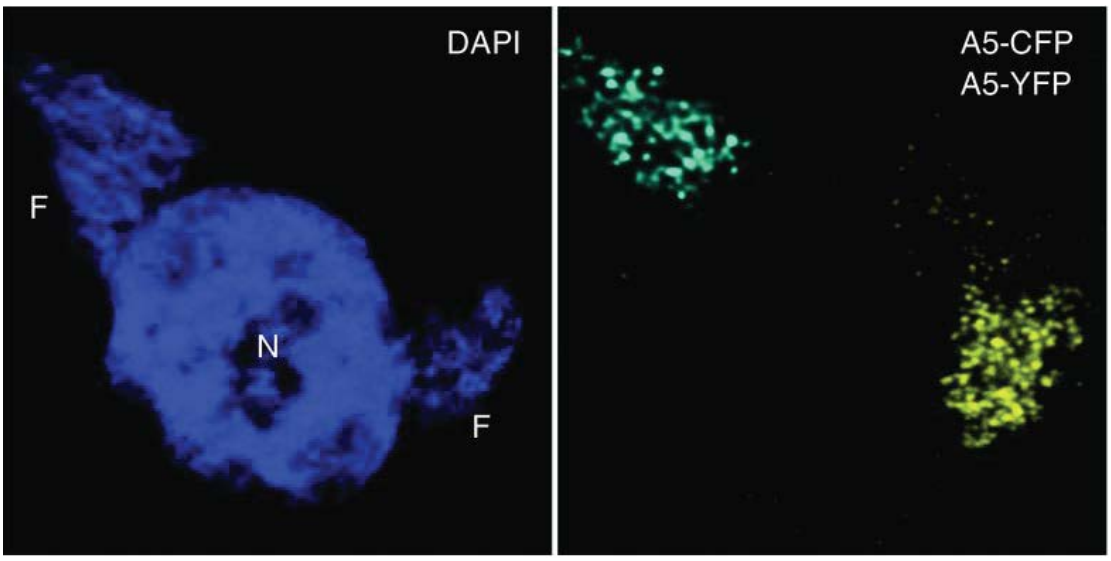

Figure 2.6 Vaccinia virus factories in cytoplasm of an infected cell

Confocal microscopy images of a HeLa cell with simultaneous infection of two recombinant VACVs, expressing either cyan fluorescent protein (CFP) or yellow fluorescent protein (YFP)-tagged A5 core protein. Blue is 4',6-diamidino-2-phenylindole (DAPI) staining of nucleus (N) and virus factories (F). Two virus factories arose in a single cell from different viruses. Figure reprinted from Katsafanas et al. (133) with permission.

encodes a protein with both nucleoside-triphosphatase (NTPase) and primase activity (137-142), B1R encodes serine/threonine protein kinase (143-145), and D4R encodes uracil DNA glycosylase (146). B1 kinase activity is important for blocking a cellular cytoplasmic protein that potentially inhibits poxviral DNA replication (147, 148). Another substrate protein for B1 kinase is encoded by the H5R gene (149), which appears to have multiple functions in DNA replication, transcription, mRNA processing, and morphogenesis (1). In addition, the A20R gene product is required for processive DNA polymerase activity (150-153). A20 was shown to interact with D4, D5 and H5 (154), suggesting that these proteins can form a complex (153). A single-stranded DNA binding protein encoded by the I3L gene (155-157) is also suggested to participate in DNA replication, but its exact role remains yet to be understood (158).

VACV replicative intermediates have genomes linked in head-to-head or tail-to-tail manner (159, 160), which are referred to as concatemers. VACV Holliday junction resolvase, encoded by the A22R gene, cleaves the concatemers into single genome units (161, 162).

Two different models have been proposed for poxvirus DNA replication, one is the self-priming model taken from the rolling hairpin strand-displacement method in the parvovirus replication model. This model was proposed due to the similarity of VACV genome and concatemers with parvovirus replication intermediates (158). More recently, reports of primase and DNA ligase requirements have rekindled the possibility of the semi-discontinuous leading-lagging strand synthesis model (163) for VACV DNA replication (164). The D5 protein, a NTPase with a C-terminal helicase,

also contains an archaeoeukaryotic primase domain in the N-terminus essential for DNA replication (141, 142). The DNA ligase requirement was evident as presence of either viral ligase encoded by the A50R gene or host DNA ligase I was necessary (165). Furthermore, a recent study using deep sequencing has mapped VACV replication origins at the nucleotide level and supported the involvement of RNA-primed, semi-discontinuous synthesis model of VACV DNA replication (166).

2.2.4 Virion maturation and egress

Electron microscopy of VACV-infected cells has shown multiple viral forms during different stages of maturation (Figure 2.7). The lower magnification electron micrograph in Figure 2.8 provides a comprehensive view of all the different forms contained within a single infected cell. Pieces of crescent-shaped membranes are the first viral membrane structures observed during infection. The crescents are found in the virus factories and they serve as starting materials that enlarge to become IVs, which then mature into MVs (167-169). MVs are the first mature form that is infectious, but it may obtain two additional membranes through wrapping of trans-Golgi or endosomal cisternae (170-172) to become wrapped virions (WVs). As the WVs egress the cell, the outermost membrane fuses with the plasma membrane, releasing the virus to the extracellular space in the EV form (Figure 2.4). The morphogenesis steps between different VACV forms will be discussed in greater detail later in 'Virus Morphogenesis' section (subsection 2.3.1).

As viral genome replication occurs before virion assembly, replicated genomes must find a way to get packaged into the virion during maturation. Electron

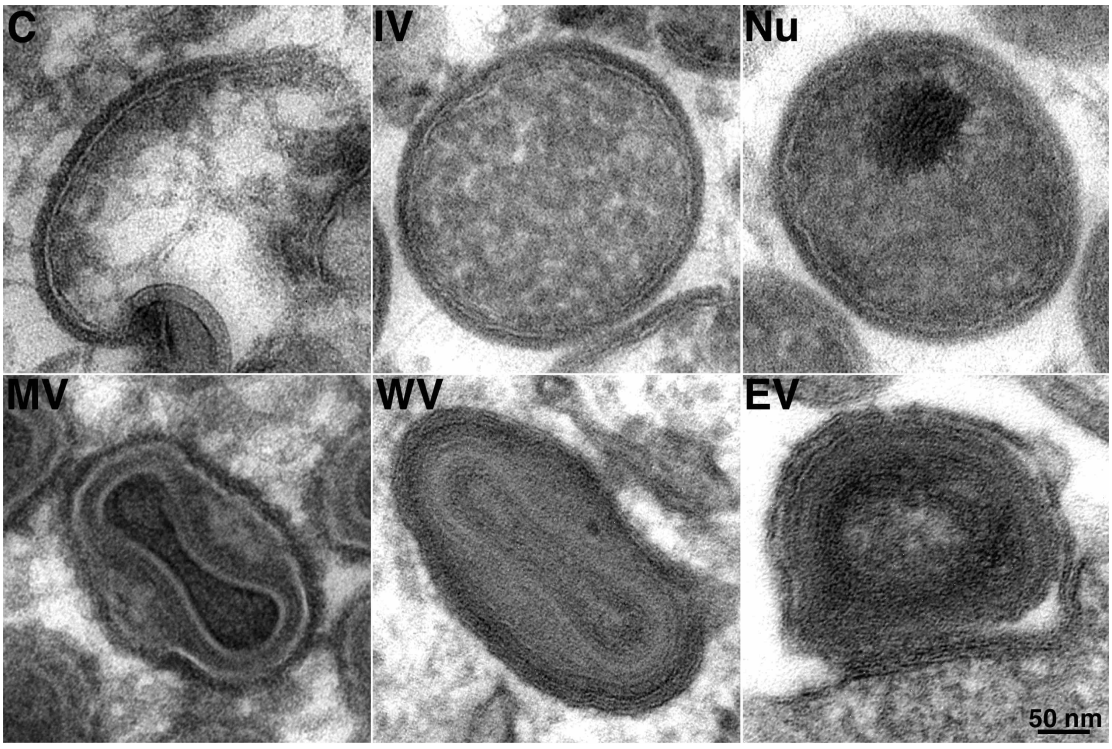

Figure 2.7 Forms of vaccinia virus in different maturation stages

Transmission electron micrographs showing a closer look at a crescent (C), immature virion (IV), nucleoid (Nu), mature virion (MV), wrapped virion (WV), and extracellular enveloped virion (EV). Scale bar measure 50 nm. Images were kindly provided by Andrea Weisberg.

microscopy has detected dense DNA entering through the virion membrane just before IVs completely close (173). An example of a nucleoid is shown in Figure 2.7. DNA accumulated as crystalloids in the cytoplasm when the drug rifampicin was used to inhibit IV formation (174). Gene products from A32L (175), I6L (176), and A13 (177) are suggested to be required for DNA packaging, although the mechanism is unknown. In addition to genomes, core proteins including the early transcription system need to be packaged in the virions as well. An electron dense mass of core proteins called 'viroplasm' gets surrounded by the crescents and enclosed as crescents grow into IVs (1). Viroplasm resembles the interior of IVs during normal infection, but accumulates into massive inclusion when virion assembly is blocked (178).

Virion maturation requires intramolecular disulfide formation or proteolytic processing of some virion proteins. The disulfide bond formation of some MV membrane proteins is critical, as repression of any one of viral redox proteins A2.5, E10, and G4 leads to a block in virion maturation (179-182). Five core proteins A3, A10, A12, G7, L4, and a membrane protein A17 are processed (1), and there are probably more that have not yet been identified. Core or membrane proteins in the IVs are unprocessed, whereas MVs contain processed proteins. The I7L gene encodes the protease responsible for cleaving these proteins at a consensus AG↓X site (183, 184). Another viral protein encoded by the G1L gene has a metalloprotease motif, but its relevance with the processing of known proteins could not be demonstrated (185). I7 protease activity is also important for MV membrane morphogenesis, which will be discussed later.

While release of MV forms can only occur by cell lysis, VACV can alternatively egress the cell in EV forms without lysis. Some MVs get wrapped to become WVs, which can migrate to the cell surface. WVs travel on microtubules for long-range intracellular movement (186-188), involving proteins encoded by the A36R and F12L ORFs. The A36 and F12 proteins are present only on WV membranes (1). Interaction between A36 and a microtubule motor protein kinesin (189, 190), and the structural similarity between F12 and kinesin light chain (191, 192) have stressed their roles in microtubular movement. As WVs reach the cortical actin network at the cell periphery, A36 is phosphorylated to regulate the transition from microtubule- to actin-based motility (193). Then the outermost membrane of WV fuses with the plasma membrane, exposing the EV form to extracellular space. A33, A34, and A36 proteins facilitate cell-to-cell spread of EVs by supporting formation of virus-tipped actin-containing projections at the cell surface (194-197).

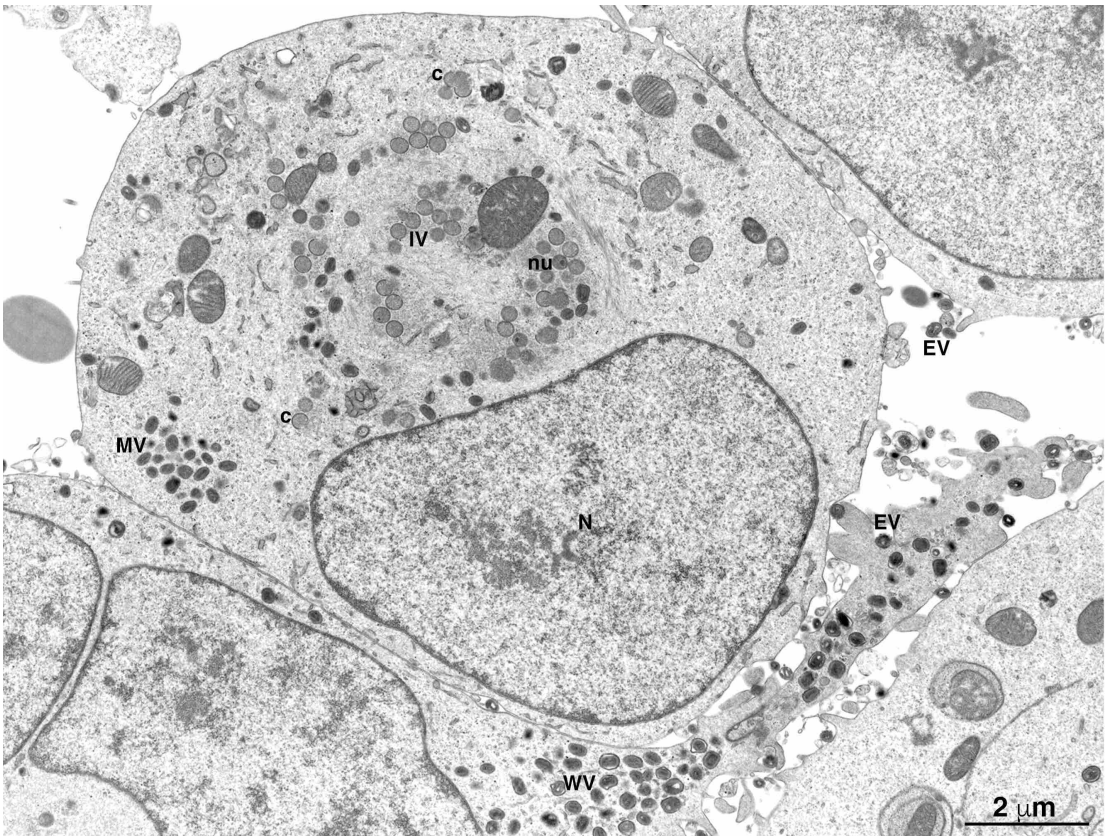

Figure 2.8 Vaccinia virus infected cell

Electron micrograph of a RK-13 (rabbit kidney) cell infected with VACV at low magnification. Abbreviations: C, crescent; IV, immature virion; Nu, nucleoid; MV, mature virion; WV, wrapped virion; EV, enveloped virion; N, nucleus. Scale bar: 2 μm. Image kindly provided by Andrea Weisberg.

2.3 Vaccinia Virus Morphogenesis

2.3.1 Overview

Morphogenesis is defined as the origin and development of structural characteristics (198). It is one of the fundamental biological processes in development of many life forms, and this includes viruses. Various families of viruses have unique shapes acquired by their intricate morphogenetic processes. Some viruses are non-enveloped, meaning they lack a phospholipid membrane bilayer and are shaped by capsid proteins that surround them. Poxviruses, however, are enveloped viruses, meaning their morphogenesis is largely dependent on phospholipid membranes. Although viral membrane morphogenesis is a part of the poxvirus replication cycle discussed in the previous section, morphogenesis of VACV crescents to MVs will be discussed separately in this section in greater depth, as this is an important topic for studies covered in subsequent chapters.

2.3.2 Crescent and immature virion morphogenesis

Crescents are the first detectable membrane structure of VACVs with free open ends in the cytoplasm (Figure 2.7). No apparent connection was observed between the crescents and the membranes of cellular organelles, leading to the notion that crescents were synthesized *de novo* (199). Other hypotheses proposed that cellular organelles are origins of viral membranes in the form of flattened cisternae, which have double-membranes (200, 201). However, questions arose as other studies showed images of single membrane structures and the controversy ended as the single

membrane was confirmed by subsequent electron tomography images (202, 203). More recently, a connection between the endoplasmic reticulum (ER) and the viral membranes was demonstrated through multiple VACV knockout mutants (Figure 2.9), which led to a break-through in understanding VACV membrane morphogenesis (178).

A group of VACV proteins conserved in chordopoxviruses, termed VMAPs (viral membrane assembly proteins), are essential in the early steps of morphogenesis (8). The up-to-date members of the VMAPs are A6 (204, 205), A11 (10, 206, 207), A30.5 (8) , H7 (208, 209), and L2 (11, 210, 211). All VMAPs are post-replicative proteins except for L2, which is expressed early. L2 and A30.5 interact with each other, and they both co-localize to the ER membrane with or without infection (8, 11). A6 and A11 have also been shown to interact, which proved to be important for the association of A11 with viral factories and membranes (207). The crystal structure of H7 was recently reported, revealing a novel phosphoinositide binding site necessary for viral replication (212).

Other morphogenesis proteins include A17, A14, and D13, which are major constituents of crescents and IVs. A17 and A14 are transmembrane proteins that interact with one another; each interrupt morphogenesis when individually repressed (213-216). A recent report on A17 (217) has suggested its resemblance to reticulons, a class of membrane proteins involved in morphogenesis of tubular ER (218). D13 is another essential protein for morphogenesis, forming a honeycomb lattice comprised of trimers around the viral membrane (Figure 2.10)(219, 220). Although D13 does

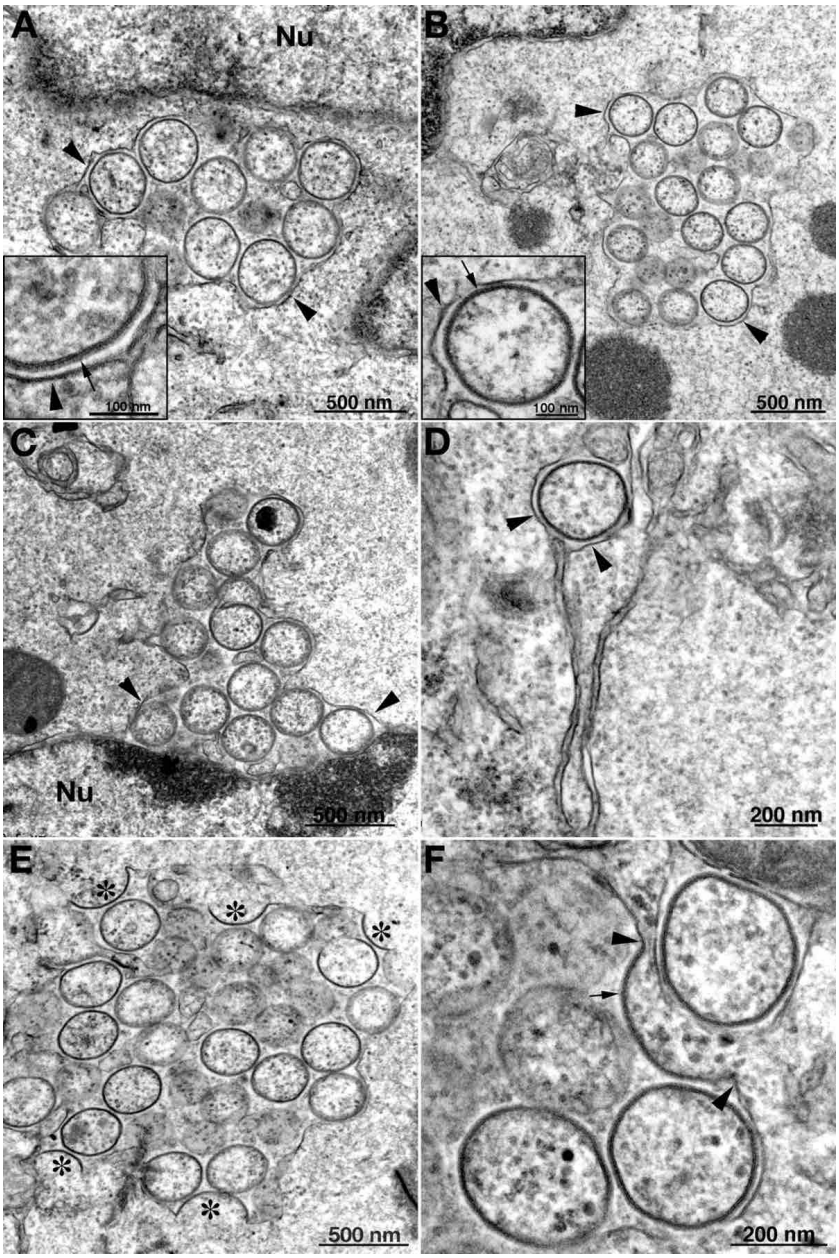

Figure 2.9 Vaccinia virus crescents and IV-like structures associated with ER

Electron micrograph showing HeLa (A) and RK-13 (B through F) cells infected with vΔA30.5. IV-like structures cluster within ER membranes, and crescents (asterisks) are continuous with the ER membrane. Arrowheads: ER membrane; arrows: spicules. Respective scale bars are at the bottom right. Figure reprinted from Maruri-Avidal et al. (8) with permission.

not have a transmembrane domain, it interacts with the N-terminus of A17 to associate with viral membranes (221, 222). Cryo-electron tomography and X-ray crystallography revealed the structure of the D13 trimers, which have double beta-barrel subunits arranged as pseudo-hexagonal trimers. (223-225). The coating by D13 scaffold protein presumably confers the curvature and spherical shaping of crescents and IV membranes.

Characterization of an L2-deletion mutant was the break-through study that first gave evidence of a direct connection of viral membranes with ER membranes (211). Analysis of the A30.5 protein and its deletion mutant have provided additional images of the connection (Figure 2.9)(8). The mutants lacked IVs and MVs but crescent structures were continuous with the ER and clusters of empty IV-like particles were observed within the ER lumen. The interior of IV-like particles did not contain dense core materials, which accumulated to form large masses of dense viroplasm. An A11-inducible mutant has also generated similar phenotypes (10), but detection of such structures has not yet been reported for either A6 or H7 mutants (178).

Based on these novel observations, a model for viral membrane formation using ER membranes was proposed as illustrated in Figure 2.11 (8, 178). This model postulates that VMAPs, presumably with cellular proteins, generate or stabilize ruptures of the ER membrane. The resulting membrane segment/crescent is stabilized by capping of L2, A30.5, and A11 on the free ends and fuses with additional segments, elongating around the core to yield spherical IVs. The IV membrane

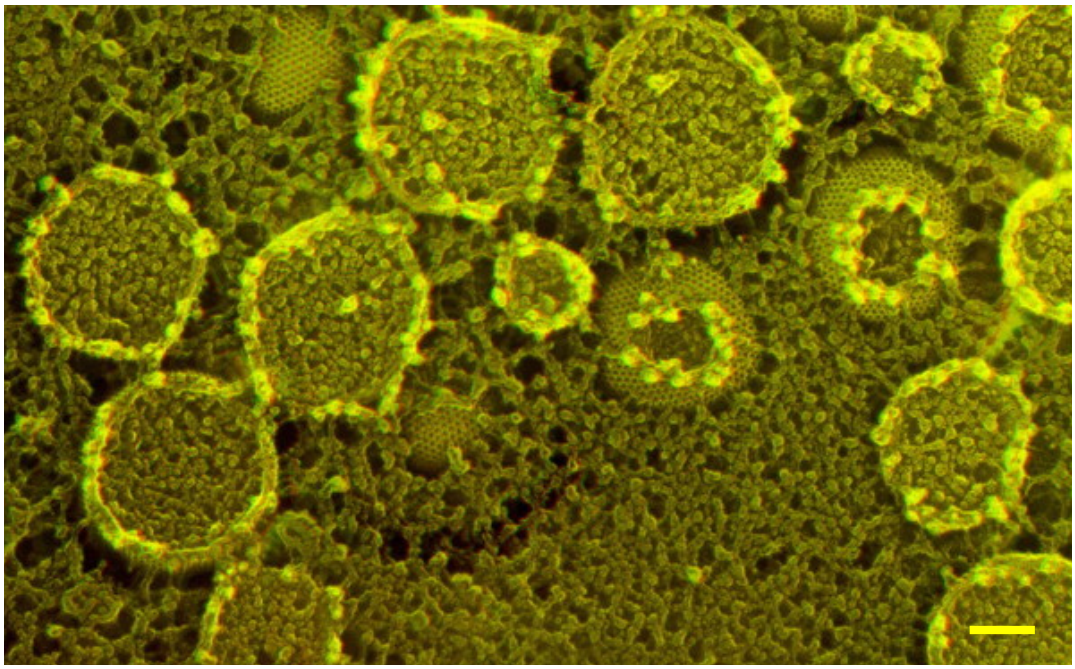

Figure 2.10 D13 honeycomb lattice of vaccinia virus IVs

3-D deep-etch electron microscope image of immunogold-labeled IVs. Antibody against a V5 epitope at the N-terminus of D13 was used. Gold particles around the sections of IV membranes are shown white (or bright yellow) as the contrast was reversed. Yellow scale bar in the bottom right measures 100 nm. Image adapted and modified from Szajner et al. (220) with reprint permission.

contains A14 and A17 with the latter acting as a clamp for D13 scaffold, giving curvature to the viral membrane. Figure 2.11 also depicts viral membrane formation in the absence of L2, A30.5, or A11, in which the crescent precursors containing A14 and A17 are continuous with the ER membrane. Incomplete ruptures may still allow D13 to enter the ER lumen and build a scaffold around the precursors, resulting in IV-like particles lacking cores. Failure to generate proper membrane fragments leads to mass accumulation of unattended core proteins (viroplasm) (178).

2.3.3 Mature virion morphogenesis

The morphologic transition from an IV to an MV is dictated by removal of the D13 scaffold from the IV membrane (219, 226, 227). As mentioned previously, scaffolding by D13 trimers hold IVs in a spherical form (Figure 2.7). When the D13 coat is removed during maturation, virions lose the spherical morphology and become brick- or barrel-shaped MVs (Figure 2.1 and 2.7). Disassociation of the D13 scaffold from the viral membrane is dependent on I7 protease activity (221). As discussed before, the I7 protease is responsible for processing multiple viral proteins including A17. The interaction between D13 and the N-terminus of A17 is lost following the proteolytic processing (221), with both N- and C-terminal ends of A17 cleaved by I7 (184, 228-230). Defects occurred in IV to MV morphogenesis when I7 expression was repressed, failing to disassemble the D13 scaffold from the particles (221). Likewise, A9 repression (231) or A6 mutation (204) resulted in a similar outcome. In addition to the change in outer membrane shape, the core transforms into a more compact, dumbbell- or hourglass-shaped core within the particle during the transition

from IV to MV (Figure 2.7). In chapter 4, a study on VACV protein I2 revealing its effect on MV morphogenesis will be discussed.

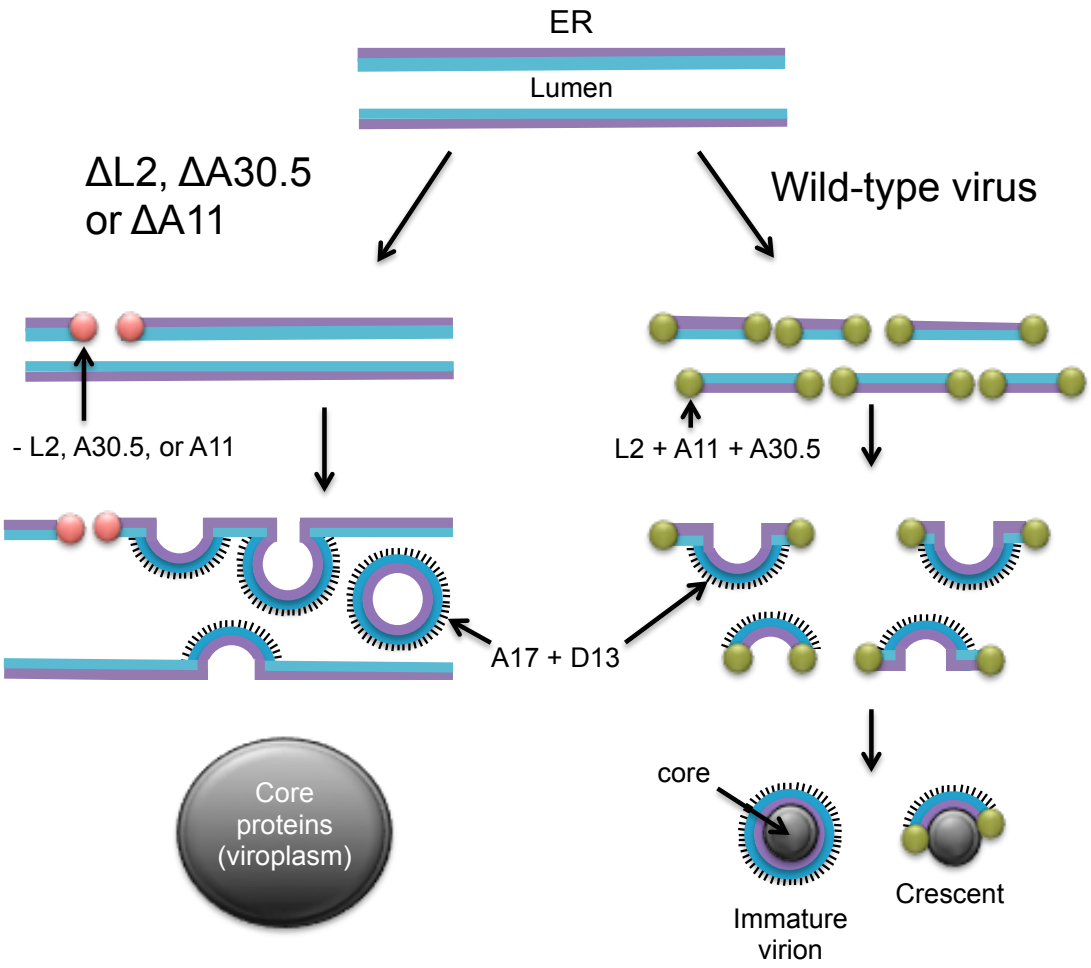

Figure 2.11 Model for vaccinia virus crescent and IV membrane formation

Diagram showing models for viral membrane formation during infection in the absence of VACV L2, A30.5, or A11 (left), compared to infection with wild-type VACV (right). Adapted and modified from Maruri et al. (8) and Moss, 2015 (178) with permissions.

Chapter 3: Investigating topology of ER-associated cellular and viral proteins with split-GFP[1]

3.1 Summary

The split GFP system was adapted for investigation of the topology of ER-associated proteins. A 215 amino acid fragment of GFP (S1-10) was expressed in the cytoplasm as an unfused protein or fused to the N-terminus of calnexin and in the ER as an intraluminal protein or fused to the C-terminus of calnexin. A 16 amino acid fragment of GFP (S11) was fused to the N- or C-terminus of the target protein. Fluorescence occurred when both GFP fragments were in the same intracellular compartment. After validation with the cellular proteins of known topology (PDI and tapasin), we investigated two vaccinia virus proteins (L2 and A30.5) of unknown topology that localize to the ER and are required for assembly of the viral membrane. Our results indicated that the N- and C-termini of L2 faced the cytoplasmic and luminal sides of the ER, respectively. In contrast both the N- and C-termini of A30.5 faced the cytoplasm. The system offers advantages for quickly determining the topology of intracellular proteins: the S11 tag is similar in length to commonly used epitope tags; multiple options are available for detecting fluorescence in live or fixed

[1] Adapted from reference 12. **Hyun SI, Maruri-Avidal L, Moss B.** 2015. Topology of Endoplasmic Reticulum-Associated Cellular and Viral Proteins Determined with Split-GFP. Traffic **16:**787-795.

cells; transfection protocols are adaptable to numerous expression systems and can enable high throughput applications.

3.2 Introduction

Membrane protein topology provides important information needed to understand protein function and intermolecular associations. Although great strides have been made in predicting topology, experimental confirmation is usually required (232). Assays based on glycosylation (233), protease susceptibility (234), fluorescence (235, 236) and luciferase activity (237, 238) have provided researchers with options to determine the topology of transmembrane proteins. Here we describe a rapid, broadly applicable approach that can be used to determine the cytoplasmic and luminal locations of the N- and C-termini of proteins that associate with the endoplasmic reticulum (ER).

The GFP from the jellyfish *Aequorea victoria* exhibits bright green fluorescence when exposed to light in the blue to ultraviolet range. Many modifications of GFP have been made including the division into separate fragments that fluoresce upon association with one another (239). One version of the split-GFP consists of self-assembling fragments of 215 amino acids comprising β-strands 1-10 (S1-10) and 16 amino acids comprising β-strand 11 (S11) (240). Recently, the system was used for in vivo localization of proteins in protozoan and plant plastids (241-243) and the *Escherichia coli* inner membrane (244). Kaddoum et al. (245) described a procedure for localizing proteins tagged with S11 by incubating fixed and permeabilized mammalian cells with purified S1-10 protein and visualizing

fluorescence. A tripartite version of split GFP was developed for detection of protein-protein interactions (246). Here we show that the S1-10 domain can be selectively targeted to cytoplasmic and ER compartments permitting rapid determination of the topology of proteins fused to S11 at the N- or C-terminus in live or fixed mammalian cells. This split-GFP method for determination of topology differs substantially from the procedure used by Wright and co-workers (236) in which a cytoplasmic full-length fluorescent protein interacts with an affinity-tagged cytosolic domain of an ER protein and from other approaches that use redox-sensitive (247) or glycosylatable (248) forms of GFP to differentiate cytoplasmic and ER luminal compartments.

3.3 Materials and Methods

3.3.1 Cells and viruses

RK-13 cells were grown in Dulbecco's minimum essential medium or in essential medium with Earle's balanced salts, containing 10% fetal bovine serum (FBS; Sigma-Aldrich), 100 units penicillin, and 100 μg streptomycin per ml (Quality Biological). The VACV Western Reserve (WR) strain was propagated as previously described (249).

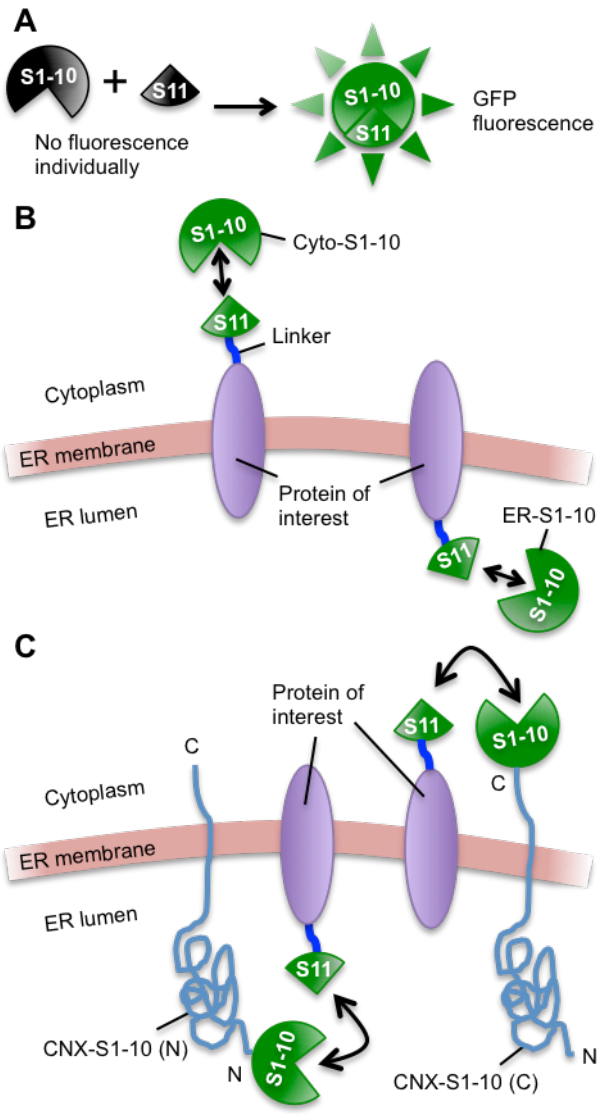

Figure 3.1 Schematic showing application of the split-GFP system for determination of the topology of ER membrane proteins

(A) The large S1-10 and small S11 fragments of GFP fluoresce upon association. (B) Fluorescence occurs if the S11 tag on the protein of interest is in the cytoplasm when co-expressed with Cyto-S1-10 or in the ER lumen when co-expressed with ER-S1-10. (C) Fluorescence occurs when the S11 tag on the protein of interest is in the cytoplasm when co-expressed with CNX-S1-10(C) or in the ER lumen when co-expressed with CNX-S1-10(N).

3.3.2 Antibodies

Anti-GFP rabbit polyclonal antibody (pAb) was obtained from Invitrogen (Cat. A11122). The mouse MAb to PDI was from Enzo Life Sciences (Cat. ADI-SPA-891). Anti-actin rabbit pAb was from Sigma (Cat. A2066).

3.3.3 Construction of plasmids

pCMV-mGFP 1-10 and pCMV-mGFP Cterm S11 were obtained from Sandia Biotech. The open reading frames (ORFs) of mGFP 1-10 (S1-10) and mGFP Cterm S11 (S11) were amplified from the plasmids by PCR, which were then used for cloning. Plasmid Cyto-S1-10 was constructed by fusing the VACV synthetic early/late promoter (250) to the S1-10 ORF. Expression of the other S1-10 fusion constructs was also regulated by the VACV synthetic early/late promoter. Plasmid ER-S1-10 was made by fusing the signal peptide sequence MGWSCIILFLVATATGAHS to the N-terminus of S1-10 and the ER retention signal peptide SEKDEL to the C-terminus. To construct calnexin-S1-10 fusion plasmids (CNX-S1-10), cellular RNA was extracted from RK-13 cells using TRIzol (Life Technologies). The extracted RNA was reverse transcribed and PCR amplified with SuperScript III One-Step RT-PCR System with Platinum Taq High Fidelity kit (Invitrogen). The template sequences for PDI-S11 and tapasin-S11 constructs were acquired using the same method except that HeLa cells were used for the tapasin sequence. The N-terminal tags of CNX-S1-10(N), PDI-S11(N) and tapasin-S11(N) were inserted 25, 18 and 20 amino acids after their start codons in order to follow the signal peptides.

Table 3.1 List of GFP S11 tagged constructs tested for membrane topology

Name of Construct	Promoter	GFP S11 Tag Location	Protein Origin
PDI-S11 (N)	VACV E/L[a]	N-terminus	Cellular
Tapasin-S11 (N)	VACV E/L, CMV[b]	N-terminus	Cellular
Tapasin-S11 (C)	VACV E/L, CMV	C-terminus	Cellular
L2-S11 (N)	Natural[c]	N-terminus	Viral
L2-S11 (C)	Natural	C-terminus	Viral
A30.5-S11 (N)	Natural	N-terminus	Viral
A30.5-S11 (C)	Natural	C-terminus	Viral

[a] Vaccinia virus synthetic early/late promoter

[b] Human cytomegalovirus (CMV) immediate-early promoter

[c] Natural promoter of each specific gene

S11 fused viral gene constructs (L2-S11(N), L2-S11(C), A30.5-S11(N), and A30.5-S11(C)) were made using genomic DNA of VACV WR strain as template for PCR amplification with primers containing S11 sequences. The natural promoter of each gene was added upstream of the ORF.

The CMV promoter driven constructs were made by inserting tapasin-S11(N), tapasin-S11(C), Cyto-S1-10, ER-S1-10 ORFs and CNX-S1-10(N) and CNX-S1-10(C) into pcDNA3.1D/V5-His-TOPO (Invitrogen) vector through directional cloning.

3.3.4 Confocal microscopy

RK-13 cells were grown on coverslips in 24-well plates. The cells were infected with 3 PFU/cell of VACV strain WR and transfected one hour later with split-GFP plasmids using Lipofectamine 2000 (Invitrogen) or with empty vector plasmids. The tranfection medium was replaced by fresh medium after 6 h. At 16 h post-transfection, the cells were washed with phosphate-buffered saline (PBS) and fixed with 4% paraformaldehyde for 15 min at room temperature (RT). A similar procedure was used for transfection of plasmids with CMV promoters except that the uninfected cells were fixed at 24 h. The fixed cells were permeabilized with 0.1% Triton X-100 for 15 min and then blocked with 10% FBS for at least 30 min at RT. Primary antibodies were added at a 1:200 dilution in PBS containing 10% FBS for overnight at 4°C. The cells were washed and treated with fluorescent dye-labeled secondary antibodies (Alexa Fluor, Molecular Probes) at 1:200 dilution for 1 h at RT. Finally, the cells were stained with 300 nM DAPI (4',6-diamidino-2-phenylindole, Molecular Probes). The coverslips were then mounted on a glass microscope slide

with ProLong Gold Antifade Reagent (Molecular Probes). Confocal images were taken using Leica TCS SP5 microscope and processed with Imaris X64 7.6.1 software including calculation of Pearson's colocalization coefficient. Fluorescence quantification was also done using Imaris X64 7.6.1 by calculating the signal from 2,000 to 17,000 cells contained within 50 microscope fields in each sample. The number of cells was kept consistent between the samples that were directly compared to one another. Background from infected cells transfected with empty vector plasmids was subtracted.

3.3.5 Western blotting

Proteins from infected/transfected cells were resolved by electrophoresis on 4 to 12% NuPAGE Bis-Tris gels followed by transfer to a nitrocellulose membrane using the iBlot system (Life Technologies). Membranes were blocked with 5% nonfat milk in PBS containing 0.05% Tween 20 (PBST) for 30 min. Blocked membranes were incubated with the primary antibody for 1 h at RT, and then were washed four times with PBST. Secondary antibody conjugated with IRDye 800CW (Li-Cor Biosciences) was incubated with the membrane (1:5000) for 1 h at RT, followed by four washes with PBST. The membranes were then developed using a Li-Cor Odyssey infrared imager (Li-Cor Biosciences).

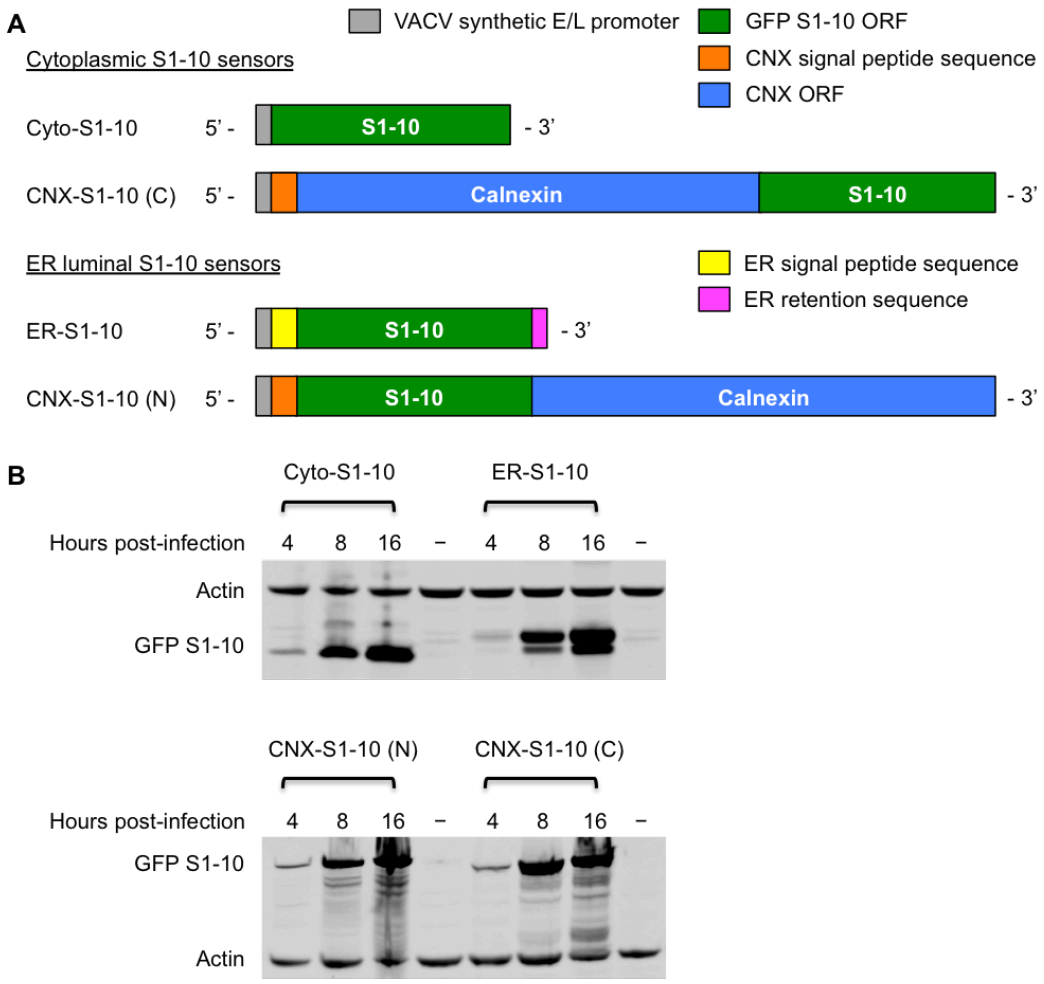

Figure 3.2 Structure and expression of GFP S1-10 proteins

(A) Diagrams of S1-10 without (Cyto-S1-10) or with signal peptide and ER retention sequence (ER-1-10) and S1-10 fused near the N-terminus of calnexin following the signal peptide (CNX-S1-10(N)) and S1-10 fused to the C-terminus of calnexin (CNX-S1-10(C)). In each case transcription was regulated by the VACV synthetic early/late promoter. (B) RK-13 cells were infected with VACV and transfected one hour later with the expression plasmids diagrammed in panel A. At 4, 8 and 16 h after infection, the cells were lysed and the proteins were resolved by SDS-polyacrylamide gel electrophoresis and detected by probing western blots with antibody to GFP and actin. ER-S1-10 presumably migrates as a doublet because of incomplete signal peptide cleavage.

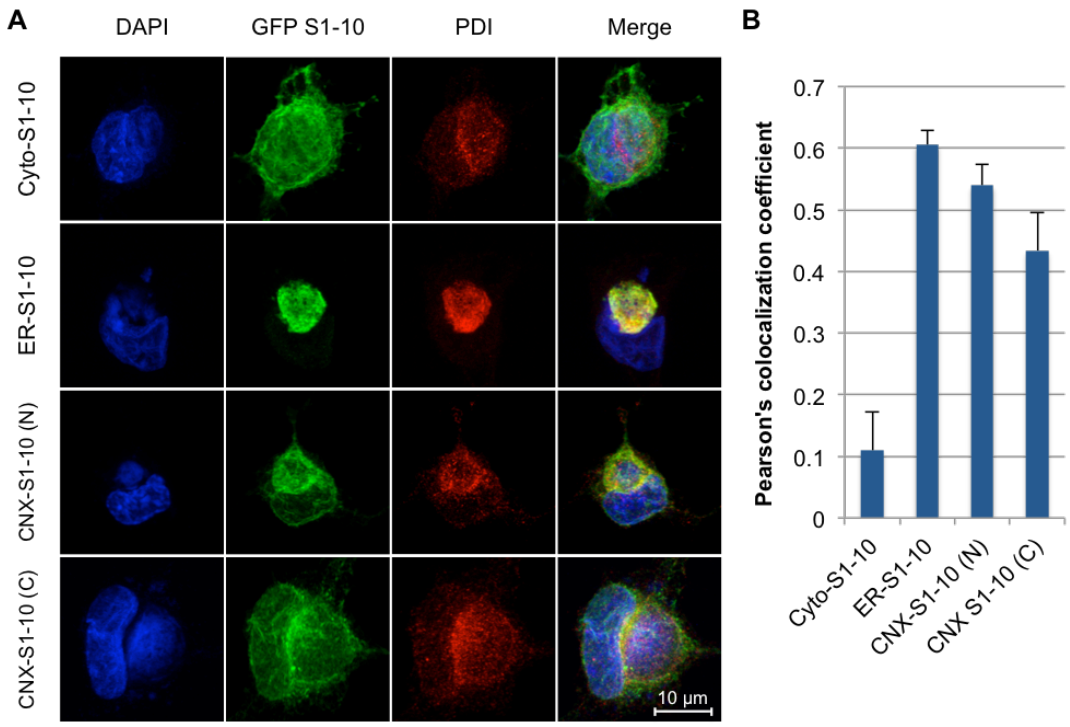

Figure 3.3 Intracellular localization of GFP S1-10 proteins

(A) Confocal microscopy of cells transfected with S1-10 expression constructs. Infections and transfections were carried out as in Figure 1B. At 16 h the cells were fixed and stained with anti-GFP rabbit PAb followed by secondary staining with Alexa Fluor 488 (green). The ER luminal protein PDI was stained with anti-PDI mouse MAb and Alexa Fluor 594 (red). DNA in nuclei and cytoplasmic virus factories were stained with DAPI (blue). Overlaps of S1-10 and PDI signals are shown as yellow in the merged images. (B) Pearson's colocalization coefficient values between S1-10 and PDI signals. A value closer to 1 indicates higher colocalization. Bars indicate standard error determined from analysis of 5 cells.

3.4 Results

3.4.1 Construction of sensors

The schematic in Figure 3.1A illustrates the occurrence of fluorescence when the S11 and S1-10 GFP fragments interact. Sensors to detect fusion proteins with S11 tags were constructed by expressing S1-10 as a soluble cytoplasmic protein (Cyto-S1-10) or an ER luminal protein (ER-S1-10) (Figure 3.1B) or by fusing S1-10 to the N- or C-termini of the transmembrane protein calnexin to produce CNX-S1-10(N) and CNX-S1-10(C), respectively (Figure 3.1C). The structural features of the four sensors are depicted in Figure 3.2A. Cyto-S1-10 is synthesized in the cytoplasm as a free protein, whereas ER-S1-10 is fused to an N-terminal signal peptide and a C-terminal ER retention sequence so that it resides within the ER lumen. The topology of calnexin dictates that the S1-10 fragment of GFP should be in the ER lumen when fused to the N-terminus and in the cytoplasm when fused to the C-terminus.

Transfection experiments indicated that the split-GFP system could be used in mammalian cells with CMV promoters or in conjunction with a VACV expression system (251). Using the latter system, the proteins were detected by Western blotting within 4 h and increased over a 16 h period (Figure 3.2B). The Cyto-S1-10 and ER-S1-10 proteins localized to cytoplasmic and ER compartments as shown by confocal microscopy (Figure 3.3A, B). Both the CNX-S1-10(N) and the CNX-S1-10(C) were associated with the ER (Figure 3.3A, B). Thus, GFP S1-10 did not perturb the localization of the sensor proteins.

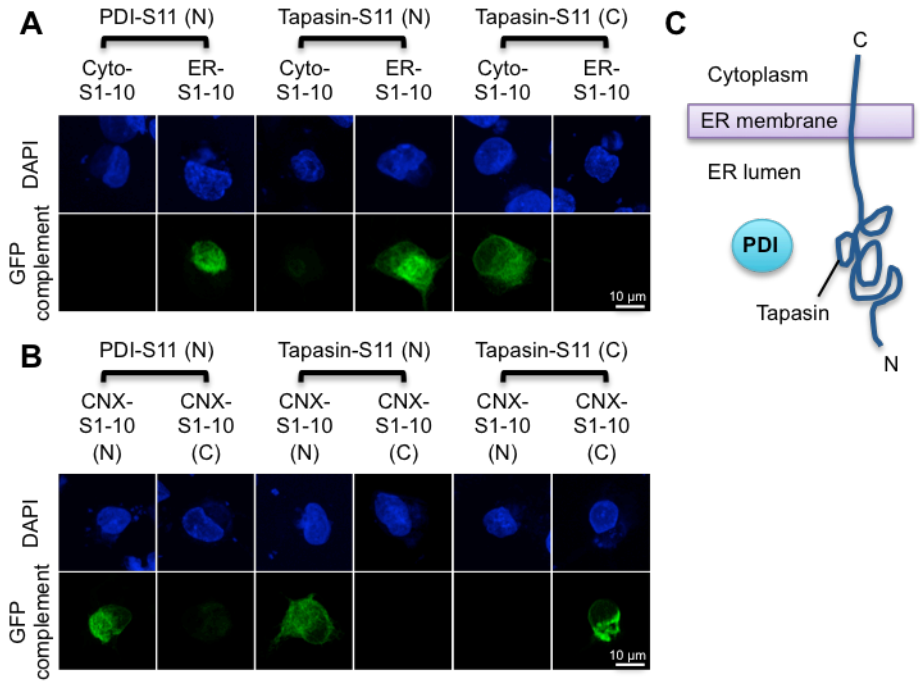

Figure 3.4 Validation of split-GFP method with cellular proteins of known ER membrane topology

(A) RK-13 cells were infected with VACV and one hour later were co-transfected with plasmids expressing PDI-S11(N) or tapasin–S11(N) or tapasin-S11(C) together with either Cyto-S1-10 or ER-S1-10. At 16 h after transfection, the cells were fixed and stained with DAPI to visualize DNA in nuclei and cytoplasmic virus factories. Fluorescence was analyzed by confocal microscopy. Blue, DAPI; green, GFP. (B) Same as panel A except that CNX-S1-10(N) or CNX-S1-10(C) was used instead of Cyto-S1-10 or ER-S1-10. (C) Diagram showing topology of PDI and tapasin.

3.4.2 Validation of the system with cellular proteins of known topology

To further validate the system, we fused S11 to the N-terminus of the luminal protein disulfide isomerase (PDI) (252), and to the N- and C-termini of tapasin, a type I membrane protein with N-terminal ER luminal and C-terminal cytoplasmic domains (253) (Table 1). Since previous studies had shown that tapasin was functional even after fusion of full-length GFP to the N- or C-termini (253, 254), we anticipated no difficulties with the short S11 fragment. DNA encoding a PDI or tapasin S11 fusion protein was co-transfected with either Cyto-S1-10 or ER-S1-10. A fluorescence signal was obtained when PDI-S11(N) was transfected with ER-S1-10 but not with Cyto-S1-10 (Figure 3.4A). A signal was obtained when tapasin-S11(N) was expressed with ER-S1-10 and when tapasin-S11(C) was expressed with Cyto-S1-10 but not the converse (Figure 3.4A). Quantification of the fluorescence is shown in Figure 3.5.

Corresponding results were obtained using CNX S1-10 constructs as sensors (Figure 3.4B; Figure 3.5). PDI-S11(N) was detected with CNX-S1-10(N) but not CNX-S1-10(C), whereas tapasin-S11(N) and tapasin-S11(C) were detected with CNX-S1-10(N) and CNX-S1-10(C), respectively. Thus, the topology of PDI and tapasin deduced by the split GFP method was consistent with the known topology of these proteins (Figure 3.4C).

The above data were obtained using the VACV expression system. The same results were obtained when tapasin-S11 and sensor constructs were expressed using CMV promoters in uninfected cells (Figure 3.6), although the expression levels at 24 h were not as high.

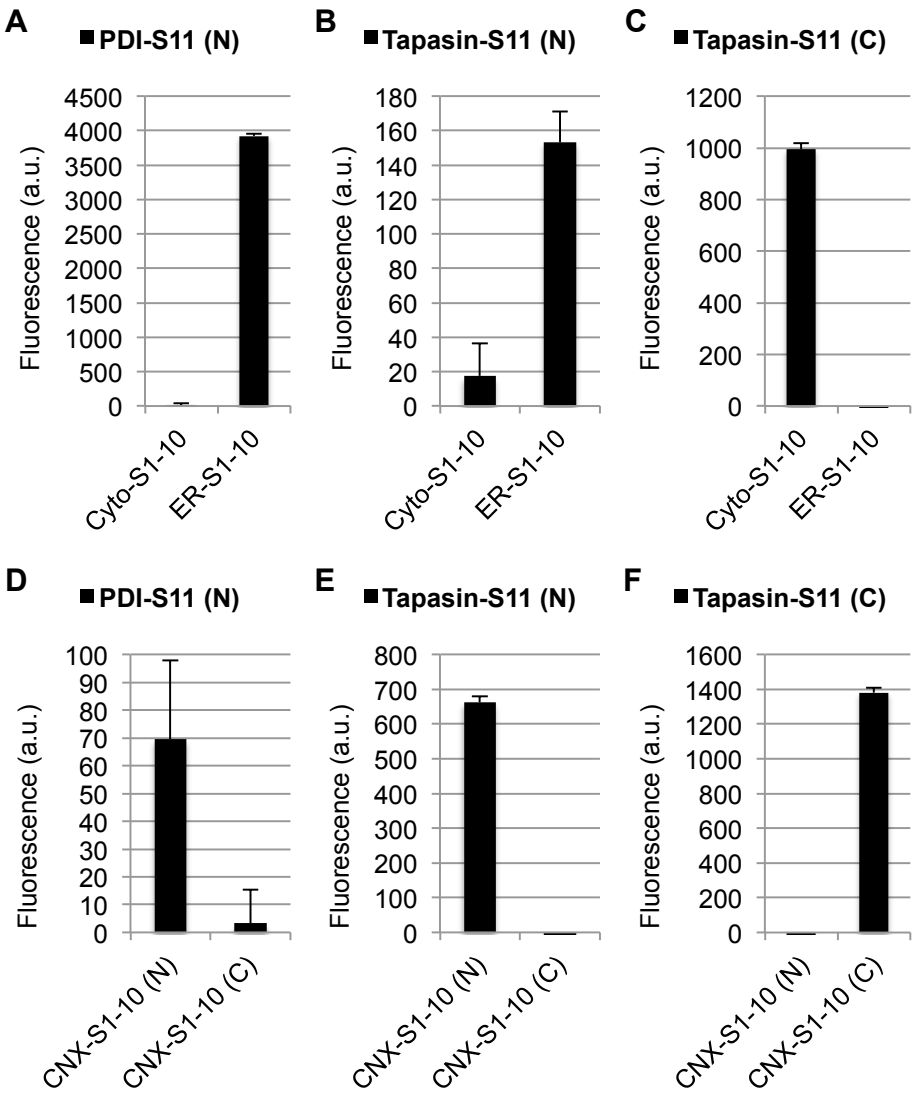

Figure 3.5 Quantification of GFP signal of cellular proteins.

(A-F) Quantification of GFP signal from each combination of S1-10 and S11 construct expressed in arbitrary units (a.u.). The fluorescence was quantified from 6,000 to 10,000 cells for each combination. The bars indicate the standard deviation of the mean determined from analysis of 50 microscopic fields.

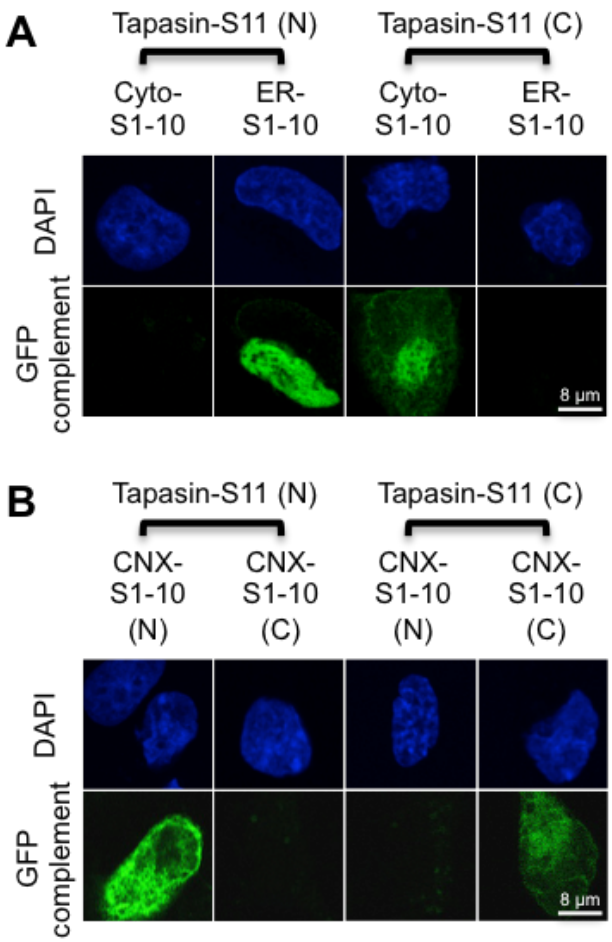

Figure 3.6 Determination of tapasin topology with split-GFP using the CMV promoter system.

(A) RK-13 cells were co-transfected with plasmids expressing tapasin-S11(N) or tapasin-S11(C) together with either Cyto-S1-10 or ER-S1-10, all expressed by the CMV promoter. At 24 h after transfection, the cells were fixed and stained as described in Figure 4A. (B) The procedures used were the same as in panel A except that the sensors were CNX-S1-10(N) and CNX-S1-10(C). Blue, DAPI; green, GFP.

3.4.3 Application of the system to investigate viral proteins of unknown topology

Having validated their use with cellular proteins of known topology, the split-GFP method was applied to VACV proteins of undetermined topology. The small L2 and A30.5 proteins, previously shown to associate independently with the ER and with each other, are crucial for formation of viral membrane structures (8, 11). L2 was predicted to have two transmembrane domains near the C-terminus and a hydrophilic N-terminus in the cytoplasm (210). For the present study, L2 was tagged with S11 at the N- or C-terminus (Table 1) and co-transfected with S1-10 sensors to determine topology. Complementation of L2-S11(N) occurred with Cyto-S1-10 but not with ER-S1-10 (Figure 3.7A; Figure 3.8A). In contrast, complementation of L2-S11(C) occurred with ER-S1-10 but not with Cyto-S1-10 (Figure 3.7A; Figure 3.8B). Corresponding results were obtained with the CNX-S1-10(N) and CNX-S1-10(C) (Figure 3.7B; Figure 3.8C, D) indicating that the N-terminus of L2 is in the cytoplasm and the C-terminus is in the ER lumen (Figure 3.7C).

The A30.5 protein was predicted to have a central transmembrane domain of only 18 amino acids (8). Both A30.5-S11(N) and A30.5-S11(C) (Table 1) were complemented by Cyto-S1-10 but not by ER-S1-10 (Figure 3.7D; Figure 3.8E, F). Consistent results were obtained with CNX-S1-10(N) and CNX-S1-10(C) (Figure 3.7E; Figure 3.8G, H) indicating that the N- and C-termini of A30.5 are both cytoplasmic. Since the hydrophobic domain is too short to pass through the ER twice, it must be embedded in the ER membrane (Figure 3.7F).

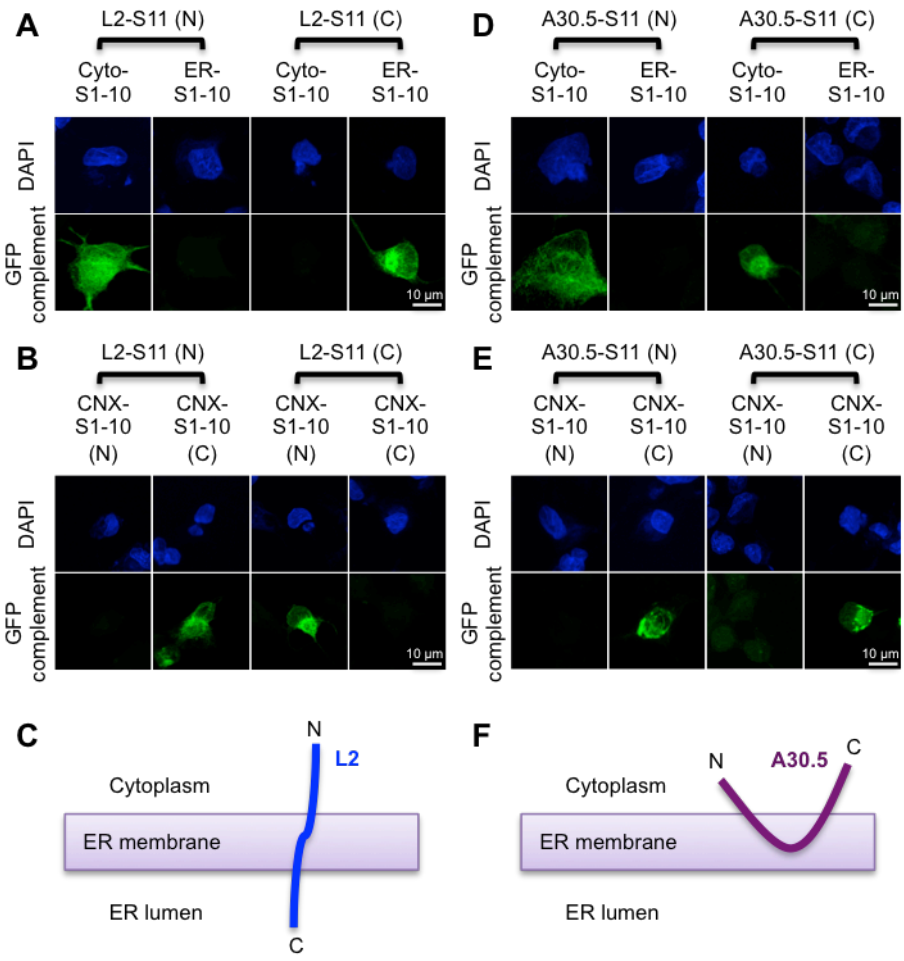

Figure 3.7 Determination of the ER membrane topology of viral proteins L2 and A30.5. (A) The experiment was carried out as described in Figure 4A a except that plasmids expressing L2-S11(N) and L2-S11(C) were co-transfected with plasmids expressing Cyto-S1-10 or ER-S1-10. (B) Same as panel A except that plasmids expressing CNX-S1-10(N) or CNX-S1-10(C) were used as sensors. (C) Diagram showing ER membrane topology of L2 deduced from GFP complementation. (D) Same as panel A except that A30.5-S11(N) and A30.5-S11(C) replaced the L2 constructs. (E) Same as panel D except that CNX-S1-10(N) and CNX-S1-10(C) were used as sensors. (F) Diagram of ER membrane topology of A30.5 deduced by split GFP complementation.

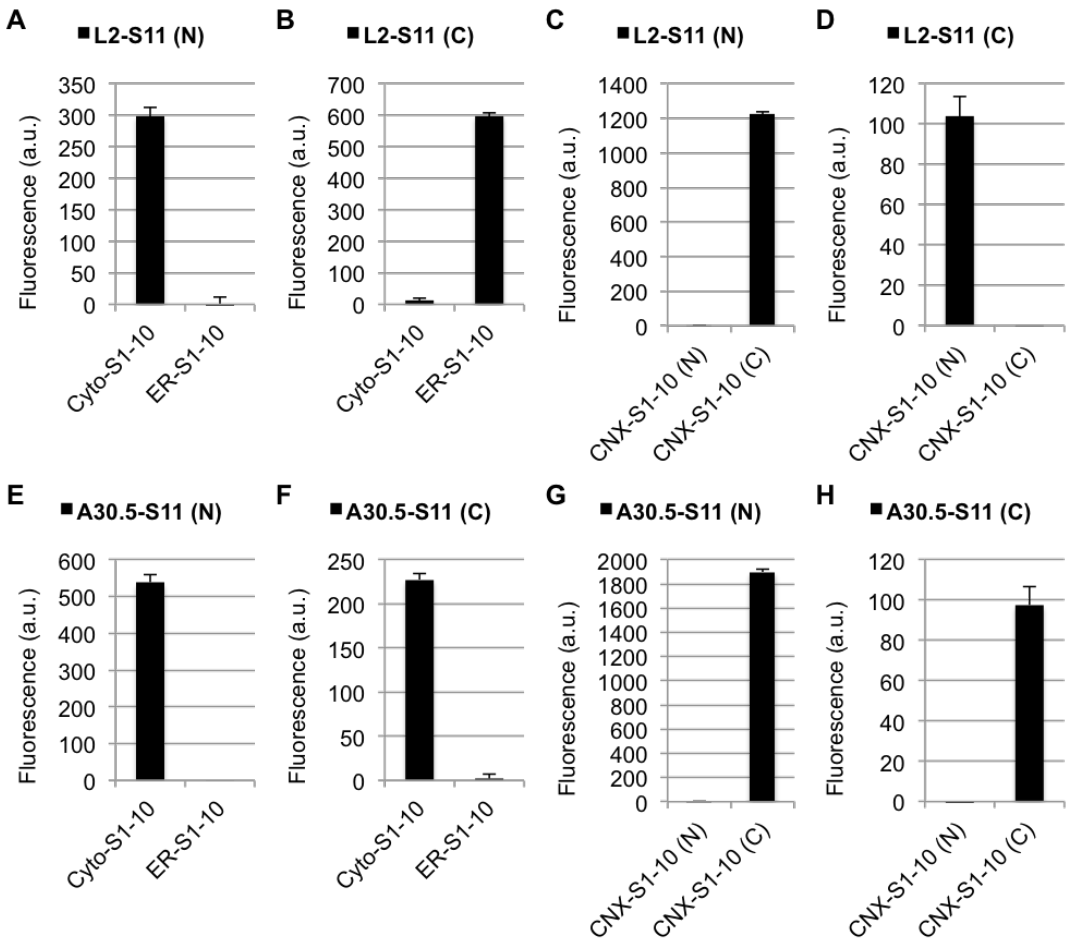

Figure 3.8 Quantification of GFP signal of viral proteins.

(A-H) Fluorescence quantified in arbitrary units (a.u.) from each set of transfections. The fluorescence was quantified from 2,000 to 17,000 cells for each combination. The bars indicate the standard deviation of the mean determined from analysis of 50 microscopic fields.

3.5 Discussion

The asymmetric self-assembling split GFP system offers advantages for quickly determining the topology of intracellular proteins: the S11 tag is similar in length to commonly used epitope tags and therefore should minimally perturb target proteins; multiple options are available for detecting fluorescence in live or fixed cells; transfection protocols are adaptable to numerous expression systems and can enable high throughput applications. Here I described application of the split GFP system for investigating the topology of ER proteins. Variations of the system employing the soluble cytoplasmic sensor together with additional sensors can likely be used to probe the topology of proteins associated with other cellular organelles such as the Golgi network, plasma membrane, endosomes and mitochondria.

Chapter 4: Vaccinia virus protein I2 is required for a critical stage in virus morphogenesis[2]

4.1 Summary

The I2L open reading frame of VACV is predicted to encode a conserved 72-amino acid protein with a C-terminal trans-membrane domain. Previous studies with a tetracycline-inducible mutant demonstrated that I2-deficient virions are blocked at the entry step of infection. The present study was motivated by a desire to understand the step in entry that is enabled by the I2 protein. Our starting point was generation of a cell line that constitutively expressed I2 and allowed the construction of the VACV I2L deletion mutant vΔI2. As anticipated, vΔI2 was unable to replicate in cells that did not express I2. Surprisingly, however, morphogenesis was interrupted after the stage of immature virion formation; dense spherical particles accumulated instead of brick-shaped mature virions with well-defined core structures. The abnormal particles retained the D13 scaffold protein of immature virions, were severely deficient in the transmembrane proteins that comprise the entry fusion complex (EFC), and had increased amounts of unprocessed membrane and core proteins. A diminished level of EFC proteins was also found when the cytoplasmic fraction of cells infected with vΔI2, which was attributed to instability due to the hydrophobicity of the EFC

[2] Some of the data from this chapter are included in a manuscript in preparation for submission (S.I. Hyun, A. Weisberg, and B. Moss, unpublished).

proteins and their failure to be inserted into viral membranes. A similar instability of EFC proteins had previously been found with unrelated mutants that also failed to form mature virions and accumulated viral membranes retaining the D13 scaffold. We concluded that I2 is required for virion morphogenesis although an additional role in chaperoning EFC proteins was not excluded.

4.2 Introduction

Poxviruses are large, double-stranded DNA viruses that replicate entirely in the cytoplasm of infected cells (1). Morphogenesis begins with the formation of crescent membranes that enlarge to form spherical IVs, which are then transformed into brick-shaped MVs (255). Studies with VACV, the prototype member of the poxvirus family, indicate that the 60 - 80 viral proteins are associated with the core and membrane fractions of MVs (256-259). These proteins enable virus attachment to the cell, fusion of viral and cellular membranes, and early gene expression. The EFC comprises 11 small trans-membrane (TM) proteins of the MV that are each required for the membrane fusion step of virus entry (55, 65). Recently, an additional protein encoded by the I2L ORF of VACV, with homologs in all chordopoxviruses, was reported to be essential for virus entry, raising the possibility that it represents an additional component of the EFC (260). The I2 protein is predicted to have 72 amino acids with a calculated mass of 8.4 kDa and a C-terminal TM domain. The protein is synthesized following viral DNA replication and is associated with purified MVs (260). Using a recombinant VACV with a tetracycline-inducible I2L ORF, Nichols and co-workers (260) showed that repression of I2L results in a profound reduction in

virus infectivity due to an inability of the virus to enter cells. Under these conditions, they noted a reduction in several EFC components in the viral membrane but considered this unlikely to account for the large decrease in the specific infectivity of I2-deficient virions, although this possibility was not entirely discounted.

The purpose of the present study was to further analyze the role of the I2 protein in VACV replication. Our starting point was to produce an I2L deletion mutant with the aid of a complementing cell line. We found that the null mutant has a primary block in virion assembly, which was not recognized in previous studies with an inducible mutant, and that the decrease in the level of EFC proteins is likely due to their instability caused by an inability to associate with viral membranes.

4.3 Materials and Methods

4.3.1 Cells and viruses

RK-13, RK-HA-I2, 293T, and BS-C-1 cells were grown in Dulbecco's minimum essential medium (DMEM) or in minimum essential medium with Earle's balanced salt (EMEM) containing 10% fetal bovine serum (Sigma-Aldrich, St. Louis, MO), 2 mM $_{L}$-glutamine, 100 units of penicillin and 100 μg of streptomycin per ml (Quality Biologicals, Gaithersburg, MD). For RK-HA-I2 cells, 2 μg/ml of puromycin was included as a selection antibiotic. The VACV Western Reserve (vWR) strain was propagated as previously described (261). The VACV I2L deletion mutant vΔI2 was propagated in RK-HA-I2 cells.

4.3.2 Construction of RK-HA-I2 cell line

RK-HA-I2 cells were created using lentiviral transduction (Figure 4.1A). Eukaryotic codon-optimized I2L ORF with N-terminal HA tag (HA-I2) was cloned into pENTR-D-TOPO (Invitrogen, Carlsbad, CA) to generate pENTR-HA-I2. LR Clonase II (Invitrogen) was used to transfer HA-I2 from pENTR-HA-I2 into pLX302, yielding pLX302-HA-I2. Lentivirus particles were produced by co-transfecting pLX302-HA-I2 (transfer vector), psPAX2 (packaging vector), and pMD2.G (VSV-G envelope vector) into 293T cells using Lipofectamine 2000 (Invitrogen). psPAX2 (Addgene plasmid # 12260) and pMD2.G (Addgene plasmid # 12259) were gifts from Didier Trono, and pLX302 (Addgene plasmid # 25896) was a gift from David Root (262). RK-13 cells were infected with the harvested lentiviruses, passaged several times under selection of 2 μg/ml puromycin selection. Puromycin resistant cells were harvested and diluted down to single cell per well in 96-well plates for clonal selection. Clones were tested for HA-I2 expression by western blotting using anti-HA monoclonal antibody (data not shown), and the best expressing clone was chosen as RK-HA-I2 cells.

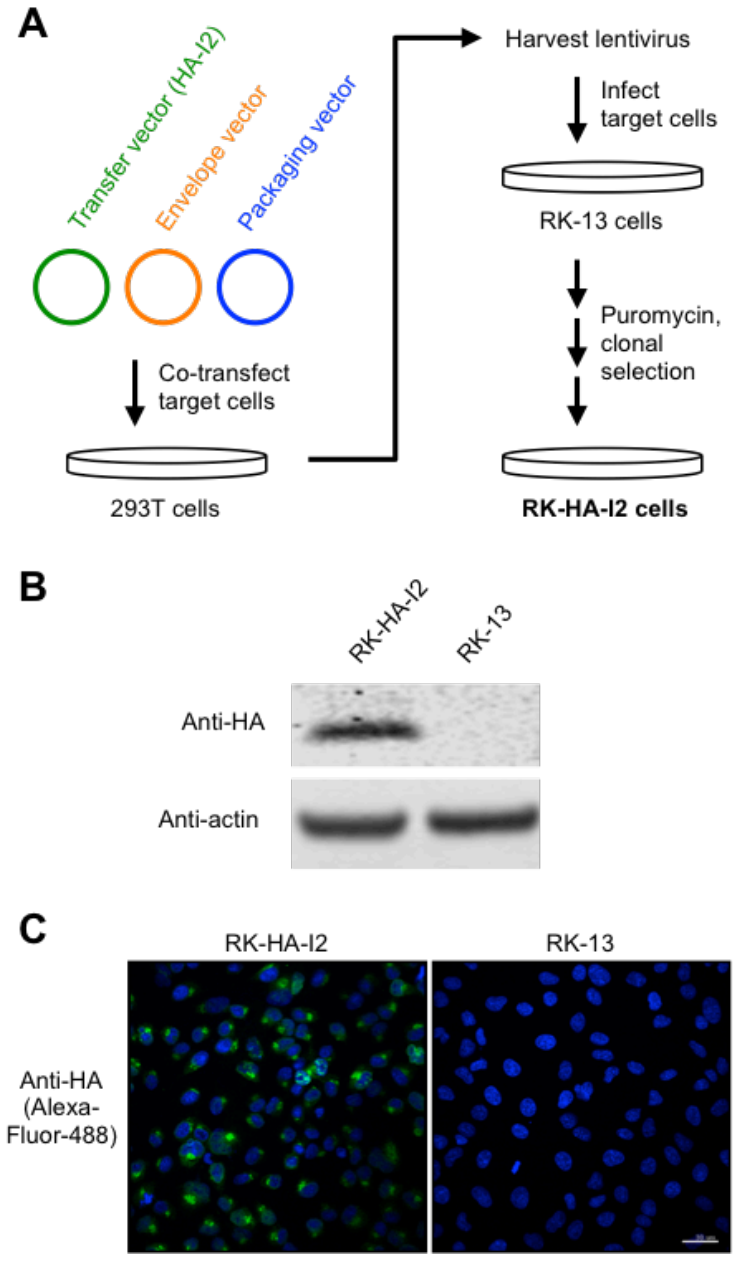

Figure 4.1 Construction and selection of RK-HA-I2 cell line

(A) Diagram of lentiviral transduction method used for making RK-HA-I2 cell line. Western blot analysis (B) and immunofluorescence labeling (C) were used to confirm the expression of HA-I2 in the selected RK-HA-I2 cell line alongside its parent RK-13 cell line as control.

4.3.3 Homologous recombination of vΔI2

DNA containing the VACV P11 promoter regulated GFP ORF was inserted between I2L ORF flanking sequences of approximately 500 bp on each side (Figure 4.2A), using In-Fusion HD Cloning Kit (Clontech, Mountain View, CA). RK-13 cells were infected with 1 PFU/cell of vWR, and transfected with the assembled DNA at 1 hour post-infection (hpi) using Lipofectamine 2000 (Invitrogen). At 24 hpi, the infected/transfected cells were collected and lysed with rapid freeze-thawing cycles and sonication. 10-fold serial dilutions of the lysate were incubated with RK-HA-I2 cell monolayers, and plaques with green fluorescence were picked. Plaque purification was repeated five times. Downstream forward primer 5'-CCGCGGCTAGTCCTATGTTGTATCAACTTC-3' and upstream reverse primer 5'-ATGATATGTATGTCCATTAAAGTTAAATTGTGTAGCGCTTCT-3' were used for PCR and sequencing to verify the deletion of the I2L ORF.

4.3.4 Construction of vGFP-I2

DNA containing the I2L ORF with N-terminal full-length GFP fusion (GFP-I2) was assembled with ~500 bp of I2L ORF flanking sequences (Figure 4.10A) into a plasmid using In-Fusion HD Cloning Kit (Clontech). Natural promoter of I2 was kept in place to regulate GFP-I2. RK-13 cells were infected with vWR and transfected with the assembled DNA for homologous recombination as described above. vGFP-I2 plaques were picked and purified as previously described, and were sequenced to verify replacement of I2L ORF with GFP-I2 ORF.

4.3.5 I2 compensatory mutant generation

RK-13 cells were infected with 0.1 PFU/cell of vΔI2 in multiple wells of 6-well plates. After 48 to 72 h, one tenth of the infected cell lysate was passed to new sets of cells. This procedure was repeated for 5 to 10 passages until several wells started showing signs of viral spread. The wells containing I2 compensatory mutants were serially diluted in ten-fold increments and plaques were picked. Selected compensatory mutants were analyzed by plaque assay and one-step growth curve. The absence of I2L ORF in the compensatory mutants was verified by PCR and whole genome sequencing. *Hind*III restriction enzyme analysis on the genome of the compensatory mutants was done as described in a previous report (50).

4.3.6 Antibodies

The mouse MAb against human influenza virus hemagglutinin (HA) was from Covance (Cat. MMS-101P, Princeton, NJ). Mouse anti-glyceraldehyde-3-phosphate dehydrogenase (GAPDH) MAb was from Santa Cruz Biotechnology (Cat. sc-32233, Dallas, TX), and rabbit anti-actin polyclonal antibody (PAb) was from Sigma-Aldrich (Cat. A2066). PAbs used for VACV protein detection were rabbit antisera to A3 (unpublished data), A10 (unpublished data), A11 (206), A17-N (230), A21 (66), A27 (60), A28 (263), D13 (226), F9 (68), F10 (264), G3 (78), G7 (265), H2 (74), H3 (266), I7 (267), L1 (268), L5 (67), and to WR strain (269). Mouse MAbs used against VACV proteins were to A14 (270) and D8 (271). PAb against GFP was from Invitrogen (A11122). Goat PAbs against protein disulfide isomerase (PDI)(sc-17222)

and calnexin (sc-6465) were from Santa Cruz Biotechnology, and Alexa Fluor secondary antibodies were from Molecular Probes (Eugene, OR).

4.3.7 Purification of viral particles

Virions of vWR and vΔI2 were first sedimented through a 36% sucrose cushion as previously described (261), then banded on a cesium chloride (CsCl) gradient (258, 272, 273). The gradient was formed by prelayering 1.3 g/ml (bottom, 3.5 ml), 1.25 g/ml (middle, 4 ml), 1.2 g/ml (top, 3.5 ml) CsCl solutions and allowing it to diffuse overnight at 4°C on a stable surface. CsCL solutions were made in 10 mM Tris-HCl calculations from (274). Sedimented virus material from the sucrose cushion was layered over the CsCl gradient and centrifuged for 4 h at 180,000 x *g* in a TH-641 rotor. Banded virions were extracted from the gradient and diluted 3-fold with 1 mM Tris-Cl. Virions were then repellected and collected by additional centrifugation.

4.3.8 Plaque assay and virus yield determination

BS-C-1, RK-13, or RK-HA-I2 cell monolayers were used for plaque assays in 6-well plates. Virus samples were serially diluted in 10-fold increments and incubated with the monolayers at 37°C. After 1 h, the medium was aspirated and replaced by medium containing 0.5% methylcellulose. At 48 hpi, the cells were stained with crystal violet at room temperature (RT) for 10 min, dried overnight, and used for

plaque counting. Counted plaques from each well were used to calculate virus yields based on their respective dilution factors.

4.3.9 Droplet digital PCR

RK-13 cells were infected with 10 PFU/cell of either vWR or vΔI2. At 10 hpi, mRNA was extracted from infected cells using Trizol LS (Invitrogen). Extracted mRNA was reverse transcribed to cDNA with SuperScript VILO MasterMix (Invitrogen). The cDNA was serially diluted and used as a template for droplet digital PCR (Bio-Rad, Hercules, CA). Following the manufacturer's protocol, the digital PCR was carried out for multiple viral transcripts with primers internally binding each ORF. The primers were designed using PrimerQuest Tool from Integrated DNA Technologies (Coralville, IA)(Table 4.1). After 40 cycles of reaction, the droplets were digitally analyzed with the droplet reader (Bio-Rad) and absolute mRNA copy numbers were obtained.

4.3.10 Radioactive pulse-labeling and chase

RK-13 cells were infected with 5 PFU/cell of vWR or vΔI2 at 37°C. After 5.5 h, the infected cells were incubated with medium lacking methionine and cysteine for 30 min at 37°C. 2.5% dialyzed FBS was used in methionine/cysteine-free medium. At 6 hpi, the cells were pulse-labeled at 37°C for 5 min with 100 μCi of [^{35}S]-methionine/cysteine (Perkin-Elmer, Waltham, MA). Following the pulse, medium was immediately switched to regular methionine/cysteine-containing medium for

chase. At various chase time points, the cells were washed with cold phosphate-buffered saline (PBS) and lysed with 1% NP-40 containing complete protease inhibitor cocktail (Roche Applied Science, Indianapolis, IN). The lysates were clarified by centrifugation and proteins were immunoprecipitated using Protein G Dynabeads (Life Technologies, Carlsbad, CA). The radiolabeled proteins were resolved in a 4 to 12% polyacrylamide gel, which subsequently was fixed in 40% methanol/10% acetic acid, soaked in 10% glycerol, dried, and exposed to a phosphor screen. Typhoon Variable Mode Imager (GE Healthcare, Chicago, IL) was used to detect radioactive bands from the phosphor screen.

4.3.11 Confocal microscopy

RK-13 cells were grown on coverslips in 24-well plates, and were infected with 3 PFU/cell of vGFP-I2. At 8 hpi, the cells were washed with PBS and fixed with 4% paraformaldehyde for 15 min at room temperature (RT). The fixed cells were permeabilized with 0.1% Triton X-100 for 15 min and then blocked with 10% FBS for at least 30 min at RT. Primary antibodies were added at a 1:200 dilution in PBS containing 10% FBS for overnight at 4°C. The cells were washed and treated with fluorescent dye-labeled secondary antibodies (Alexa Fluor, Molecular Probes) at 1:200 dilution for 1 h at RT. Subsequently, the cells were stained with 300 nM DAPI (4’,6-diamidino-2-phenylindole, Molecular Probes). The coverslips were then mounted on a glass microscope slide with ProLong Gold Antifade Reagent (Molecular Probes). Confocal images were taken using Leica TCS SP5 microscope and processed with Imaris X64 7.6.1 software.

Table 4.1 List of primers used for droplet digital PCR

Viral gene	Sequence (5' - 3')
L1 F	AACCATGGATGTAACCTCACTG
L1 R	TTCTGTAGCGGCTGATAACAC
L5 F	AATACCCGATCCTATTGATAGATTACG
L5 R	CGCAGATGTTTGAGTTGTCATC
A28 F	ATGTAAAGCAAAAGTGGAGATGTG
A28 R	TGTTGCATCGTGTTAAATTTTCTAATG
G3 F	ACTTCAGGCAGCTGTAATGGA
G3 R	CGACGGTTGATGCATCGGTA
H2 F	CAAGCTATTAGGCGAGGTACTG
H2 R	TGTTGAGCAGATGGATCGAC
A3 F	GGCTAGACCTATAAACGGCATC
A3 R	TTGATAGAAATCGGACTGTCGG
D8 F	GTATAAATTGAACGACGACACGC
D8 R	TCTCAAATCGGACAACCATCTC
D13 F	TCTATCCGGAGTTATGACAAACG
D13 R	GAATCTTCCCATACCTTTAACTTCTG
I2 F	GCCGCTATATTTGGTGTATTTATGG
I2 R	AACCAATACCAACCCCAACA
F10 F	GTGGGCCATGGGATTAAACTA
F10 R	CAATGAGAGTTCCTGACCATCC

Abbreviations: F, forward; R, reverse

4.3.12 Transmission electron microscopy

Infected RK-13 or RK-HA-I2 cells in 60-mm plates were fixed with 2% glutaraldehyde in 0.1 M sodium cacodylate buffer, postfixed in 1% reduced osmium tetroxide, dehydrated in a series of ethanol incubations with final dehydrations in propylene oxide, and embedded in EmBed-812 resin (Electron Microscopy Sciences, Hatfield, PA)(210). Procedures for cryosectioning and immunogold labeling were described previously (275). Cryosections were picked up on grids, thawed, washed free of sucrose, and stained with rabbit polyclonal D13 antibody, and then protein-A-conjugated to 10-nm gold spheres (University Medical Center, Utrecht, Netherlands). Specimens were viewed with an FEI Tecnai Spirit transmission electron microscope (FEI, Hillsboro, OR).

4.3.13 Western blotting and signal quantification

Proteins from cells or purified virions were prepared with NuPAGE (Life Technologies) lithium dodecyl sulfate buffer and reducing agent, resolved by electrophoresis on 4 to 12% NuPAGE Bis-Tris gels, and transferred to nitrocellulose membranes using the iBlot system (Life Technologies). Membranes were blocked with 5% nonfat milk in Tris-buffered saline (TBS) containing 0.05% Tween 20 (TBST) or with Odyssey Blocking Buffer (Li-Cor Biosciences, Lincoln, NE) for 30 min to 1 h. Blocked membranes were incubated with the primary antibody for 1 h at RT or for overnight at 4°C, and washed four times with TBST. Secondary antibody conjugated with IRDye 800CW or 680RD (Li-Cor Biosciences) was incubated with the membrane (1:10000) for 1 h at RT, followed by four washes with TBST. The

membranes were scanned using Li-Cor Odyssey infrared imager, and band signal intensities were acquired with Image Studio software (Li-Cor Biosciences).

4.3.14 Whole genome sequencing

Approximately 2 x 10^7 infected RK-13 cells were Dounce homogenized and sedimented through a 36% sucrose cushion as previously described (261). The pellet was resuspended in 200 µl of PBS, and DNA was extracted using Qiagen DNA Blood Kit (Qiagen, Hilden, Germany). Extracted DNA samples were processed into paired-end libraries with the Illumina TruSeq DNA (Illumina, San Diego, CA) protocol. The libraries were sequenced on the HiSeq 2000 next-generation sequencer (Illumina), generating reads of ~100 bp in length. The reads were mapped to VACV genome and analyzed using Integrative Genomics Viewer (Broad Institute, Cambridge, MA) or Geneious software (Biomatters, Auckland, New Zealand).

4.3.15 Chemical cross-linking and immunoprecipitation

RK-13 cells were infected with vWR or vGFP-I2 at 3 PFU/cell. At 8 or 16 hpi, one half of the samples were chemically cross-linked using 1% paraformaldehyde for 30 min at RT and quenched for 15 min with 5 mM glycine. Crosslinked and non-crosslinked cells were lysed with immunoprecipitation (IP) buffer composed of: 1% NP-40, 50 mM Tris-HCl (pH 7.4), 150 mM NaCl, 1 mM EDTA, and complete protease inhibitor cocktail (Roche Applied Science). The lysates were clarified by centrifugation and precleared with protein G Dynabeads (Invitrogen) or GFP-Trap

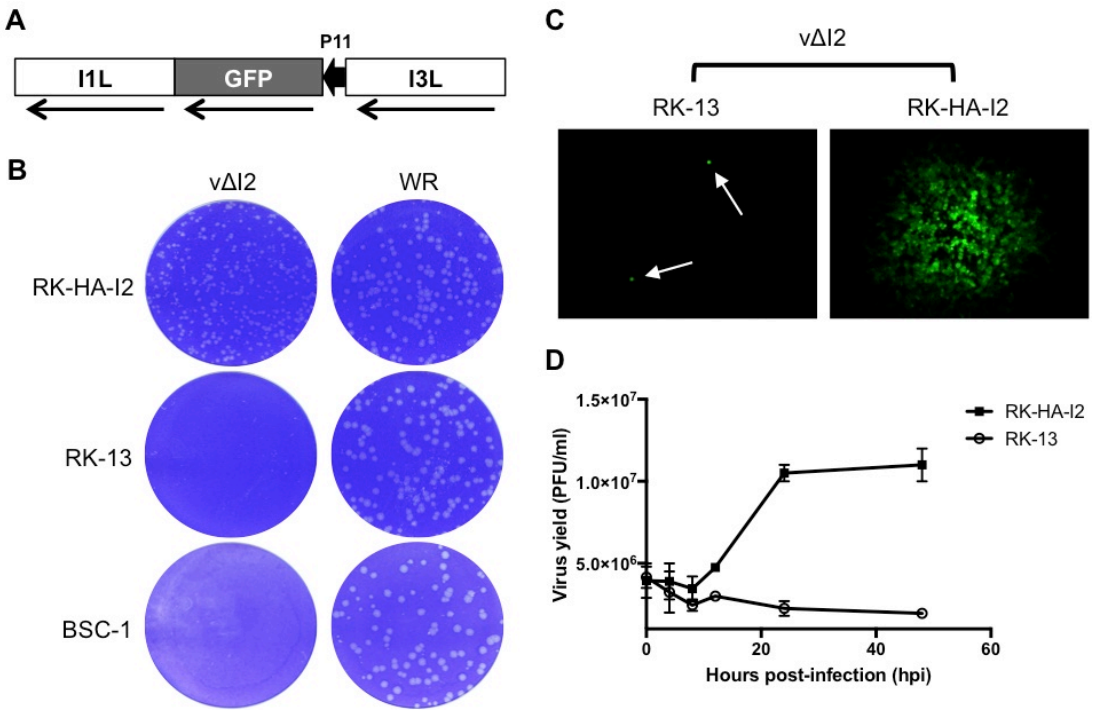

Figure 4.2 Construction of the I2L deletion mutant

(A) Diagram of vΔI2 construction design showing flanking genes of I2, which is replaced by P11 promoter-regulated GFP. (B) Plaque phenotypes of vΔI2 and wild-type vaccinia virus WR strain (vWR). RK-HA-I2, RK-13, and BS-C-1 cells were infected at multiplicity of 0.0007 PFU/cell of vΔI2 or vWR. At 48 hpi, the infected cells were washed and stained with crystal violet. (C) Enlarged fluorescent plaque images. RK-13 and RK-HA-I2 cells were infected as in panel B. At 48 hpi, the cells were imaged under fluorescence microscope. White arrows indicate cells infected with vΔI2, which failed spreading to neighboring cells. (D) One-step growth curves of vΔI2. RK-HA-I2 and RK-13 cells were infected with 3 PFU/cell of vΔI2. The infected cells were collected at 0, 4, 8, 12, 24, and 48 hpi. Virus titers for each time points were determined by plaque assay using RK-HA-I2 cells. The experiment was done twice, and the mean with range (bar) is shown.

magnetic beads (Chromotek, Martinsried, Germany). GFP-I2 was bound with anti-GFP PAb (Invitrogen, A11122), or with GFP-Trap magnetic beads following manufacturer protocols.

4.4 Results

4.4.1 Construction of an I2L deletion mutant

Because repression of gene expression by inducible mutants can be incomplete, we decided to construct an I2L deletion mutant. However, since I2 is essential for replication, it was first necessary to make a cell line that expresses I2 and can complement a virus null mutant. We chose rabbit kidney RK-13 cells because they are permissive for VACV and have previously been used to make complementing cell lines that express other VACV genes (276, 277). A eukaryotic codon-optimized version of the I2 ORF with a N-terminal HA tag was incorporated into a lentiviral vector, which was then used for gene delivery to RK-13 cells (Figure 4.1A). Transduced cells were isolated by antibiotic selection and clonally purified. Western blotting (Figure 4.1B) and fluorescence microscopy demonstrated expression of HA-I2 by the RK-HA-I2 cells (Figure 4.1C).

To delete the I2L ORF of VACV, DNA encoding GFP regulated by the VACV late P11 promoter was flanked by sequences upstream and downstream of I2L (Figure 4.2A) and transfected into RK-13 cells that were infected by VACV to allow homologous recombination. The mutant viruses formed green fluorescent plaques on RK-HA-I2 cells and were clonally purified by repeated plaque picking. Loss of the

I2L ORF was confirmed by sequencing. As expected, vΔI2 was unable to form large plaques in the parental RK-13 cells or in BS-C-1 cells (Figure 4.2B). At high magnification, single RK-13 cells infected with vΔI2 could be detected by their fluorescence but spread to neighboring cells did not occur (Figure 4.2C). Furthermore, vΔI2 replicated to high titer in RK-HA-I2 cells but not in RK-13 cells (Figure 4.2D)

4.4.2 Replication of vΔI2 blocked during morphogenesis

RK-13 and RK-HA-I2 cells were infected with vΔI2 and examined by transmission electron microcopy in order to determine the stage at which virus replication was inhibited. We discovered that morphogenesis was grossly disrupted in non-complementing RK-13 and BS-C-1 cells. The cytoplasm contained large, granular, bodies with crescent membranes on their periphery and relatively normal looking IVs but MVs were not found (Figure 4.3A, B, E, and F). Instead of MVs, there were dense spherical virions (or incomplete MVs). These images contrasted with the overall normal appearance of IV, MVs and wrapped MVs in RK-HA-I2 cells infected with vΔI2 (Figure 4.3C and D) and with similar structures in RK-13 and RK-HA-I2 cells infected with the parental wild type VACV (not shown).

The transformation of spherical IVs to brick-shaped MVs is accompanied by disassembly of the external scaffold formed by trimers of the D13 protein (219, 220). The latter step is accompanied by the processing of the A17 membrane protein that is associated with the D13 trimers (221, 222). Antibody to the D13 protein and protein A conjugated to gold spheres were used to localize the scaffold protein in RK-13 and

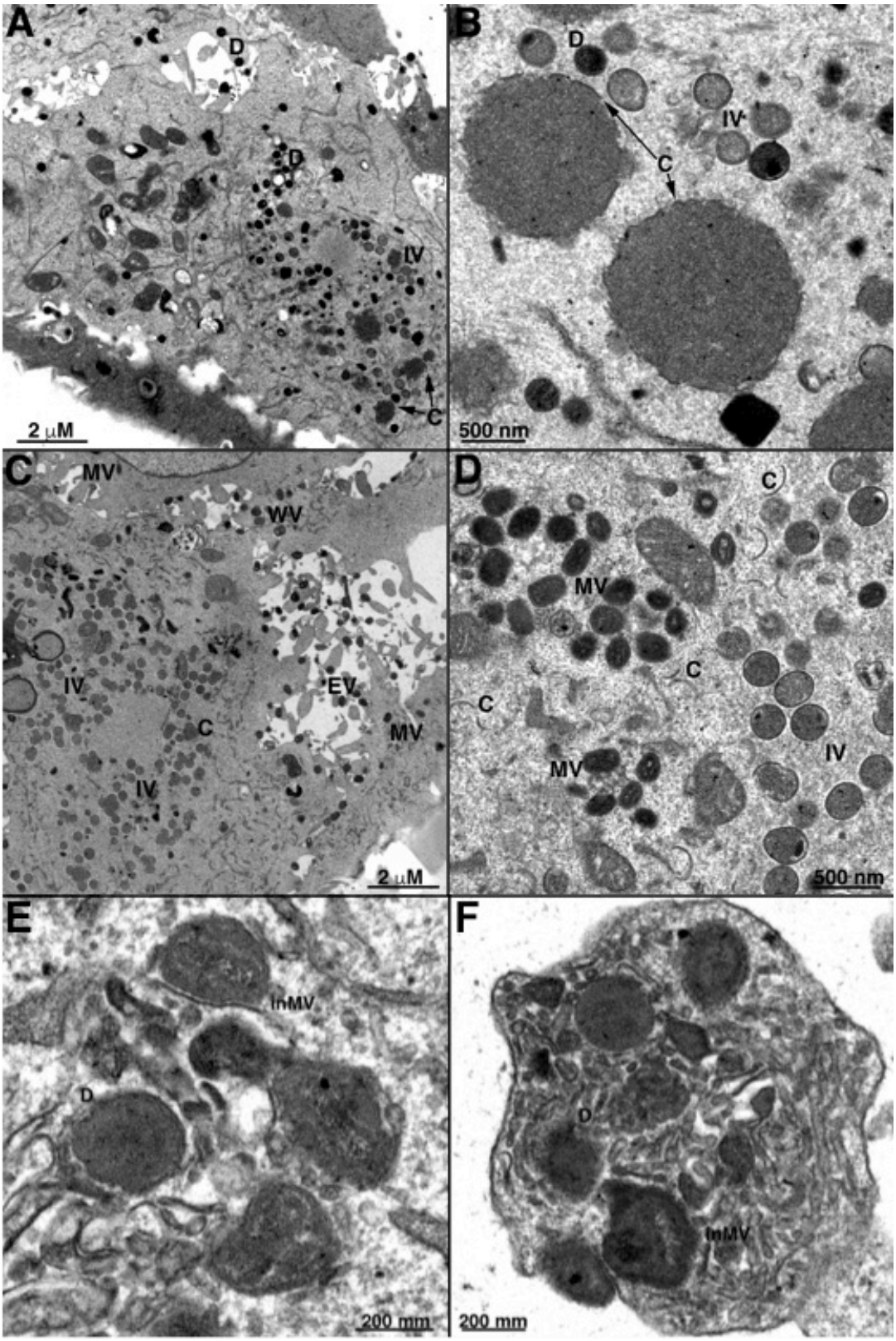
A
D
D
IV
C
2 μM
B
D
IV
C
500 nm
C
MV
WV
IV
EV
C
MV
IV
2 μM
D
C
MV
C
C
IV
MV
500 nm
E
InMV
D
200 mm
F
D
InMV
200 mm

Figure 4.3 Transmission electron micrographs of cells infected with vΔI2

RK-13 cells (A, B), RK-HA-I2 cells (C, D), and BS-C-1 cells (E, F) were infected with 3 PFU/cell of vΔI2. At 18 hpi, the cells were harvested, fixed, and prepared for transmission electron microscopy. C: crescent, D: dense virion, IV: immature virion, InMV: incomplete mature virion, MV: mature virion, WV: wrapped virion, EV: enveloped virion. Scale bars are located on the bottom left or right of each panel.

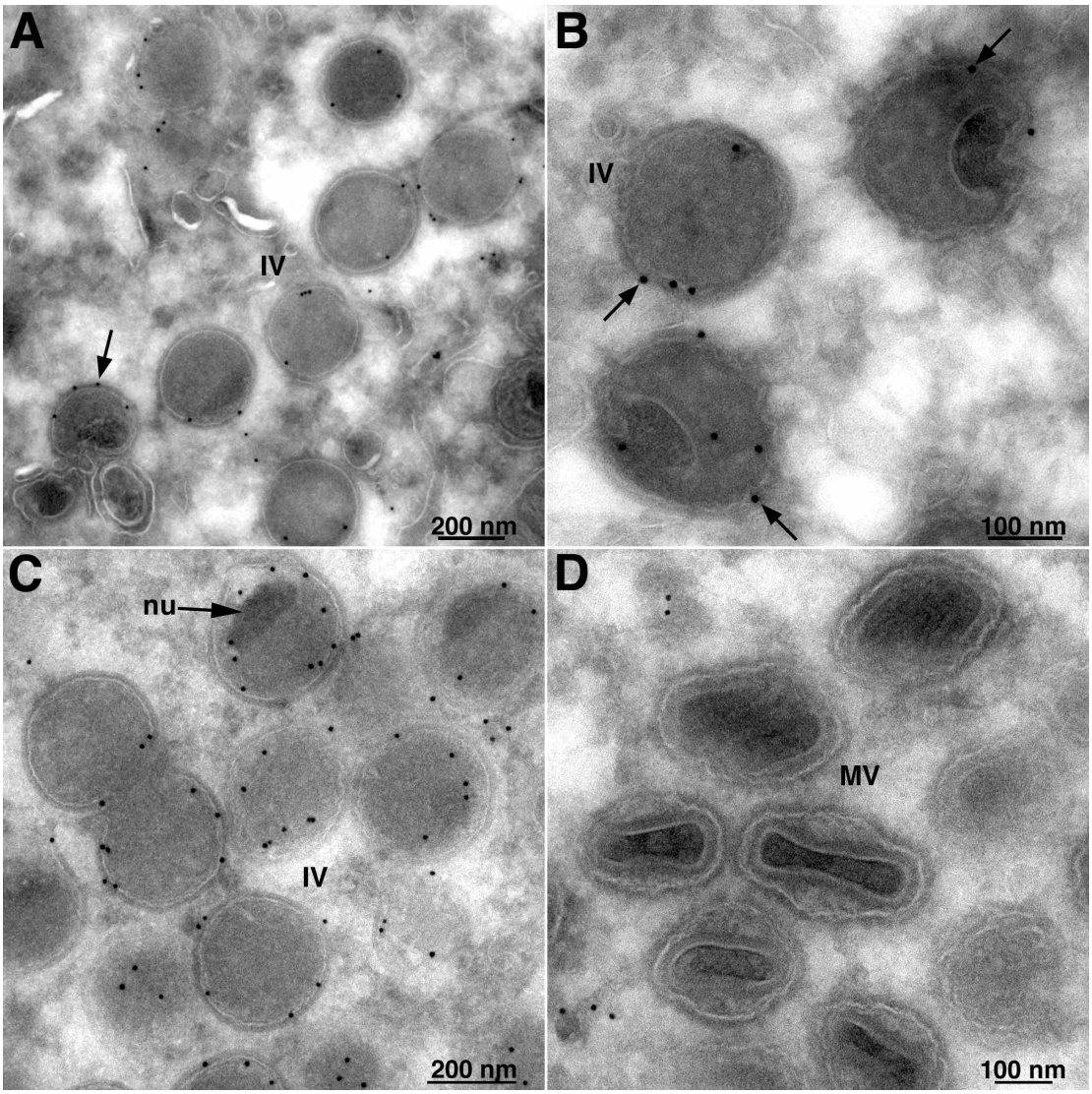

Figure 4.4 Immuno-electron microscopy images showing localization of D13 in IVs and dense virions

RK-13 cells (A, B) and RK-HA-I2 cells (C, D) were infected with 3 PFU/cell of vΔI2. Cells were collected at 18 hpi for fixation and preparation for immuno-electron microscopy using primary polyclonal antibody to D13. IV: immature virion, nu: nucleoid, MV: mature virion. Arrows indicate gold spheres labeling. Scale bars are on the bottom right of each image.

RK-HA-I2 cells infected with vΔI2. D13 was associated with the IVs and the dense spherical particles in in RK-13 cells (Figure 4.4A and B). In RK-HA-I2 cells, D13 was also associated with IVs but not MVs (Figure 4.4C and D). Thus, I2 deficiency prevented the removal of the D13 scaffold and further steps of morphogenesis. The accumulation of dense spherical particles retaining D13 was previously noted when the synthesis of the I7 protease was repressed (221).

4.4.3 I2-deficient virus particles have low levels of EFC proteins

Nichols and co-workers (260) previously compared the proteins associated with I2–deficient virus particles made in the absence of tetracycline inducer and wild type virus particles by western blotting. They found normal amounts of most proteins but an approximate 5-fold decrease in A21, G3 and A28, which are each components of the EFC. We carried out a similar comparison of vΔI2 and wild type virus particles assembled in RK-13 cells. Specific antibodies were used to analyze 15 proteins of which seven were components of the EFC, seven were other membrane and core proteins and one was the D13 scaffold protein. There was on average a 10-fold reduction in the amount of each EFC protein in the I2-deficient virus particles compared to the amounts in wild type virus particles (Figure 4.5A). In contrast, there were similar amounts of the other proteins with one striking exception, a 30-fold increase in D13 in the I2-deficient virus particles (Figure 4.5B). The retention of D13 was consistent with the immunogold labeling of the dense spherical particles (Fig, 4A, B). Another notable difference was greater amounts of unprocessed A3 and A17

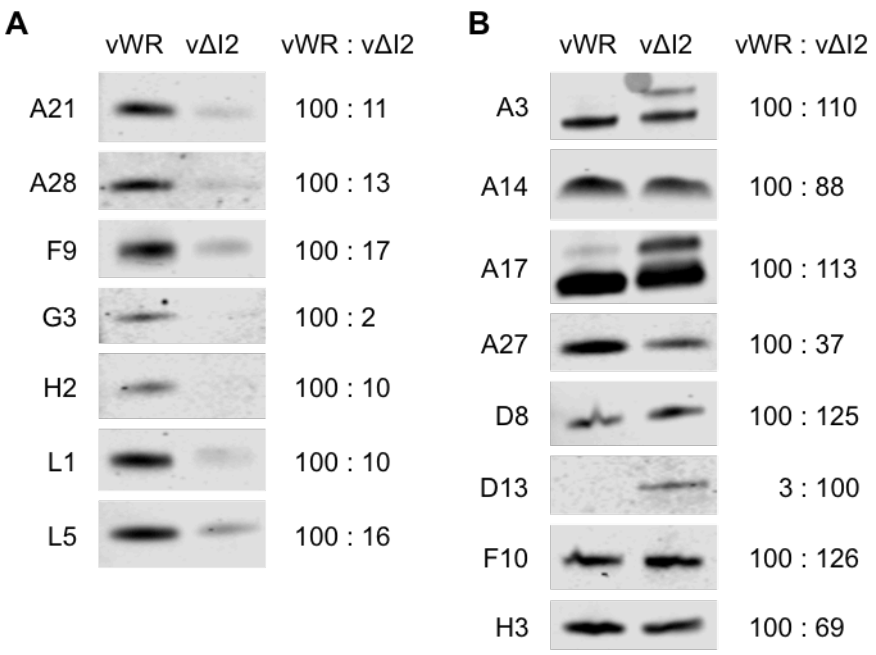

Figure 4.5 Proteins in cesium chloride (CsCl) gradient purified virions

vWR and vΔI2 lanes refer to vWR and vΔI2 virions, respectively. (A) Western blots probing for vaccinia virus entry/fusion proteins. (B) Western blots for other vaccinia proteins including attachment, core, and morphogenesis proteins. vWR:vΔI2 shows relative band intensities of vΔI2 samples compared to vWR samples, which is scaled to 100. D13 is an exception where vΔI2 sample is scaled to 100.

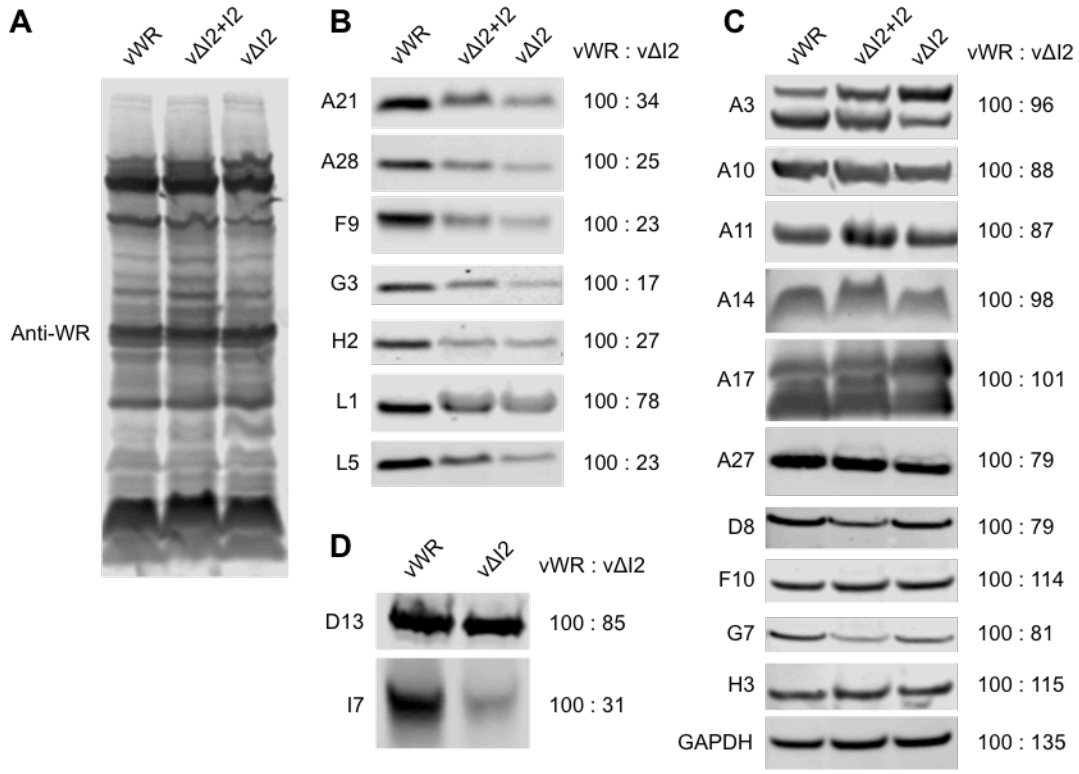

Figure 4.6 Proteins in total infected cell extracts

Either RK-13 or RK-HA-I2 cells were infected with 3 PFU/cell and lysed at 20 hpi. vWR and vΔI2 lanes refer to RK-13 cells infected with vWR and vΔI2, respectively. vΔI2+I2 lanes represent RK-HA-I2 cells infected with vΔI2. (A) Overall expression of vaccinia virus proteins visualized using anti-WR. Western blots probing vaccinia entry/fusion proteins (B), other proteins such as vaccinia attachment, core, morphogenesis, and cellular loading control protein (C). (D) D13 and I7 were additionally analyzed in RK-13 cells only.

proteins seen as higher bands in the western blots (Figure 4.5B), consistent with a perturbation in morphogenesis.

4.4.4 Decreased accumulation of EFC proteins in vΔI2-infected RK-13 cells

In view of the greatly diminished amounts of the EFC proteins in the purified virus particles, we were curious to determine their abundance in infected cells. Lysates of RK-13 cells infected with WT VACV or vΔI2 and of RK-HA-I2 cells infected with vΔI2 were analyzed by SDS-PAGE and western blotting. The pattern of abundant viral proteins appeared indistinguishable when the blot was probed with antiserum from rabbits that were infected with VACV (269), indicating the absence of a general effect on viral protein synthesis (Figure 4.6A). Nevertheless, there were lower amounts of the EFC proteins in RK-13 cells infected with vΔI2 compared to vWR (Figure 4.6B). Although there was some variation, the difference was about 4-fold. This effect was partially overcome when RK-HA-I2 cells were infected with vΔI2 (Figure 4.4B). In contrast, the abundance of the non-EFC proteins was very similar in the cells infected with vWR and vΔI2, although again we noted greater amounts of unprocessed A3 and A17 in cells infected with vΔI2 (Figure 4.6C).

We also compared the levels of the scaffold protein D13 and I7, the proteinase responsible for cleavage of both A3 and A17 and needed for disassembly of D13, in RK-13 cells infected with vΔI2. Although D13 was present in similar amounts, I7 was reduced about 3-fold (Figure 4.6D). As the previous report (184) with the repression of I7 expression showed similar defective dense virions in EM (Figure 4.7A), I7 repression was expected to give similar effects to EFC protein levels as it

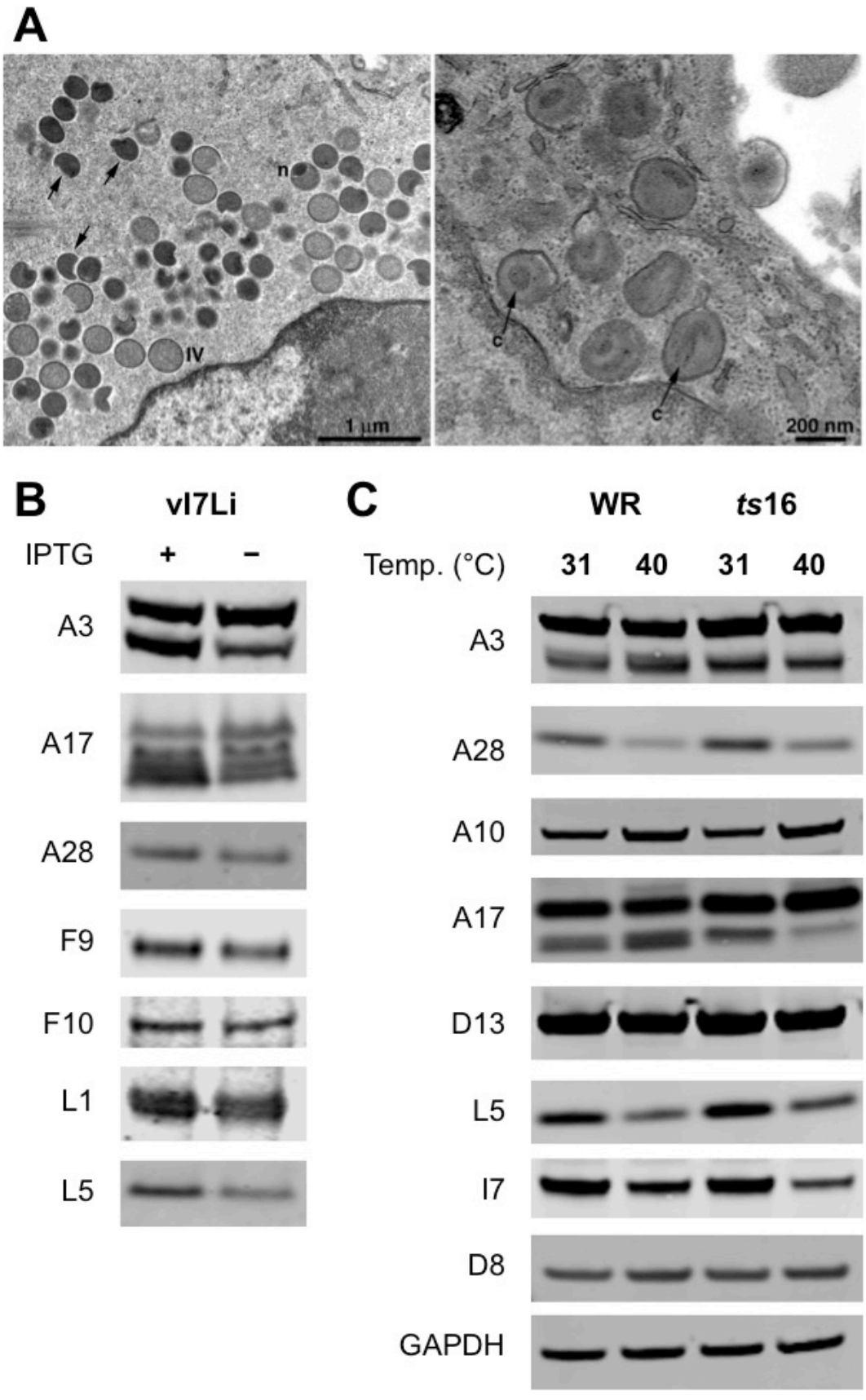
A
n
IV
1 μm
c
c
200 nm
B
vI7Li
IPTG
+
−
A3
A17
A28
F9
F10
L1
L5
C
WR
ts16
Temp. (°C)
31
40
31
40
A3
A28
A10
A17
D13
L5
I7
D8
GAPDH

Figure 4.7 Inducible and temperature-sensitive mutants of I7

(A) Transmission electron micrographs of BS-C-1 cells infected for 24 h with vI7Li in the absence of IPTG. Arrows on the left panel point to irregularly shaped dense particles, and arrows with 'c' indicate poorly formed cores. Abbreviations: n, nucleoid; IV, immature virion. The micrographs were reprinted from Ansarah-Sobrinho et al. (184) with permission. (B) vI7Li (184) was used to infect RK-13 cells at 3 PFU/cell at 37°C with (+) or without (-) 25 μM isopropyl β-D-1-thiogalactopyranoside (IPTG). At 20 hpi, the cells were lysed and analyzed by SDS-PAGE and western blotting. (C) Temperature-sensitive mutant of I7 (*ts*16)(267, 278) was used to infect BS-C-1 cells at 5 PFU/cell. After initial incubation at 31°C for 1 h of virus absorption, the cells were separately incubated in 31 or 40°C for 18 h. Then the cells were harvested, lysed, resolved by SDS-PAGE and analyzed by immunoblotting. GAPDH was used as a loading control.

did in I2 deletion mutant. However, I7 repression by an inducible or a temperature-sensitive mutant did not produce a dramatic effect on the EFC protein levels (Figure 4.7B and C). Regardless, a virus with a complete knockout of the I7L gene would be more appropriate for direct comparison.

Time course expression analysis showed that late protein synthesis was first seen around 6 and 8 hpi with vΔI2 and slightly later with vWR (Figure 4.8A). Background bands at earlier time points were more visible with vΔI2 than vWR (Figure 4.8A) as there are presumably more proteins associated with the virus inoculum due to its high particle to PFU ratio suggested by the lower virus titer.

The low amounts of the EFC proteins could be due to diminished synthesis or protein instability. To distinguish between these possibilities we carried out digital PCR to determine mRNA levels and pulse-labeling with radioactive amino acids to determine protein synthesis and stability. The viral mRNAs encoding EFC and non-EFC proteins were similar in quantity in RK-13 cells infected with vWR or vΔI2 suggesting that the difference in protein levels did not have a transcriptional basis (Figure 4.8B). We chose to analyze the synthesis and stability of L1 because of the availability of a MAb that could be used for immunoaffinity capture (279, 280). Likewise, F9 PAb and D8 MAb were also used. After a 5 min labeling period, the intensity of the L1 and F9 bands from RK-13 cells infected with vWR and vΔI2 were similar suggesting similar rates of translation. However, the vΔI2 bands declined more rapidly during a 2 h chase indicating greater instability (Figure 4.8C, D, and E). The control D8 bands did not show decreasing trend throughout the chase for both

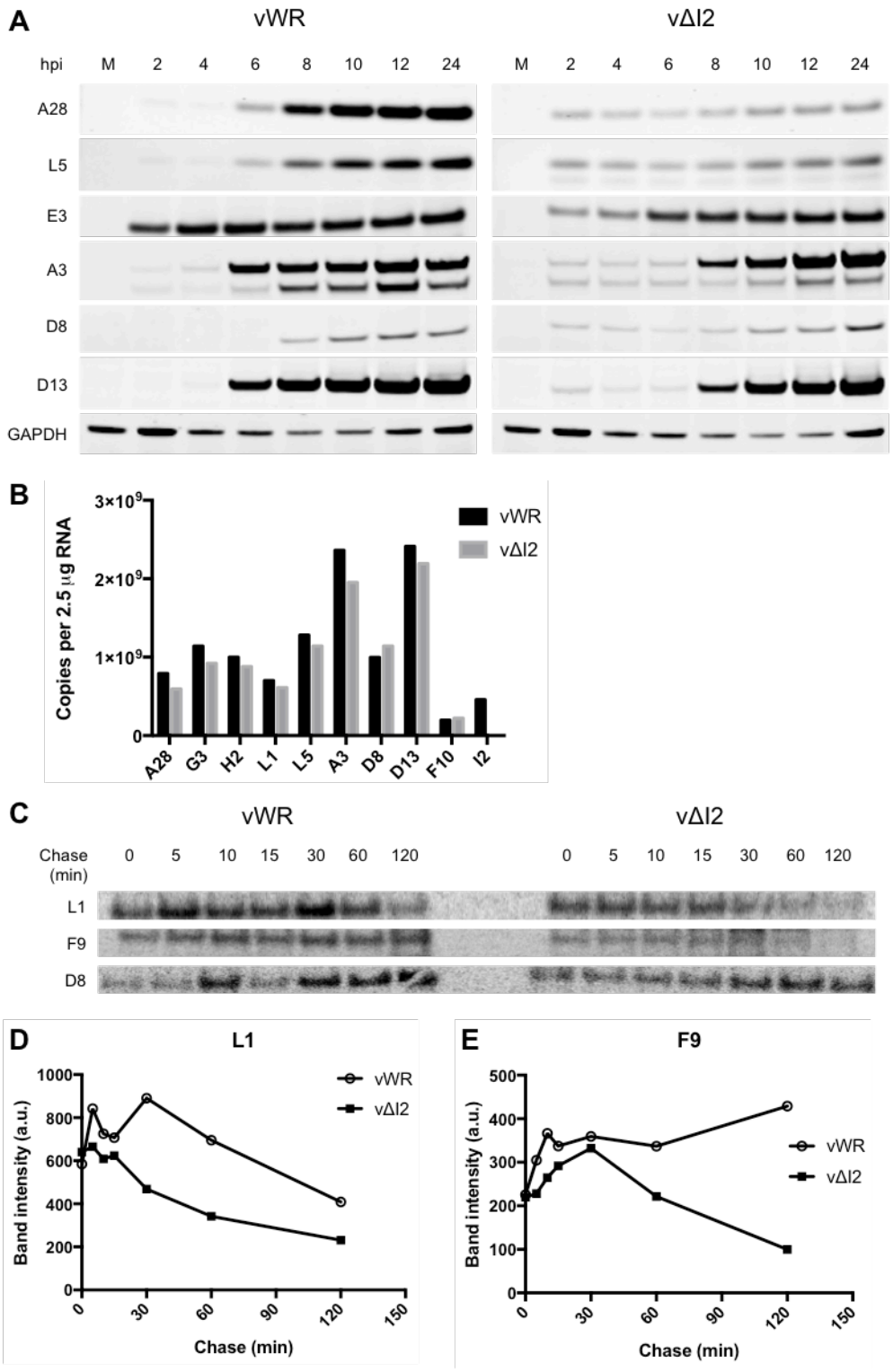
A
vWR
vΔI2
hpi
M
2
4
6
8
10
12
24
A28
L5
E3
A3
D8
D13
GAPDH
B
Copies per 2.5 μg RNA
3×10^9
2×10^9
1×10^9
0
vWR
vΔI2
A28
G3
H2
L1
L5
A3
D8
D13
F10
I2
C
vWR
vΔI2
Chase (min)
0
5
10
15
30
60
120
L1
F9
D8
D
L1
Band intensity (a.u.)
1000
800
600
400
200
0
vWR
vΔI2
0
30
60
90
120
150
Chase (min)
E
F9
Band intensity (a.u.)
500
400
300
200
100
0
vWR
vΔI2
0
30
60
90
120
150
Chase (min)

Figure 4.8 Expression of EFC proteins

(A) Time course expression profile. RK-13 cells were infected with 10 PFU/cell of vWR and vΔI2. M: mock infection. At indicated time points, the cells were lysed and analyzed by SDS-PAGE and immunoblotting with specific antibodies to individual proteins. (B) mRNA levels. RK-13 cells were infected at a multiplicity of 10 PFU/cell with vWR or vΔI2. At 10 hpi, RNA was extracted from infected cells and reverse-transcribed to cDNA. Primers for indicated genes were used for digital PCR and the number of copies of each mRNA in 2.5 µg of total RNA was determined. (C) Pulse-chase. RK-13 cells were infected with 5 PFU/cell of vWR or vΔI2. At 6 hpi, the cells were pulse-labeled with 100 µCi of [^{35}S]-methionine-cysteine for 5 min in methionine-cysteine-deficient medium and then chased in label-free normal medium. At the indicated time, lysates were prepared and L1, F9 and D8 proteins were immunopurified with specific antibodies and analyzed by SDS polyacrylamide gel electrophoresis and autoradiography. Band intensities for L1 (D) and F9 (E) were acquired from audioradiographs in panel C using ImageJ, and were plotted in arbitrary units (a.u.).

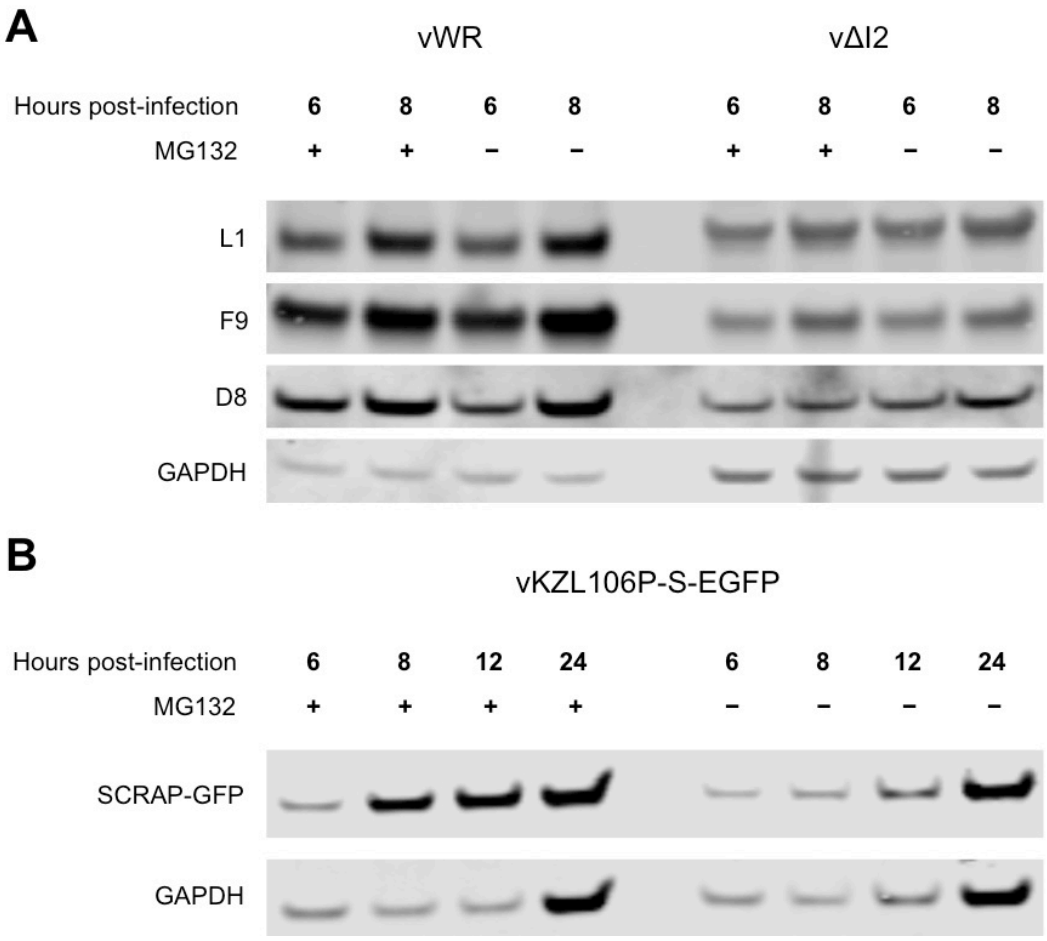

Figure 4.9 MG132 proteasome inhibitor effect on EFC proteins

RK-13 cells were infected with 10 PFU/cell of vWR, vΔI2 (A), or vKZL106P-S-EGFP (B). At 6 hpi, the cells were treated with (+) or without (-) 10 uM MG132 and lysed at indicated times. Lysates were resolved by SDS-PAGE and probed for each of the protein shown. PAbs and MAbs to individual viral proteins, GFP, and GAPDH were used. vKZL106P-S-EGFP, a gift from Jon Yewdell lab, was used as a control as it expresses SCRAP-GFP that has been previously shown to be degraded by the proteasome (281). GAPDH was used as the loading control.

vWR and vΔI2 as expected (Figure 4.8C). A proteasome inhibitor MG132 treatment could not stabilize the EFC proteins (Figure 4.9).

4.4.5 Intracellular localization and protein-protein interaction of I2

To determine intracellular localization of I2, we constructed a recombinant VACV expressing N-terminal GFP-tagged I2 called vGFP-I2 (Figure 4.10A). GFP-I2 replaced the original I2L ORF and natural I2 promoter was used to regulate its expression. vGFP-I2 was replication-competent, though slightly less productive than wild type (data not shown). Green fluorescence from GFP-I2 was weaker than what was observed from P11 promoter regulated GFP (data not shown), suggesting natural I2 expression is not as strong.

In confocal microscopy, GFP-I2 localized to the viral factory in the cytoplasm. Other viral factory proteins A11 and A14 overlapped with GFP-I2, although GFP-I2 signals covered larger area than the other two (Figure 4.10B and C). When stained for I7, GFP-I2 signals co-localized well with the I7 signal (Figure 4.10D). Although I2 has a putative transmembrane domain, I2 only partially overlapped with ER marker proteins calnexin and PDI (protein disulfide isomerase)(Figure 4.10B and C) suggesting that it did not specifically localize with this cellular organelle.

Another potential use of vGFP-I2 was to detect proteins that associate with I2 by immunoprecipitation of the GFP fusion tag. vGFP-I2 infected cells were either cross-linked with 1% paraformaldehyde or left non-cross-linked. vWR infected cells

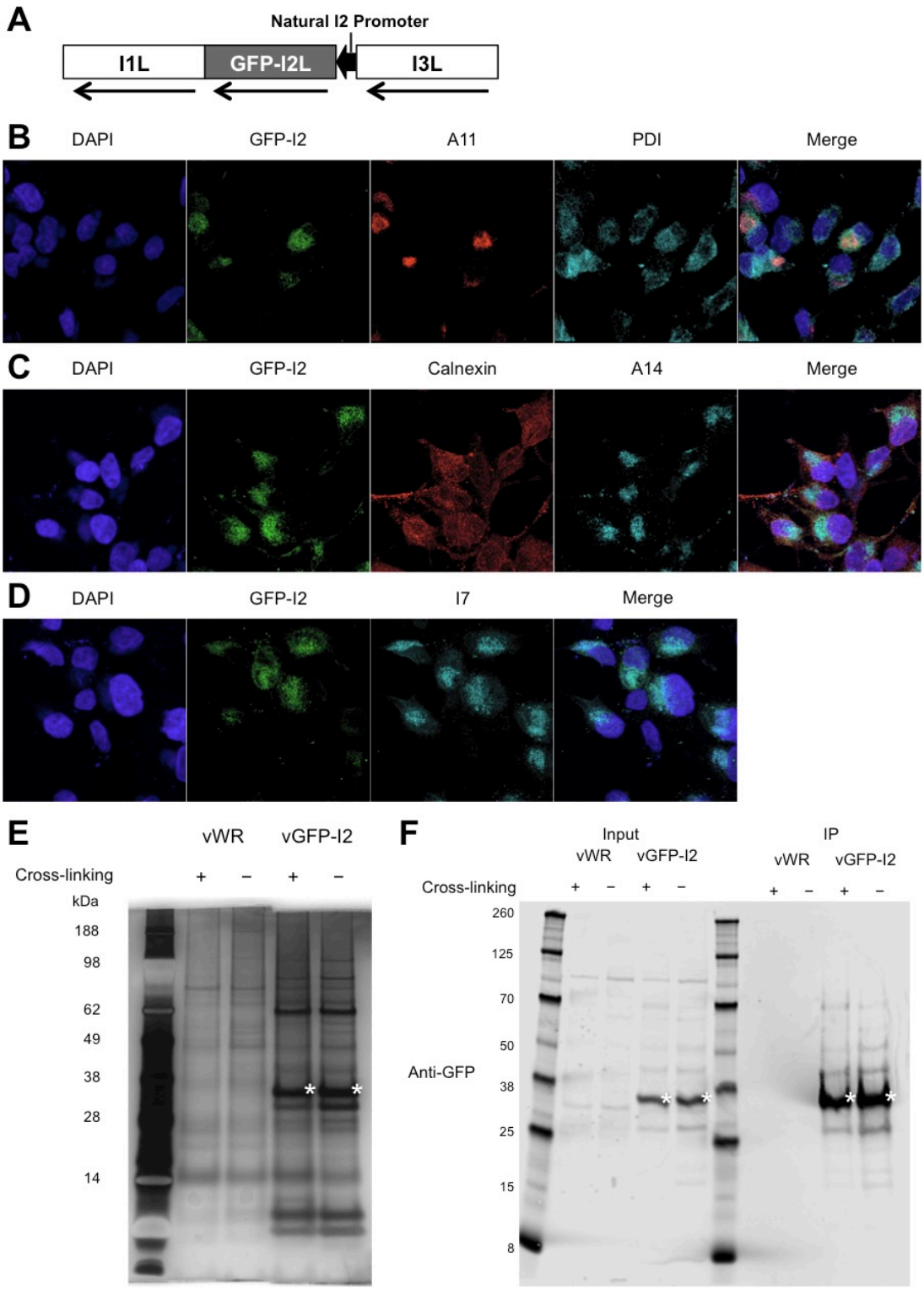
A
Natural I2 Promoter
I1L
GFP-I2L
I3L
B
DAPI
GFP-I2
A11
PDI
Merge
C
DAPI
GFP-I2
Calnexin
A14
Merge
D
DAPI
GFP-I2
I7
Merge
E
vWR
vGFP-I2
Cross-linking
+ − + −
kDa
188
98
62
49
38
28
14
F
Input
vWR
vGFP-I2
IP
vWR
vGFP-I2
Cross-linking
+ − + −
+ − + −
260
125
70
50
38
25
15
8
Anti-GFP

Figure 4.10 Intracellular localization and immunoprecipitation of GFP-I2

(A) Diagram of vGFP-I2 construction. GFP-I2L fusion DNA was inserted between the I1L and I3L ORFs that flank the original I2L ORF. Natural I2L promoter regulates the transcription of GFP-I2L. Arrows indicate the direction of transcription. (B, C, and D) Immunofluorescence microscopy of RK-13 cells infected with 3 PFU/cell of vGFP-I2. At 8 hpi the cells were fixed and stained with mouse MAb to A14, goat PAbs against PDI, calnexin, or rabbit PAbs to A11, I7 followed by secondary staining with Alexa Fluor 568 (red) or 647 (cyan). Nuclear DNA and cytoplasmic viral DNA were stained with 4',6-diamidino-2-phenylindole (DAPI, blue). Green fluorescence from GFP-I2 is shown in green. Merge shows overlay of all images in each panel. (E and F) RK-13 cells were infected with vWR or vGFP-I2 at 3 multiplicity of infection. At 16 hpi, the infected cells were cross-linked (+) with 1% paraformaldehyde (one half the samples were not cross-linked, -), lysed and incubated with GFP-Trap magnetic beads for immunoprecipitation (IP) of GFP-I2. Following the IP, samples were resolved by SDS-PAGE and analyzed by silver staining (E) or by western blot using anti-GFP rabbit polyclonal antibody (F). GFP-I2 bands (35 kDa) are marked with white asterisks. Molecular weights are labeled on the left side of each panel in kilodaltons (kDa).

were used as a negative control. A ladder of multiple bands was seen above and below the 35 kDa GFP-I2 band (white asterisks) for both cross-linked and non-cross-linked samples in total protein staining (Figure 4.10E). Similar trend with fewer bands was observed in a western blot analysis using anti-GFP polyclonal antibody (Figure 4.10F). However, the input samples in Figure 4.10F also showed nearly identical ladder patterns. Therefore, no proteins associated with I2 were detected by this method.

4.4.6 Analysis of I2 compensatory mutants

To screen for the possibility that spontaneous mutations could overcome the replication defect due to the absence of I2, we continuously passaged vΔI2 in five separate passage lines using RK-13 cells. At as early as the fifth passage, I2 compensatory mutants were found replicating in non-complementing RK-13 cells without I2. Among the five different passage lines, three clones were isolated from line number 2 (vcI2-2a, vcI2-2b, and vcI2-2c) and one clone was isolated from line number 5 (vcI2-5a). Remaining passage lines, however, did not contain any compensatory mutants throughout ten passages. While vΔI2 could not form any plaque in the non-complementing cells, the isolated compensatory mutants were able to form plaques although they were smaller than those of vWR (Figure 4.11A). The vcI2-2a formed smaller plaques than other clones vcI2-2b, vcI2-2c, and vcI2-5a (Figure 4.11A), corresponding with the results from one-step growth curve analysis (Figure 4.11B).

In principle, the increased replication of the mutant viruses could be due to changes in gene sequences or expression. Previous studies have identified duplications and transpositions that resulted in the increase of overall genome sizes (48, 282). Elde and co-workers (282) reported that poxviruses rapidly adapted in response to changing host responses with gene amplifications. To determine if our compensatory mutants have used such modification strategy to overcome the absence of I2, we digested the viral genome with the *Hind*III restriction enzyme. Notably, vcI2-2c had two additional fragments (marked with white asterisks) when compared to vWR and vΔI2 genomes (Figure 4.11C). If there was simply a duplication, then we would not have expected to see all of the original size fragments. One explanation is that the duplication was unstable and was continuously being lost. With the exception of vcI2-2a that showed no difference with the parent vΔI2, other clones (vcI2-2b and vcI2-5a) also showed the same additional bands in the *Hind*III restriction analysis (data not shown). Fragment close to the 6557 bp sized ladder was slightly larger for vΔI2 and vcI2-2c than vWR, as null-I2 mutants contained a larger GFP ORF instead of the I2L ORF of vWR within the fragment (Figure 4.11C).

To further analyze the modifications made in the genomes of I2 compensatory mutants, whole genome sequencing was done with the Illumina system. Millions of reads of about 100 bp in length were generated and mapped to the VACV genome. As expected, both vΔI2 and its compensatory mutants were missing the I2L ORF. The I2 compensatory mutants merely contained several point mutations and small deletions compared to the reference genome in GenBank, but these were also present in the parental virus. The difference between the parent vΔI2 and compensatory mutants

were rather identified in the number of reads mapped to certain regions of the genome. Peaks were generated across the VACV genome, with the height of the peak dependent on the number of mapped reads. While vΔI2 peaks plateaued throughout the genome before the inverted terminal repetitions (ITRs), vcI2-2c peaks doubled and tripled in height at around the 176,000 and 188,000 nucleotide positions, respectively (arrows, Figure 4.11D). With the exception of vcI2-2b, all other I2 compensatory mutants showed the same duplication/triplication patterns (data not shown). Because nucleotide position scale in Figure 4.11D is not entirely accurate due to incompletely mapped reads that extended the ends of the genome, the duplicated/triplicated regions were extracted separately and re-aligned to the VACV genome. As a result, the predicted start position for duplication was found to be around 171323, and at around 182233 for triplication. 32 ORFs were encoded within the duplicated/triplicated sequences, as listed in Table 4.2. The results of the sequence analysis were consistent with the finding of additional fragments by restriction enzyme digestion.

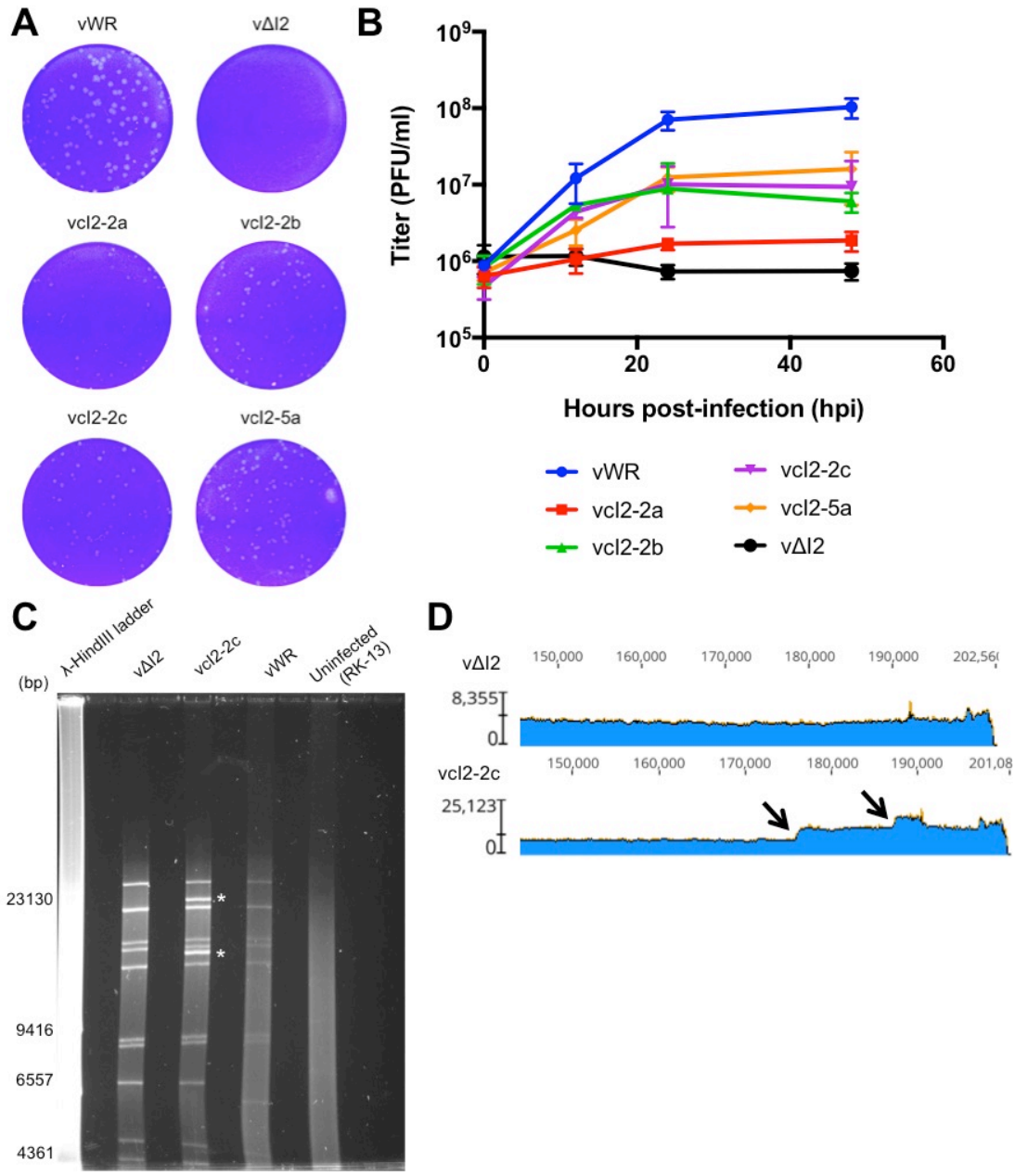

Figure 4.11 Analysis of I2 compensatory mutants

(A) Plaque assay of RK-13 cells infected with vWR, vΔI2, or with four other I2 compensatory mutants. Each virus stock was serially diluted and incubated in a 6-well plate containing monolayers of the RK-13 cells. After 48 h, the cells were washed and stained with crystal violet. (B) One-step growth curve analysis of the four I2 compensatory mutants along with vWR and vΔI2. Infected RK-13 cells were harvested at indicated times (0, 12, 24, and

48 h) and disrupted by repeated freeze-thaw cycles followed by sonication. Ten-fold dilutions of the lysates were plated for virus yield determination. The experiment was done three times and the mean is plotted with error bars representing the standard deviation. Blue: vWR, black: vΔI2, red: vcI2-2a, green: vcI2-2b, magenta: vcI2-2c, orange: vcI2-5a. (C) *Hind*III restriction enzyme analysis of vWR, vΔI2, and vcI2-2c genomes. RK-13 cellular DNA was analyzed as a control. The λ-*Hind*III ladder is shown on the left labeled in base pairs (bp). White asterisks indicate additional *Hind*III fragments of vcI2-2c not present in vΔI2 or vWR genome fragments. (D) Peaks showing whole genome sequencing reads of vΔI2 and vcI2-2c mapped to VACV genome. The reads are approximately 100 bp in length and the height of the blue peaks represents the number of reads assembled to the corresponding region of the genome. Nucleotide position of the genome is labeled along the top and the scale on the left reflects the number of mapped reads according to the height of the peak. The arrows point to increases (bumps) in the number of mapped reads suggesting duplication and triplication of indicated regions.

Table 4.2 List of ORFs within duplicated/triplicated regions of vaccinia virus I2 compensatory mutant

Position in genome[a]	Open reading frame
171323 to 182232	hypothetical protein[b] hypothetical protein ankyrin-like protein[c] hypothetical protein B19R B18R B17L B15R B13R B12R B11R hypothetical protein B9R B8R
182233 to end (194711)	B29R TNF-alpha-receptor-like protein[d] hypothetical protein B28R ankyrin-like protein ankyrin-like protein hypothetical protein B25R epidermal growth factor-like protein (EGF-like protein)[e] ITR paralog: VACWR009, C11R gene hypothetical protein ITR paralog: VACWR010, C10L gene zinc finger-like; apoptosis[f] ITR paralog: VACWR011 gene zinc finger-like protein[g] C13L C12L hypothetical protein

[a] Nucleotide position starting from the left end of the genome

[b-g] Refer to ORFs that have not been annotated

4.5 Discussion

Nichols and co-workers (260) previously reported that the I2L gene encodes a membrane protein with an essential role in virion entry. We were interested in following up this study in order to determine the stage of entry that was affected and therefore decided to construct an I2L deletion mutant for high stringency. Several previous studies successfully constructed and propagated VACV mutants with deletions of essential genes by making a complementary cell line that expresses the missing gene (8, 211, 276, 277). We introduced an HA-tagged I2 gene regulated by a eukaryotic promoter into RK-13 cells using a lentivirus vector and screened antibiotic-resistant mutants for expression of the HA tag. The cell line isolated stably expressed HA-I2 though the level was less than achieved by virus infection. Nevertheless, we succeeded in deleting the I2L gene from VACV and propagating the mutant in the cell line achieving yields about a log lower than that of wild type virus. As anticipated, the virus was unable to replicate in cells not expressing I2, confirming the requirement for this gene. We were surprised, however, to discover a block in morphogenesis. Although IVs appeared normal, spherical dense particles accumulated instead of brick-shaped MVs. Although these particles contained normal amounts of most core and membrane proteins, they were greatly deficient in EFC proteins, had an increased amount of the D13 scaffold protein, and increased amounts of unprocessed A3 and A17 proteins. Thus, failure to disassemble the scaffold appeared to be a major defect that was previously reported to occur when I7, the proteinase responsible for cleavage of A17 as well as several core proteins, was

repressed (221). Coincidentally, we noted that there was a reduced amount of I7 detected in cytoplasmic extracts of RK-13 cells infected with vΔI2.

The EFC proteins have either N- or C-terminal transmembrane domains but lack signal peptides and their modes of insertion into the viral membrane have not been investigated. However, electron microscopic studies showed that in contrast to A17, which is detected in both IVs and MVs, L1 is only detected in MVs suggesting that insertion of the EFC proteins may occur after removal of the D13 scaffold (279). In the present study, we found that the EFC proteins were also diminished when the total cell lysate was analyzed, though not to the same extent as in purified virus particles. A specific diminution in EFC proteins was previously noted when the formation of IVs was impaired resulting in the absence of MVs due to deletion or repression of viral membrane assembly proteins (VMAPs) notably A6, A11, A30.5, H7 and L2 (8, 10, 205, 206, 208, 209, 211). A common feature of the I2 deletion mutant and the VMAP mutants is the failure to form membranes lacking the D13 scaffold. We suggest that the EFC proteins are only able to insert into the viral membrane after removal of D13 and that they are unstable because of their hydrophobicity when prevented from inserting into viral membranes. The two major modes of protein degradation in eukaryotic cells are the ubiquitin-proteasome and autophagy-lysosomal pathways. We were unable to stabilize the EFC proteins by addition of the proteasome inhibitor MG132 and which if either of the canonical pathways is involved is uncertain at this time.

As discussed above, the simplest model to explain the defect in replication of the I2 deletion mutant is that the protein is involved in the final stages of IV assembly

or disassembly and that the deficiency of EFC proteins is secondary (Figure 4.12). However, it is possible that I2 has multiple functions in association with the localization or activation of I7 proteinase or in chaperoning the EFC proteins. The study highlights the need to better understand the pathway of insertion of the EFC proteins in the viral membrane. Studies on protein interaction and compensatory mutants of I2 may provide insights to the stronger understanding of I2. Further discussions regarding those studies will be provided in chapter 5.

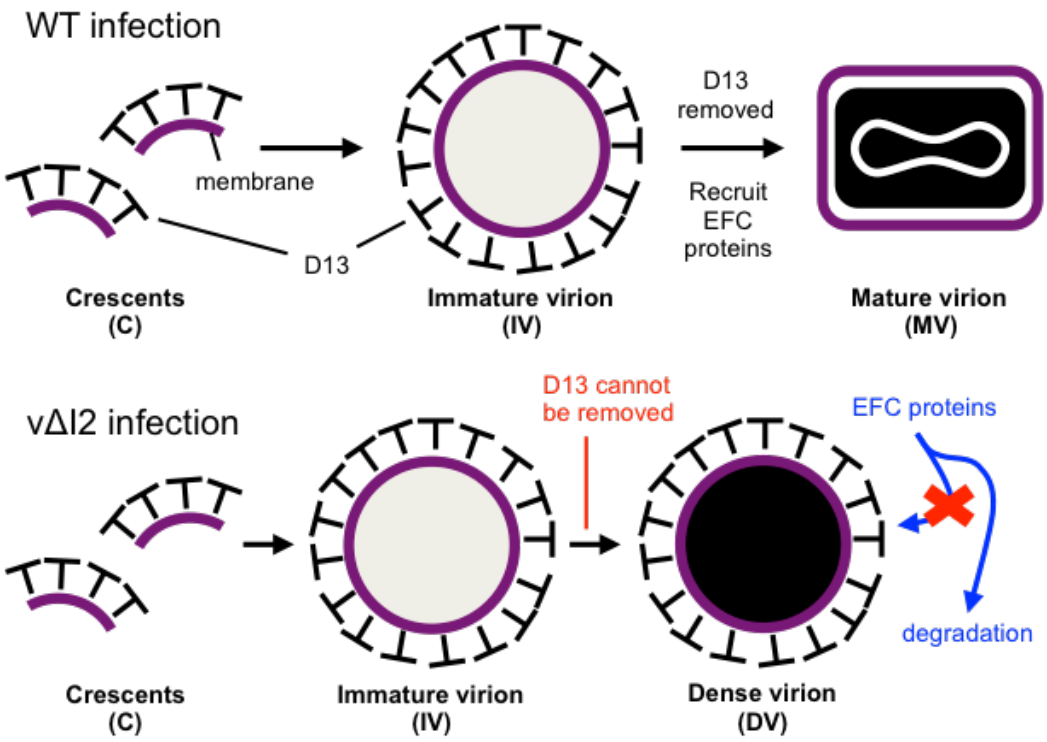

Figure 4.12 Model for defects caused by the absence of I2

During a wild type (WT) VACV infection, crescents membranes coated with the D13 scaffold protein form, enlarge to form spherical immature virions (IVs) containing the DNA and core proteins. Further morphogenesis involves processing of the A17 membrane protein by I7 proteinase, removal of the D13 scaffold, recruitment of the EFC proteins and a change in shape. The IVs also form during infection with the I2 deletion mutant vΔI2, but the D13 scaffold protein is not removed and the change to the brick-shape with a well-defined core does not occur. Under these conditions, the EFC proteins fail to be inserted into the viral membrane and exhibit enhanced degradation.

Chapter 5: Discussion

5.1 Use of Split-GFP for Vaccinia Virus Morphogenesis Studies

With recent studies reporting evidence of ER membranes as the source of poxviral membranes (8, 211), we were highly interested in uncovering the intricate mechanism of how the virus makes use of the cellular membrane. There is a vast amount of uncertainty in VACV morphogenesis from the start to the end. The recent studies merely gave us a starting point, which is the ER membrane. Yet this is invaluable information that was greatly missed during the past years of poxvirus research. It generated numerous questions related to the use of ER membrane by the virus, from how the membrane is sectioned into pieces to how the virus stabilizes the breaks. It is not just one or two proteins that are necessary for VACV morphogenesis, but already a large number of VACV proteins have been shown to be required for morphogenesis (178). Moreover, the involvement of host cell proteins cannot be ruled out. At the moment, it seems that great efforts are going to be needed towards the complete understanding of morphogenesis, but every step should help to reach the goal.

The split-GFP project was started to reveal the ER membrane topology of VACV morphogenesis proteins, and we believe that this step would guide us to more directed studies of morphogenesis. Despite the existing reports of various methods of

determining protein topology (9, 233, 234, 236-238, 283-285), we wanted to develop a new method that is quick and versatile. In chapter 3, we were able to determine the topology of VMAPs L2 and A30.5, providing useful information when designing studies to reveal the function and mechanism of interaction between those proteins. Fluorescence signals from the N-terminus of L2 were detected in the cytoplasm and those of C-terminus were detected in the ER lumen. For A30.5, both the N- and C-terminus were shown to be facing the cytoplasm. With this information, we can predict that the L2-A30.5 interaction occurs at the cytoplasmic side of the ER membrane. This method can be used in various occasions such as when designing constructs for mutagenesis studies or when considering models of multiple proteins in a complex. The split-GFP method is not limited to viral proteins but also is applicable to cellular proteins as previously shown, which is a bonus.

The versatility offered by the split-GFP method extends beyond rapid determination of protein topology. As mentioned before, the system can be used in live cells in addition to fixed cells (12), meaning high-throughput applications such as small interfering RNA (siRNA) screening can be coupled with split-GFP. Indeed, we have made attempts to design a siRNA screen to determine host cell proteins necessary for VACV morphogenesis. If a viral protein switches its ER-associated membrane topology during morphogenesis, a block in the process before the transition would yield a different topology when compared to normal conditions. If split-GFP tag can be used on that particular protein, then theoretically siRNA screening can identify host genes that, when silenced, can prevent the topology transition of the viral protein. We have tried to use VACV A14 and A17 proteins for

this purpose, but were unable to acquire their membrane topology with our split-GFP method perhaps because of their multiple locations in viral and cellular membranes. The size of the GFP-S11 tag is similar to that of small epitope tags and most proteins can be tagged with minimal perturbation, which is encouraging in the search for new candidate proteins. While trying such high-throughput analysis using split-GFP could seem ambitious, it suggests how this method can be modified or combined with other techniques to develop innovative strategies for studying VACV morphogenesis.

5.2 Versatile Approaches for Studying Vaccinia Virus Protein I2

When the role of I2 in VACV entry was suggested (260), we were interested in determining the function of I2 in allowing entry of the virus into host cells. The possibility of I2 serving as a transporter for other EFC proteins was also considered based on the previous report (260) showing 5-fold less EFC protein levels on purified virions made under repressed I2 expression. We were therefore surprised by the results indicating I2's role in morphogenesis presented in chapter 4. Yet it had allowed another contribution to the understanding of VACV morphogenesis in conjunction with studies covered in chapter 3. While L2 and A30.5 (chapter 3) are critical for the beginning or early stage of viral membrane morphogenesis, I2 (chapter 4) has a crucial role in the later stage. Overall, this work has reiterated the complexity of virus morphogenesis by highlighting that there still could be unknown proteins taking actions in different stages of morphogenesis.

Prior to this study, the removal of D13 scaffold from the IV membrane was thought to be dependent only on the processing of A17 by the I7 protease (221). It

turned out that the process is not as simple, however, with I2 also proven to be required for the D13 removal. The deletion of I2 therefore blocked the transition from IV to MV, yielding defective dense virions that remained spherical and retained D13 coat. Perhaps I2 could be working as a cofactor of I7, similar to adenovirus protease that requires an 11 amino acid cofactor for activation (286-288). In this context, there was a reduction of I7 in cells infected with vΔI2. Experiments with I7 repression could not demonstrate a similar effect on the EFC protein levels as vΔI2, but a deletion-I7L virus may generate more robust evidence for the correlation between I2 and I7.

The initial intent of studying virus entry was partially fulfilled as this project did not solely focus on the morphogenesis aspects, but also implemented numerous experiments with the EFC proteins. Entry protein levels were first analyzed both in purified virions and in total cell lysates in the absence of I2. This answered one of the questions we had from the beginning of this study, which was about whether EFC proteins are inserted into membranes prior to the start of viral membrane formation or not. The blockage of EFC protein localization on viral membranes caused by retention of D13 scaffold has revealed that EFC proteins are localized after the IV formation. The proteins without the accessibility for proper localization were degraded, as determined by the pulse-chase experiment. The proteasome inhibitor MG132, however, could not stabilize the EFC proteins. MG132 perhaps needed to be treated at earlier time point, but 6 hpi had to be used as earlier treatment was reported to cause defects in viral replication (289). A question was raised on whether the hydrophobic transmembrane (TM) domains in the EFC proteins enhanced the

degradation (290) in the absence of I2. Plasmids were constructed to express HA-tagged A28 and F9 with or without the TM domains, but the experiment was not successful as the proteins without TM domains were unstable regardless of I2 presence (not shown).

To further characterize the I2 protein a versatile recombinant VACV with a tag on I2 was made, and the vGFP-I2 was constructed. It could be used for confocal microscopy, immunoprecipitation, mass spectrometry, and immuno-electron microscopy. The green fluorescence from GFP-I2 was relatively weaker than that of P11 promoter-regulated GFP by naked eye, implicating that I2 naturally has low level of expression. Confocal microscopy analysis of GFP-I2 with other viral proteins had shown localization of I2 in the viral factories. When stained for I7, GFP-I2 signals co-localized with the I7 signal. This suggested that I2 might interact with I7, but co-localization in confocal microscopy alone was not enough to confirm the interaction. When GFP-I2 was immunoprecipitated, I7 proteinase was not found despite paraformaldehyde cross-linking prior to the immunoprecipitation. Silver staining and western blot analysis of the immunopurified samples did show faint signs of additional proteins, but mass spectrometry could not show any specific proteins that interact with I2.

When a protein critical for virus replication is absent, it could be interesting and sometimes extremely useful to look at the genetic response from the virus. Unlike RNA viruses, DNA viruses are generally more stable in terms of spontaneous mutations. Infection of RNA viruses such as human immunodeficiency virus (HIV) is difficult to prevent with vaccines because of their escape mutants generated from high

mutation rates. Poxviruses and other DNA viruses are less mutagenic, and the eradication of smallpox would not have been possible if it had higher mutation rates. Despite the low mutation rates, poxviruses have their own ways to adapt rapidly to unfavorable conditions (282). Although rare, modifications to the genome in forms of point mutation, insertion, deletion, gene amplification and genomic accordions have been reported (48, 282, 291, 292). Likewise, we wanted to see if VACV could eventually compensate the loss of I2L gene through genomic or gene modification as this could provide a clue to the function of the protein. We were fortunate to find four clones that could replicate without the I2 protein. Whole genome sequencing of the I2 compensatory mutants showed no amino acid changes but rather duplication and triplication of certain regions of the genome. It was expected to find amino acid level mutations for proteins such as D13 or I7 that directly correlate to morphogenesis defects found in vΔI2, but the genome amplification was equally interesting as it suggested the compensation of I2's role with other gene(s). We first thought the right end of the genome was amplified and transpositions into the left side of the genome based on the previous case in rabbit poxvirus (48). However, *Hind*III restriction enzyme analysis showed appearance of two additional fragments instead of the expected changes in existing fragments. This result suggests that the duplication is unstable and that it is continuously deleted so that there is always a mixture of wild type genomes and genomes with duplications. While this complicates the genomic modification model in our I2 compensatory mutants, it suggests yet another novel strategy that can be used by poxviruses.

5.3 Future Directions

Overall, this work has mainly focused on VACV morphogenesis specifically in two areas: the early stage where ER membranes are modified for viral membrane formation, and the later stage where IVs mature into MVs. The future directions are therefore aimed towards unveiling the mechanism of viral membrane formation as well as its transitions.

As a follow-up to the split-GFP project, future experiments should focus on analyzing the segments or ruptures of the ER membrane regarding how they are generated and stabilized. Topological analysis of all the viral membrane proteins and cellular proteins with potential function in viral morphogenesis would give a head start when modeling protein interactions necessary for the ruptures. Based on topology results in chapter 3, mutagenesis of L2 and A30.5 can be done to map critical domains for interaction. Furthermore, live cell imaging experiments can be used to confirm the breaking of ER membranes. The split-GFP method was used in an attempt to see if luminal GFP-S11 tag is released by ER membrane breaks, but was unsuccessful presumably because the ruptures are stabilized. ER luminal calcium, however, can be more readily released being harder to contain even with a minuscule rupture. Live cell imaging studies using fluorescence labeling of calcium and ER membrane may be able to provide another evidence for ER membrane ruptures during VACV infection.

As discussed before, the use of high-throughput siRNA screening using split-GFP tagged proteins may help to identify host cell proteins necessary for VACV morphogenesis. A protein with distinct topological states between normal and

defective morphogenesis conditions needs to be identified first. Once such a protein is found, it can be tagged with the GFP-S11 tag and separate expression of GFP-S1-10 within a different compartment will generate a condition where no green fluorescence is produced under normal conditions. When morphogenesis is blocked by siRNA silencing of certain host mRNA, the GFP-S11 tag could be available for interaction with the GFP-S1-10 and give fluorescence. This can be done the other way around where it normally gives fluorescence when morphogenesis occurs, but does not when morphogenesis is blocked. Identification of host cell protein with a role in VACV morphogenesis will be a great step forward in understanding the mechanism.

There are many additional experiments that could be done to further understand the role of I2. We now know why D13 scaffold is not removed and how it causes a defect in the late stage of morphogenesis, but the mechanism of I2's action is not known. The correlation between I2 and I7 must be studied in more detail. Only IPTG inducible and temperature-sensitive mutants are available for I7, and these could not show large differences in EFC protein levels that were expected. Inducible or temperature-sensitive mutants are often leaky, which in some cases is enough to alter experimental results. A complete deletion I7 mutant could show phenotypes that are more dramatic, similar to how the deletion I2 mutant surprised us with the block in morphogenesis. Thus, acquisition of the deletion I7 mutant would generate more confidence in the analysis of the I2 and I7 mechanism.

When the function of a protein is unknown, identifying any other interacting protein can often provide useful hints. Unfortunately for I2, its interaction with other proteins could not be demonstrated with the GFP-I2 fusion protein. Various attempts

including immunoprecipitation and even mass spectrometry could not show anything, but perhaps tagging I2 with HA or V5 tags may produce different results.

Especially with the difficulties in detecting protein interactions of I2, hopes are high on the I2 compensatory mutants for revealing the function of I2. Identifying another protein that can replace the role of I2 would be massive. If it is a protein with a known function, it should strongly suggest that I2 has a similar function. Even if it is not a previously characterized protein, it would be mean that another viral morphogenesis protein is discovered. However, the whole genome sequencing suggested that the compensatory effect was not from point mutations but from large duplications of genome segments. The duplicated/triplicated regions contain 32 ORFs, and work needs to be done to narrow this list down. Perhaps additional passaging of the mutants may naturally select for more narrow modifications, similar to the transition from gene accordions to point mutations reported in another study (282). The *Hind*III restriction enzyme analysis requires further experiments as well. Isolation of the two additional *Hind*III fragments in the compensatory mutant genomes may enable us to locate the sites where amplified regions have transpositioned in the genome. It is likely that the duplication is unstable and that it is continuously lost so that there is always a mixture of genomes when there is selection pressure. Another novel idea is that the duplicated DNA exists separately outside of the viral genome, when under selection pressure from the absence of I2. Maintaining such epigenomic DNA is probably less efficient, and removing the selection pressure by infecting in RK-HA-I2 cells may cause the mutants to dispose of the additional

DNA. This type of compensation by non-genomic DNA has not been reported before for poxviruses and would be a novel finding if true.

A significant amount of work has been put into analyzing EFC protein expression in the deletion I2 mutant. We have shown that EFC proteins are subject to more rapid degradation when they fail to localize on the viral membrane. Yet the mechanism for degradation could not be shown with experiments involving the treatment of proteasome inhibitor MG132, detection of ubiquitin, or removal of TM domains. Additional proteasome inhibitors may be tested, as well as autophagy and lysosome inhibitors. Hydrophobic properties of the TM domains are suspected to cause degradation when the proteins are mis-localized, but more experiments are needed for confirmation. Our interest in signal sequences is not limited to degradation signals. The absence of any known signal sequence within the EFC proteins make it difficult to understand how the proteins are transported to the viral membranes. Identification of such signals is of a great interest and it can lead to the understanding of EFC protein transport mechanism, which will surely benefit the VACV morphogenesis and maturation studies.

Bibliography

1. **Moss B.** 2013. Poxviridae, p 2129-2159. *In* Knipe DM, Howley PM, Cohen JL, Griffin DE, Lamb RA, Martin MA, Racaniello VR, Roizman B (ed), Fields Virology, 6 ed, vol 2. Lippincott Williams & Wilkins, Philadelphia, PA.

2. **Fenner F.** 1993. Smallpox: emergence, global spread, and eradication. Hist Philos Life Sci **15:**397-420.

3. **Tucker JB, Zilinskas RA.** 2003. The 1971 smallpox outbreak in the Soviet city of Aralsk: implications for Variola virus as a bioterrorist threat. Introduction. Crit Rev Microbiol **29:**81-95.

4. **Kantele A, Chickering K, Vapalahti O, Rimoin AW.** 2016. Emerging diseases-the monkeypox epidemic in the Democratic Republic of the Congo. Clin Microbiol Infect **22:**658-659.

5. **Moss B.** 2013. Reflections on the early development of poxvirus vectors. Vaccine **31:**4220-4222.

6. **Chan WM, McFadden G.** 2014. Oncolytic Poxviruses. Annu Rev Virol **1:**119-141.

7. **Kirn DH, Thorne SH.** 2009. Targeted and armed oncolytic poxviruses: a novel multi-mechanistic therapeutic class for cancer. Nat Rev Cancer **9:**64-71.

8. **Maruri-Avidal L, Weisberg AS, Moss B.** 2013. Direct Formation of Vaccinia Viral Membranes from the Endoplasmic Reticulum in the Absence of the Newly Characterized L2-Interacting A30.5 Protein. J Virol doi:10.1128/JVI.02137-13.

9. **von Heijne G.** 2006. Membrane-protein topology. Nat Rev Mol Cell Biol **7:**909-918.

10. **Maruri-Avidal L, Weisberg AS, Moss B.** 2013. Association of the vaccinia virus a11 protein with the endoplasmic reticulum and crescent precursors of immature virions. J Virol **87:**10195-10206.

11. **Maruri-Avidal L, Weisberg AS, Moss B.** 2011. Vaccinia virus L2 protein associates with the endoplasmic reticulum near the growing edge of crescent precursors of immature virions and stabilizes a subset of viral membrane proteins. J Virol **85:**12431-12441.

12. **Hyun SI, Maruri-Avidal L, Moss B.** 2015. Topology of Endoplasmic Reticulum-Associated Cellular and Viral Proteins Determined with Split-GFP. Traffic **16:**787-795.

13. **International Committee on Taxonomy of Viruses., King AMQ.** 2012. Virus taxonomy : classification and nomenclature of viruses : ninth report of the International Committee on Taxonomy of Viruses. Academic Press, London ; Waltham, MA.

14. **Anonymous.** 2015. Virus Taxonomy: 2015 Release, *on* International Committee on Taxonomy of Viruses. http://www.ictvonline.org/virustaxonomy.asp. Accessed Feb 8, 2017.

15. **Thomas K, Tompkins DM, Sainsbury AW, Wood AR, Dalziel R, Nettleton PF, McInnes CJ.** 2003. A novel poxvirus lethal to red squirrels (Sciurus vulgaris). J Gen Virol **84:**3337-3341.

16. **Bracht AJ, Brudek RL, Ewing RY, Manire CA, Burek KA, Rosa C, Beckmen KB, Maruniak JE, Romero CH.** 2006. Genetic identification of novel poxviruses of cetaceans and pinnipeds. Arch Virol **151:**423-438.

17. **Himsworth CG, McInnes CJ, Coulter L, Everest DJ, Hill JE.** 2013. Characterization of a novel poxvirus in a North American red squirrel (Tamiasciurus hudsonicus). J Wildl Dis **49:**173-179.

18. **Gjessing MC, Yutin N, Tengs T, Senkevich T, Koonin E, Ronning HP, Alarcon M, Ylving S, Lie KI, Saure B, Tran L, Moss B, Dale OB.** 2015. Salmon Gill Poxvirus, the Deepest Representative of the Chordopoxvirinae. J Virol **89:**9348-9367.

19. **Airas N, Hautaniemi M, Syrja P, Knuuttila A, Putkuri N, Coulter L, McInnes CJ, Vapalahti O, Huovilainen A, Kinnunen PM.** 2016. Infection with Possible Novel Parapoxvirus in Horse, Finland, 2013. Emerg Infect Dis **22:**1242-1245.

20. **O'Dea MA, Tu SL, Pang S, De Ridder T, Jackson B, Upton C.** 2016. Genomic characterization of a novel poxvirus from a flying fox: evidence for a new genus? J Gen Virol **97:**2363-2375.

21. **Koonin EV, Yutin N.** 2010. Origin and evolution of eukaryotic large nucleo-cytoplasmic DNA viruses. Intervirology **53:**284-292.

22. **Arslan D, Legendre M, Seltzer V, Abergel C, Claverie JM.** 2011. Distant Mimivirus relative with a larger genome highlights the fundamental features of Megaviridae. Proc Natl Acad Sci U S A **108:**17486-17491.

23. **Philippe N, Legendre M, Doutre G, Coute Y, Poirot O, Lescot M, Arslan D, Seltzer V, Bertaux L, Bruley C, Garin J, Claverie JM, Abergel C.** 2013. Pandoraviruses: amoeba viruses with genomes up to 2.5 Mb reaching that of parasitic eukaryotes. Science **341:**281-286.

24. **Legendre M, Bartoli J, Shmakova L, Jeudy S, Labadie K, Adrait A, Lescot M, Poirot O, Bertaux L, Bruley C, Coute Y, Rivkina E, Abergel C, Claverie JM.** 2014. Thirty-thousand-year-old distant relative of giant icosahedral DNA viruses with a pandoravirus morphology. Proc Natl Acad Sci U S A **111:**4274-4279.

25. **Fenner F.** 1988. Smallpox and its eradication. World Health Organization, Geneva.

26. **Belongia EA, Naleway AL.** 2003. Smallpox vaccine: the good, the bad, and the ugly. Clin Med Res **1:**87-92.

27. **Hanna W, Baxby D.** 2002. Studies in smallpox and vaccination. 1913. Rev Med Virol **12:**201-209.

28. **Fenner F.** 1977. The eradication of smallpox. Prog Med Virol **23:**1-21.

29. **Moss B.** 2011. Smallpox vaccines: targets of protective immunity. Immunol Rev **239:**8-26.

30. **Riedel S.** 2005. Edward Jenner and the history of smallpox and vaccination. Proc (Bayl Univ Med Cent) **18:**21-25.

31. **Huygelen C.** 1996. [Jenner's cowpox vaccine in light of current vaccinology]. Verh K Acad Geneeskd Belg **58:**479-536; discussion 537-478.

32. **Plotkin SA, Orenstein WA.** 1999. Vaccines, 3rd ed. W.B. Saunders Co., Philadelphia.

33. **Cyrklaff M, Risco C, Fernandez JJ, Jimenez MV, Esteban M, Baumeister W, Carrascosa JL.** 2005. Cryo-electron tomography of vaccinia virus. Proc Natl Acad Sci U S A **102:**2772-2777.

34. **Roos N, Cyrklaff M, Cudmore S, Blasco R, Krijnse-Locker J, Griffiths G.** 1996. A novel immunogold cryoelectron microscopic approach to investigate the structure of the intracellular and extracellular forms of vaccinia virus. EMBO J **15:**2343-2355.

35. **Griffiths G, Wepf R, Wendt T, Locker JK, Cyrklaff M, Roos N.** 2001. Structure and assembly of intracellular mature vaccinia virus: isolated-particle analysis. J Virol **75:**11034-11055.

36. **Zwartouw HT.** 1964. The Chemical Composition of Vaccinia Virus. J Gen Microbiol **34:**115-123.

37. **Gupta A, Akin, D., and Bashir, R.** 2004. Single virus particle mass detection using microresonators with nanoscale thickness. Appl Physics Lett **84:**1976-1978.

38. **Johnson L, Gupta, A.K., Ghafoor, A., Akin, D., and Bashir, R.** 2006. Characterization of vaccinia virus particles using microscale silicon cantilever resonators and atomic force microscopy. Sensors and Actuators B Chemical **115:**189-197.

39. **Roening G, Holowczak JA.** 1974. Evidence for the presence of RNA in the purified virions of vaccinia virus. J Virol **14:**704-708.

40. **Lanzer W, Holowczak JA.** 1975. Polyamines in vaccinia virions and polypeptides released from viral cores by acid extraction. J Virol **16:**1254-1264.

41. **Goebel SJ, Johnson GP, Perkus ME, Davis SW, Winslow JP, Paoletti E.** 1990. The complete DNA sequence of vaccinia virus. Virology **179:**247-266, 517-263.

42. **Garon CF, Barbosa E, Moss B.** 1978. Visualization of an inverted terminal repetition in vaccinia virus DNA. Proc Natl Acad Sci U S A **75:**4863-4867.

43. **Baroudy BM, Venkatesan S, Moss B.** 1982. Incompletely base-paired flip-flop terminal loops link the two DNA strands of the vaccinia virus genome into one uninterrupted polynucleotide chain. Cell **28:**315-324.

44. **Hruby DE.** 1990. Vaccinia virus vectors: new strategies for producing recombinant vaccines. Clin Microbiol Rev **3:**153-170.

45. **Al Ali S, Baldanta S, Fernández-Escobar M, Guerra S.** 2016. Use of Reporter Genes in the Generation of Vaccinia Virus-Derived Vectors. Viruses **8:**134.

46. **Merchlinsky M, Garon CF, Moss B.** 1988. Molecular cloning and sequence of the concatemer junction from vaccinia virus replicative DNA. Viral nuclease cleavage sites in cruciform structures. J Mol Biol **199:**399-413.

47. **Wittek R, Cooper JA, Barbosa E, Moss B.** 1980. Expression of the vaccinia virus genome: analysis and mapping of mRNAs encoded within the inverted terminal repetition. Cell **21:**487-493.

48. **Moyer RW, Graves RL, Rothe CT.** 1980. The white pock (mu) mutants of rabbit poxvirus. III. Terminal DNA sequence duplication and transposition in rabbit poxvirus. Cell **22:**545-553.

49. **Moyer RW, Rothe CT.** 1980. The white pock mutants of rabbit poxvirus. I. Spontaneous host range mutants contain deletions. Virology **102:**119-132.

50. **Wittek R, Moss B.** 1980. Tandem repeats within the inverted terminal repetition of vaccinia virus DNA. Cell **21:**277-284.

51. **Upton C, Slack S, Hunter AL, Ehlers A, Roper RL.** 2003. Poxvirus orthologous clusters: toward defining the minimum essential poxvirus genome. J Virol **77:**7590-7600.

52. **McCarron RJ, Cabrera CV, Esteban M, McAllister WT, Holowczak JA.** 1978. Structure of vaccinia DNA: analysis of the viral genome by restriction endonucleases. Virology **86:**88-101.

53. **Mackett M, Archard LC.** 1979. Conservation and variation in Orthopoxvirus genome structure. J Gen Virol **45:**683-701.

54. **Moss B.** 2006. Poxvirus entry and membrane fusion. Virology **344:**48-54.

55. **Moss B.** 2016. Membrane fusion during poxvirus entry. Semin Cell Dev Biol **60:**89-96.

56. **Chung CS, Hsiao JC, Chang YS, Chang W.** 1998. A27L protein mediates vaccinia virus interaction with cell surface heparan sulfate. J Virol **72:**1577-1585.

57. **Hsiao JC, Chung CS, Chang W.** 1999. Vaccinia virus envelope D8L protein binds to cell surface chondroitin sulfate and mediates the adsorption of intracellular mature virions to cells. J Virol **73:**8750-8761.

58. **Lin CL, Chung CS, Heine HG, Chang W.** 2000. Vaccinia virus envelope H3L protein binds to cell surface heparan sulfate and is important for intracellular mature virion morphogenesis and virus infection in vitro and in vivo. J Virol **74:**3353-3365.

59. **Chiu WL, Lin CL, Yang MH, Tzou DL, Chang W.** 2007. Vaccinia virus 4c (A26L) protein on intracellular mature virus binds to the extracellular cellular matrix laminin. J Virol **81:**2149-2157.

60. **Howard AR, Senkevich TG, Moss B.** 2008. Vaccinia virus A26 and A27 proteins form a stable complex tethered to mature virions by association with the A17 transmembrane protein. J Virol **82:**12384-12391.

61. **Moss B.** 2012. Poxvirus cell entry: how many proteins does it take? Viruses **4:**688-707.

62. **Ravanello MP, Hruby DE.** 1994. Conditional lethal expression of the vaccinia virus L1R myristylated protein reveals a role in virion assembly. J Virol **68:**6401-6410.

63. **Senkevich TG, Ward BM, Moss B.** 2004. Vaccinia virus A28L gene encodes an essential protein component of the virion membrane with intramolecular disulfide bonds formed by the viral cytoplasmic redox pathway. J Virol **78:**2348-2356.

64. **Senkevich TG, Moss B.** 2005. Vaccinia virus H2 protein is an essential component of a complex involved in virus entry and cell-cell fusion. J Virol **79:**4744-4754.

65. **Senkevich TG, Ojeda S, Townsley A, Nelson GE, Moss B.** 2005. Poxvirus multiprotein entry-fusion complex. Proc Natl Acad Sci U S A **102:**18572-18577.

66. **Townsley AC, Senkevich TG, Moss B.** 2005. Vaccinia virus A21 virion membrane protein is required for cell entry and fusion. J Virol **79:**9458-9469.

67. **Townsley AC, Senkevich TG, Moss B.** 2005. The product of the vaccinia virus L5R gene is a fourth membrane protein encoded by all poxviruses that is required for cell entry and cell-cell fusion. J Virol **79:**10988-10998.

68. **Brown E, Senkevich TG, Moss B.** 2006. Vaccinia virus F9 virion membrane protein is required for entry but not virus assembly, in contrast to the related L1 protein. J Virol **80:**9455-9464.

69. **Izmailyan RA, Huang CY, Mohammad S, Isaacs SN, Chang W.** 2006. The envelope G3L protein is essential for entry of vaccinia virus into host cells. J Virol **80:**8402-8410.

70. **Ojeda S, Domi A, Moss B.** 2006. Vaccinia virus G9 protein is an essential component of the poxvirus entry-fusion complex. J Virol **80:**9822-9830.

71. **Ojeda S, Senkevich TG, Moss B.** 2006. Entry of vaccinia virus and cell-cell fusion require a highly conserved cysteine-rich membrane protein encoded by the A16L gene. J Virol **80:**51-61.

72. **Turner PC, Dilling BP, Prins C, Cresawn SG, Moyer RW, Condit RC.** 2007. Vaccinia virus temperature-sensitive mutants in the A28 gene produce non-infectious virions that bind to cells but are defective in entry. Virology **366:**62-72.

73. **Bisht H, Weisberg AS, Moss B.** 2008. Vaccinia virus l1 protein is required for cell entry and membrane fusion. J Virol **82:**8687-8694.

74. **Nelson GE, Wagenaar TR, Moss B.** 2008. A conserved sequence within the H2 subunit of the vaccinia virus entry/fusion complex is important for interaction with the A28 subunit and infectivity. J Virol **82:**6244-6250.

75. **Satheshkumar PS, Moss B.** 2009. Characterization of a newly identified 35-amino-acid component of the vaccinia virus entry/fusion complex conserved in all chordopoxviruses. J Virol **83:**12822-12832.

76. **Doms RW, Blumenthal R, Moss B.** 1990. Fusion of intra- and extracellular forms of vaccinia virus with the cell membrane. J Virol **64:**4884-4892.

77. **Townsley AC, Weisberg AS, Wagenaar TR, Moss B.** 2006. Vaccinia virus entry into cells via a low-pH-dependent endosomal pathway. J Virol **80:**8899-8908.

78. **Wagenaar TR, Ojeda S, Moss B.** 2008. Vaccinia virus A56/K2 fusion regulatory protein interacts with the A16 and G9 subunits of the entry fusion complex. J Virol **82:**5153-5160.

79. **Wolfe CL, Moss B.** 2011. Interaction between the G3 and L5 proteins of the vaccinia virus entry-fusion complex. Virology **412:**278-283.

80. **Schmidt FI, Bleck CK, Helenius A, Mercer J.** 2011. Vaccinia extracellular virions enter cells by macropinocytosis and acid-activated membrane rupture. EMBO J **30:**3647-3661.

81. **Yang Z, Bruno DP, Martens CA, Porcella SF, Moss B.** 2010. Simultaneous high-resolution analysis of vaccinia virus and host cell transcriptomes by deep RNA sequencing. Proc Natl Acad Sci U S A **107:**11513-11518.

82. **Davison AJ, Moss B.** 1989. Structure of vaccinia virus early promoters. J Mol Biol **210:**749-769.

83. **Davison AJ, Moss B.** 1989. Structure of vaccinia virus late promoters. J Mol Biol **210:**771-784.

84. **Baldick CJ, Jr., Keck JG, Moss B.** 1992. Mutational analysis of the core, spacer, and initiator regions of vaccinia virus intermediate-class promoters. J Virol **66:**4710-4719.

85. **Yang Z, Moss B.** 2009. Interaction of the vaccinia virus RNA polymerase-associated 94-kilodalton protein with the early transcription factor. J Virol **83:**12018-12026.

86. **Mallardo M, Schleich S, Krijnse Locker J.** 2001. Microtubule-dependent organization of vaccinia virus core-derived early mRNAs into distinct cytoplasmic structures. Mol Biol Cell **12:**3875-3891.

87. **Carter GC, Rodger G, Murphy BJ, Law M, Krauss O, Hollinshead M, Smith GL.** 2003. Vaccinia virus cores are transported on microtubules. J Gen Virol **84:**2443-2458.

88. **Kates JR, McAuslan BR.** 1967. Poxvirus DNA-dependent RNA polymerase. Proc Natl Acad Sci U S A **58:**134-141.

89. **Munyon W, Paoletti E, Grace JT, Jr.** 1967. RNA polymerase activity in purified infectious vaccinia virus. Proc Natl Acad Sci U S A **58:**2280-2287.

90. **Kates J, Beeson J.** 1970. Ribonucleic acid synthesis in vaccinia virus. II. Synthesis of polyriboadenylic acid. J Mol Biol **50:**19-33.

91. **Wei CM, Moss B.** 1975. Methylated nucleotides block 5'-terminus of vaccinia virus messenger RNA. Proc Natl Acad Sci U S A **72:**318-322.

92. **Broyles SS, Yuen L, Shuman S, Moss B.** 1988. Purification of a factor required for transcription of vaccinia virus early genes. J Biol Chem **263:**10754-10760.

93. **Broyles SS, Fesler BS.** 1990. Vaccinia virus gene encoding a component of the viral early transcription factor. J Virol **64:**1523-1529.

94. **Gershon PD, Moss B.** 1990. Early transcription factor subunits are encoded by vaccinia virus late genes. Proc Natl Acad Sci U S A **87:**4401-4405.

95. **Ahn BY, Moss B.** 1992. RNA polymerase-associated transcription specificity factor encoded by vaccinia virus. Proc Natl Acad Sci U S A **89:**3536-3540.

96. **Ahn BY, Gershon PD, Moss B.** 1994. RNA polymerase-associated protein Rap94 confers promoter specificity for initiating transcription of vaccinia virus early stage genes. J Biol Chem **269:**7552-7557.

97. **Deng L, Shuman S.** 1994. A role for the H4 subunit of vaccinia RNA polymerase in transcription initiation at a viral early promoter. J Biol Chem **269:**14323-14328.

98. **Baroudy BM, Moss B.** 1980. Purification and characterization of a DNA-dependent RNA polymerase from vaccinia virions. J Biol Chem **255:**4372-4380.

99. **Broyles SS, Moss B.** 1986. Homology between RNA polymerases of poxviruses, prokaryotes, and eukaryotes: nucleotide sequence and transcriptional analysis of vaccinia virus genes encoding 147-kDa and 22-kDa subunits. Proc Natl Acad Sci U S A **83:**3141-3145.

100. **Ahn BY, Gershon PD, Jones EV, Moss B.** 1990. Identification of rpo30, a vaccinia virus RNA polymerase gene with structural similarity to a eucaryotic transcription elongation factor. Mol Cell Biol **10:**5433-5441.

101. **Ahn BY, Jones EV, Moss B.** 1990. Identification of the vaccinia virus gene encoding an 18-kilodalton subunit of RNA polymerase and demonstration of a 5' poly(A) leader on its early transcript. J Virol **64:**3019-3024.

102. **Broyles SS, Pennington MJ.** 1990. Vaccinia virus gene encoding a 30-kilodalton subunit of the viral DNA-dependent RNA polymerase. J Virol **64:**5376-5382.

103. **Quick SD, Broyles SS.** 1990. Vaccinia virus gene D7R encodes a 20,000-dalton subunit of the viral DNA-dependent RNA polymerase. Virology **178:**603-605.

104. **Amegadzie BY, Ahn BY, Moss B.** 1991. Identification, sequence, and expression of the gene encoding a Mr 35,000 subunit of the vaccinia virus DNA-dependent RNA polymerase. J Biol Chem **266:**13712-13718.

105. **Ahn BY, Rosel J, Cole NB, Moss B.** 1992. Identification and expression of rpo19, a vaccinia virus gene encoding a 19-kilodalton DNA-dependent RNA polymerase subunit. J Virol **66:**971-982.

106. **Amegadzie BY, Ahn BY, Moss B.** 1992. Characterization of a 7-kilodalton subunit of vaccinia virus DNA-dependent RNA polymerase with structural similarities to the smallest subunit of eukaryotic RNA polymerase II. J Virol **66:**3003-3010.

107. **Rosales R, Harris N, Ahn BY, Moss B.** 1994. Purification and identification of a vaccinia virus-encoded intermediate stage promoter-specific transcription factor that has homology to eukaryotic transcription factor SII (TFIIS) and an additional role as a viral RNA polymerase subunit. J Biol Chem **269:**14260-14267.

108. **Katsafanas GC, Moss B.** 1999. Histidine codons appended to the gene encoding the RPO22 subunit of vaccinia virus RNA polymerase facilitate the isolation and purification of functional enzyme and associated proteins from virus-infected cells. Virology **258:**469-479.

109. **Broyles SS, Moss B.** 1987. Sedimentation of an RNA polymerase complex from vaccinia virus that specifically initiates and terminates transcription. Mol Cell Biol **7:**7-14.

110. **Yuen L, Moss B.** 1987. Oligonucleotide sequence signaling transcriptional termination of vaccinia virus early genes. Proc Natl Acad Sci U S A **84:**6417-6421.

111. **Rosales R, Sutter G, Moss B.** 1994. A cellular factor is required for transcription of vaccinia viral intermediate-stage genes. Proc Natl Acad Sci U S A **91:**3794-3798.

112. **Sanz P, Moss B.** 1999. Identification of a transcription factor, encoded by two vaccinia virus early genes, that regulates the intermediate stage of viral gene expression. Proc Natl Acad Sci U S A **96:**2692-2697.

113. **Yang Z, Reynolds SE, Martens CA, Bruno DP, Porcella SF, Moss B.** 2011. Expression profiling of the intermediate and late stages of poxvirus replication. J Virol **85:**9899-9908.

114. **Keck JG, Baldick CJ, Jr., Moss B.** 1990. Role of DNA replication in vaccinia virus gene expression: a naked template is required for transcription of three late trans-activator genes. Cell **61:**801-809.

115. **Kovacs GR, Moss B.** 1996. The vaccinia virus H5R gene encodes late gene transcription factor 4: purification, cloning, and overexpression. J Virol **70:**6796-6802.

116. **Dellis S, Strickland KC, McCrary WJ, Patel A, Stocum E, Wright CF.** 2004. Protein interactions among the vaccinia virus late transcription factors. Virology **329:**328-336.

117. **Oda KI, Joklik WK.** 1967. Hybridization and sedimentation studies on "early" and "late" vaccinia messenger RNA. J Mol Biol **27:**395-419.

118. **Sebring ED, Salzman NP.** 1967. Metabolic properties of early and late vaccinia virus messenger ribonucleic acid. J Virol **1:**550-558.

119. **Vos JC, Stunnenberg HG.** 1988. Derepression of a novel class of vaccinia virus genes upon DNA replication. EMBO J **7:**3487-3492.

120. **Baldick CJ, Jr., Moss B.** 1993. Characterization and temporal regulation of mRNAs encoded by vaccinia virus intermediate-stage genes. J Virol **67:**3515-3527.

121. **Shors T, Keck JG, Moss B.** 1999. Down regulation of gene expression by the vaccinia virus D10 protein. J Virol **73:**791-796.

122. **Parrish S, Moss B.** 2006. Characterization of a vaccinia virus mutant with a deletion of the D10R gene encoding a putative negative regulator of gene expression. J Virol **80:**553-561.

123. **Parrish S, Resch W, Moss B.** 2007. Vaccinia virus D10 protein has mRNA decapping activity, providing a mechanism for control of host and viral gene expression. Proc Natl Acad Sci U S A **104:**2139-2144.

124. **Parrish S, Hurchalla M, Liu SW, Moss B.** 2009. The African swine fever virus g5R protein possesses mRNA decapping activity. Virology **393:**177-182.

125. **Liu SW, Wyatt LS, Orandle MS, Minai M, Moss B.** 2014. The D10 decapping enzyme of vaccinia virus contributes to decay of cellular and viral mRNAs and to virulence in mice. J Virol **88:**202-211.

126. **Mahr A, Roberts BE.** 1984. Arrangement of late RNAs transcribed from a 7.1-kilobase EcoRI vaccinia virus DNA fragment. J Virol **49:**510-520.

127. **Stark GR, Kerr IM, Williams BR, Silverman RH, Schreiber RD.** 1998. How cells respond to interferons. Annu Rev Biochem **67:**227-264.

128. **Silverman RH.** 2007. Viral encounters with 2',5'-oligoadenylate synthetase and RNase L during the interferon antiviral response. J Virol **81:**12720-12729.

129. **Perdiguero B, Esteban M.** 2009. The interferon system and vaccinia virus evasion mechanisms. J Interferon Cytokine Res **29:**581-598.

130. **Liu SW, Katsafanas GC, Liu R, Wyatt LS, Moss B.** 2015. Poxvirus decapping enzymes enhance virulence by preventing the accumulation of dsRNA and the induction of innate antiviral responses. Cell Host Microbe **17:**320-331.

131. **Cairns J.** 1960. The initiation of vaccinia infection. Virology **11:**603-623.

132. **Harford CG, Hamlin A, Rieders E.** 1966. Electron microscopic autoradiography of DNA synthesis in cells infected with vaccinia virus. Exp Cell Res **42:**50-57.

133. **Katsafanas GC, Moss B.** 2007. Colocalization of transcription and translation within cytoplasmic poxvirus factories coordinates viral expression and subjugates host functions. Cell Host Microbe **2:**221-228.

134. **Challberg MD, Englund PT.** 1979. Purification and properties of the deoxyribonucleic acid polymerase induced by vaccinia virus. J Biol Chem **254:**7812-7819.

135. **Earl PL, Jones EV, Moss B.** 1986. Homology between DNA polymerases of poxviruses, herpesviruses, and adenoviruses: nucleotide sequence of the vaccinia virus DNA polymerase gene. Proc Natl Acad Sci U S A **83:**3659-3663.

136. **McDonald WF, Traktman P.** 1994. Vaccinia virus DNA polymerase. In vitro analysis of parameters affecting processivity. J Biol Chem **269:**31190-31197.

137. **Evans E, Traktman P.** 1987. Molecular genetic analysis of a vaccinia virus gene with an essential role in DNA replication. J Virol **61:**3152-3162.

138. **Roseman NA, Hruby DE.** 1987. Nucleotide sequence and transcript organization of a region of the vaccinia virus genome which encodes a constitutively expressed gene required for DNA replication. J Virol **61:**1398-1406.

139. **Evans E, Traktman P.** 1992. Characterization of vaccinia virus DNA replication mutants with lesions in the D5 gene. Chromosoma **102:**S72-82.

140. **Evans E, Klemperer N, Ghosh R, Traktman P.** 1995. The vaccinia virus D5 protein, which is required for DNA replication, is a nucleic acid-independent nucleoside triphosphatase. J Virol **69:**5353-5361.

141. **De Silva FS, Lewis W, Berglund P, Koonin EV, Moss B.** 2007. Poxvirus DNA primase. Proc Natl Acad Sci U S A **104:**18724-18729.

142. **De Silva FS, Paran N, Moss B.** 2009. Products and substrate/template usage of vaccinia virus DNA primase. Virology **383:**136-141.

143. **Banham AH, Smith GL.** 1992. Vaccinia virus gene B1R encodes a 34-kDa serine/threonine protein kinase that localizes in cytoplasmic factories and is packaged into virions. Virology **191:**803-812.

144. **Lin S, Chen W, Broyles SS.** 1992. The vaccinia virus B1R gene product is a serine/threonine protein kinase. J Virol **66:**2717-2723.

145. **Rempel RE, Traktman P.** 1992. Vaccinia virus B1 kinase: phenotypic analysis of temperature-sensitive mutants and enzymatic characterization of recombinant proteins. J Virol **66:**4413-4426.

146. **Millns AK, Carpenter MS, DeLange AM.** 1994. The vaccinia virus-encoded uracil DNA glycosylase has an essential role in viral DNA replication. Virology **198:**504-513.

147. **Nichols RJ, Wiebe MS, Traktman P.** 2006. The vaccinia-related kinases phosphorylate the N' terminus of BAF, regulating its interaction with DNA and its retention in the nucleus. Mol Biol Cell **17:**2451-2464.

148. **Wiebe MS, Traktman P.** 2007. Poxviral B1 kinase overcomes barrier to autointegration factor, a host defense against virus replication. Cell Host Microbe **1:**187-197.

149. **Beaud G, Beaud R, Leader DP.** 1995. Vaccinia virus gene H5R encodes a protein that is phosphorylated by the multisubstrate vaccinia virus B1R protein kinase. J Virol **69:**1819-1826.

150. **Ishii K, Moss B.** 2001. Role of vaccinia virus A20R protein in DNA replication: construction and characterization of temperature-sensitive mutants. J Virol **75:**1656-1663.

151. **Klemperer N, McDonald W, Boyle K, Unger B, Traktman P.** 2001. The A20R protein is a stoichiometric component of the processive form of vaccinia virus DNA polymerase. J Virol **75:**12298-12307.

152. **Punjabi A, Boyle K, DeMasi J, Grubisha O, Unger B, Khanna M, Traktman P.** 2001. Clustered charge-to-alanine mutagenesis of the vaccinia virus A20 gene: temperature-sensitive mutants have a DNA-minus phenotype and are defective in the production of processive DNA polymerase activity. J Virol **75:**12308-12318.

153. **Ishii K, Moss B.** 2002. Mapping interaction sites of the A20R protein component of the vaccinia virus DNA replication complex. Virology **303:**232-239.

154. **McCraith S, Holtzman T, Moss B, Fields S.** 2000. Genome-wide analysis of vaccinia virus protein-protein interactions. Proc Natl Acad Sci U S A **97:**4879-4884.

155. **Davis RE, Mathews CK.** 1993. Acidic C terminus of vaccinia virus DNA-binding protein interacts with ribonucleotide reductase. Proc Natl Acad Sci U S A **90:**745-749.

156. **Rochester SC, Traktman P.** 1998. Characterization of the single-stranded DNA binding protein encoded by the vaccinia virus I3 gene. J Virol **72:**2917-2926.

157. **Greseth MD, Boyle KA, Bluma MS, Unger B, Wiebe MS, Soares-Martins JA, Wickramasekera NT, Wahlberg J, Traktman P.** 2012. Molecular genetic and biochemical characterization of the vaccinia virus I3 protein, the replicative single-stranded DNA binding protein. J Virol **86:**6197-6209.

158. **Moss B.** 2013. Poxvirus DNA replication. Cold Spring Harb Perspect Biol **5**.

159. **Moyer RW, Graves RL.** 1981. The mechanism of cytoplasmic orthopoxvirus DNA replication. Cell **27:**391-401.

160. **Baroudy BM, Venkatesan S, Moss B.** 1983. Structure and replication of vaccinia virus telomeres. Cold Spring Harb Symp Quant Biol **47 Pt 2:**723-729.

161. **Garcia AD, Aravind L, Koonin EV, Moss B.** 2000. Bacterial-type DNA holliday junction resolvases in eukaryotic viruses. Proc Natl Acad Sci U S A **97:**8926-8931.

162. **Garcia AD, Moss B.** 2001. Repression of vaccinia virus Holliday junction resolvase inhibits processing of viral DNA into unit-length genomes. J Virol **75:**6460-6471.

163. **Olgiati DD, Pogo BG, Dales S.** 1976. Evidence for RNA linked to nascent DNA in HeLa cells. J Cell Biol **68:**557-566.

164. **Esteban M, Holowczak JA.** 1977. Replication of vaccinia DNA in mouse L cells. I. In vivo DNA synthesis. Virology **78:**57-75.

165. **Paran N, De Silva FS, Senkevich TG, Moss B.** 2009. Cellular DNA ligase I is recruited to cytoplasmic vaccinia virus factories and masks the role of the vaccinia ligase in viral DNA replication. Cell Host Microbe **6:**563-569.

166. **Senkevich TG, Bruno D, Martens C, Porcella SF, Wolf YI, Moss B.** 2015. Mapping vaccinia virus DNA replication origins at nucleotide level by deep sequencing. Proc Natl Acad Sci U S A **112:**10908-10913.

167. **Morgan C, Wyckoff RW.** 1950. The electron microscopy of fowl pox virus within the chorioallantoic membrane. J Immunol **65:**285-295.

168. **Gaylord WH, Jr., Melnick JL.** 1953. Intracellular forms of pox viruses as shown by the electron microscope (Vaccinia, Ectromelia, Molluscum Contagiosum). J Exp Med **98:**157-172.

169. **Morgan C, Ellison SA, Rose HM, Moore DH.** 1954. Structure and development of viruses observed in the electron microscope. II. Vaccinia and fowl pox viruses. J Exp Med **100:**301-310.

170. **Hiller G, Weber K.** 1985. Golgi-derived membranes that contain an acylated viral polypeptide are used for vaccinia virus envelopment. J Virol **55:**651-659.

171. **Tooze J, Hollinshead M, Reis B, Radsak K, Kern H.** 1993. Progeny vaccinia and human cytomegalovirus particles utilize early endosomal cisternae for their envelopes. Eur J Cell Biol **60:**163-178.

172. **Schmelz M, Sodeik B, Ericsson M, Wolffe EJ, Shida H, Hiller G, Griffiths G.** 1994. Assembly of vaccinia virus: the second wrapping cisterna is derived from the trans Golgi network. J Virol **68:**130-147.

173. **Morgan C.** 1976. The insertion of DNA into vaccinia virus. Science **193:**591-592.

174. **Grimley PM, Rosenblum EN, Mims SJ, Moss B.** 1970. Interruption by Rifampin of an early stage in vaccinia virus morphogenesis: accumulation of membranes which are precursors of virus envelopes. J Virol **6:**519-533.

175. **Cassetti MC, Merchlinsky M, Wolffe EJ, Weisberg AS, Moss B.** 1998. DNA packaging mutant: repression of the vaccinia virus A32 gene results in noninfectious, DNA-deficient, spherical, enveloped particles. J Virol **72:**5769-5780.

176. **Grubisha O, Traktman P.** 2003. Genetic analysis of the vaccinia virus I6 telomere-binding protein uncovers a key role in genome encapsidation. J Virol **77:**10929-10942.

177. **Unger B, Traktman P.** 2004. Vaccinia virus morphogenesis: a13 phosphoprotein is required for assembly of mature virions. J Virol **78:**8885-8901.

178. **Moss B.** 2015. Poxvirus membrane biogenesis. Virology doi:10.1016/j.virol.2015.02.003.

179. **Senkevich TG, White CL, Koonin EV, Moss B.** 2000. A viral member of the ERV1/ALR protein family participates in a cytoplasmic pathway of disulfide bond formation. Proc Natl Acad Sci U S A **97:**12068-12073.

180. **Senkevich TG, White CL, Koonin EV, Moss B.** 2002. Complete pathway for protein disulfide bond formation encoded by poxviruses. Proc Natl Acad Sci U S A **99:**6667-6672.

181. **Senkevich TG, White CL, Weisberg A, Granek JA, Wolffe EJ, Koonin EV, Moss B.** 2002. Expression of the vaccinia virus A2.5L redox protein is required for virion morphogenesis. Virology **300:**296-303.

182. **White CL, Senkevich TG, Moss B.** 2002. Vaccinia virus G4L glutaredoxin is an essential intermediate of a cytoplasmic disulfide bond pathway required for virion assembly. J Virol **76:**467-472.

183. **VanSlyke JK, Franke CA, Hruby DE.** 1991. Proteolytic maturation of vaccinia virus core proteins: identification of a conserved motif at the N termini of the 4b and 25K virion proteins. J Gen Virol **72 (Pt 2):**411-416.

184. **Ansarah-Sobrinho C, Moss B.** 2004. Role of the I7 protein in proteolytic processing of vaccinia virus membrane and core components. J Virol **78:**6335-6343.

185. **Ansarah-Sobrinho C, Moss B.** 2004. Vaccinia virus G1 protein, a predicted metalloprotease, is essential for morphogenesis of infectious virions but not for cleavage of major core proteins. J Virol **78:**6855-6863.

186. **Geada MM, Galindo I, Lorenzo MM, Perdiguero B, Blasco R.** 2001. Movements of vaccinia virus intracellular enveloped virions with GFP tagged to the F13L envelope protein. J Gen Virol **82:**2747-2760.

187. **Hollinshead M, Rodger G, Van Eijl H, Law M, Hollinshead R, Vaux DJ, Smith GL.** 2001. Vaccinia virus utilizes microtubules for movement to the cell surface. J Cell Biol **154:**389-402.

188. **Rietdorf J, Ploubidou A, Reckmann I, Holmstrom A, Frischknecht F, Zettl M, Zimmermann T, Way M.** 2001. Kinesin-dependent movement on microtubules precedes actin-based motility of vaccinia virus. Nat Cell Biol **3:**992-1000.

189. **Ward BM, Moss B.** 2004. Vaccinia virus A36R membrane protein provides a direct link between intracellular enveloped virions and the microtubule motor kinesin. J Virol **78:**2486-2493.

190. **Jeshtadi A, Burgos P, Stubbs CD, Parker AW, King LA, Skinner MA, Botchway SW.** 2010. Interaction of poxvirus intracellular mature virion proteins with the TPR domain of kinesin light chain in live infected cells revealed by two-photon-induced fluorescence resonance energy transfer fluorescence lifetime imaging microscopy. J Virol **84:**12886-12894.

191. **Herrero-Martinez E, Roberts KL, Hollinshead M, Smith GL.** 2005. Vaccinia virus intracellular enveloped virions move to the cell periphery on microtubules in the absence of the A36R protein. J Gen Virol **86:**2961-2968.

192. **Morgan GW, Hollinshead M, Ferguson BJ, Murphy BJ, Carpentier DC, Smith GL.** 2010. Vaccinia protein F12 has structural similarity to kinesin light chain and contains a motor binding motif required for virion export. PLoS Pathog **6:**e1000785.

193. **Newsome TP, Scaplehorn N, Way M.** 2004. SRC mediates a switch from microtubule- to actin-based motility of vaccinia virus. Science **306:**124-129.

194. **Wolffe EJ, Katz E, Weisberg A, Moss B.** 1997. The A34R glycoprotein gene is required for induction of specialized actin-containing microvilli and efficient cell-to-cell transmission of vaccinia virus. J Virol **71:**3904-3915.

195. **Roper RL, Wolffe EJ, Weisberg A, Moss B.** 1998. The envelope protein encoded by the A33R gene is required for formation of actin-containing microvilli and efficient cell-to-cell spread of vaccinia virus. J Virol **72:**4192-4204.

196. **Sanderson CM, Frischknecht F, Way M, Hollinshead M, Smith GL.** 1998. Roles of vaccinia virus EEV-specific proteins in intracellular actin tail formation and low pH-induced cell-cell fusion. J Gen Virol **79 (Pt 6):**1415-1425.

197. **Wolffe EJ, Weisberg AS, Moss B.** 1998. Role for the vaccinia virus A36R outer envelope protein in the formation of virus-tipped actin-containing microvilli and cell-to-cell virus spread. Virology **244:**20-26.

198. **Anonymous.** 2017. English Oxford Living Dictionaries. Oxford University Press.

199. **Dales S, Mosbach EH.** 1968. Vaccinia as a model for membrane biogenesis. Virology **35:**564-583.

200. **Sodeik B, Doms RW, Ericsson M, Hiller G, Machamer CE, van 't Hof W, van Meer G, Moss B, Griffiths G.** 1993. Assembly of vaccinia virus: role of the intermediate compartment between the endoplasmic reticulum and the Golgi stacks. J Cell Biol **121:**521-541.

201. **Risco C, Rodriguez JR, Lopez-Iglesias C, Carrascosa JL, Esteban M, Rodriguez D.** 2002. Endoplasmic reticulum-Golgi intermediate compartment

membranes and vimentin filaments participate in vaccinia virus assembly. J Virol **76:**1839-1855.

202. **Chichon FJ, Rodriguez MJ, Risco C, Fraile-Ramos A, Fernandez JJ, Esteban M, Carrascosa JL.** 2009. Membrane remodelling during vaccinia virus morphogenesis. Biol Cell **101:**401-414.

203. **Chlanda P, Carbajal MA, Cyrklaff M, Griffiths G, Krijnse-Locker J.** 2009. Membrane rupture generates single open membrane sheets during vaccinia virus assembly. Cell Host Microbe **6:**81-90.

204. **Meng X, Embry A, Sochia D, Xiang Y.** 2007. Vaccinia virus A6L encodes a virion core protein required for formation of mature virion. J Virol **81:**1433-1443.

205. **Meng X, Embry A, Rose L, Yan B, Xu C, Xiang Y.** 2012. Vaccinia virus A6 is essential for virion membrane biogenesis and localization of virion membrane proteins to sites of virion assembly. J Virol **86:**5603-5613.

206. **Resch W, Weisberg AS, Moss B.** 2005. Vaccinia virus nonstructural protein encoded by the A11R gene is required for formation of the virion membrane. J Virol **79:**6598-6609.

207. **Wu X, Meng X, Yan B, Rose L, Deng J, Xiang Y.** 2012. Vaccinia virus virion membrane biogenesis protein A11 associates with viral membranes in a manner that requires the expression of another membrane biogenesis protein, A6. J Virol **86:**11276-11286.

208. **Satheshkumar PS, Weisberg A, Moss B.** 2009. Vaccinia virus H7 protein contributes to the formation of crescent membrane precursors of immature virions. J Virol **83:**8439-8450.

209. **Meng X, Wu X, Yan B, Deng J, Xiang Y.** 2013. Analysis of the role of vaccinia virus H7 in virion membrane biogenesis with an H7-deletion mutant. J Virol **87:**8247-8253.

210. **Maruri-Avidal L, Domi A, Weisberg AS, Moss B.** 2011. Participation of vaccinia virus l2 protein in the formation of crescent membranes and immature virions. J Virol **85:**2504-2511.

211. **Maruri-Avidal L, Weisberg AS, Bisht H, Moss B.** 2013. Analysis of viral membranes formed in cells infected by a vaccinia virus L2-deletion mutant suggests their origin from the endoplasmic reticulum. J Virol **87:**1861-1871.

212. **Kolli S, Meng X, Wu X, Shengjuler D, Cameron CE, Xiang Y, Deng J.** 2015. Structure-function analysis of vaccinia virus H7 protein reveals a novel phosphoinositide binding fold essential for poxvirus replication. J Virol **89:**2209-2219.

213. **Rodriguez D, Risco C, Rodriguez JR, Carrascosa JL, Esteban M.** 1996. Inducible expression of the vaccinia virus A17L gene provides a synchronized system to monitor sorting of viral proteins during morphogenesis. J Virol **70:**7641-7653.

214. **Wolffe EJ, Moore DM, Peters PJ, Moss B.** 1996. Vaccinia virus A17L open reading frame encodes an essential component of nascent viral membranes that is required to initiate morphogenesis. J Virol **70:**2797-2808.

215. **Rodriguez JR, Risco C, Carrascosa JL, Esteban M, Rodriguez D.** 1998. Vaccinia virus 15-kilodalton (A14L) protein is essential for assembly and attachment of viral crescents to virosomes. J Virol **72:**1287-1296.

216. **Traktman P, Liu K, DeMasi J, Rollins R, Jesty S, Unger B.** 2000. Elucidating the essential role of the A14 phosphoprotein in vaccinia virus morphogenesis: construction and characterization of a tetracycline-inducible recombinant. J Virol **74:**3682-3695.

217. **Erlandson KJ, Bisht H, Weisberg AS, Hyun SI, Hansen BT, Fischer ER, Hinshaw JE, Moss B.** 2016. Poxviruses Encode a Reticulon-Like Protein that Promotes Membrane Curvature. Cell Rep **14:**2084-2091.

218. **Voeltz GK, Prinz WA, Shibata Y, Rist JM, Rapoport TA.** 2006. A class of membrane proteins shaping the tubular endoplasmic reticulum. Cell **124:**573-586.

219. **Heuser J.** 2005. Deep-etch EM reveals that the early poxvirus envelope is a single membrane bilayer stabilized by a geodetic "honeycomb" surface coat. J Cell Biol **169:**269-283.

220. **Szajner P, Weisberg AS, Lebowitz J, Heuser J, Moss B.** 2005. External scaffold of spherical immature poxvirus particles is made of protein trimers, forming a honeycomb lattice. J Cell Biol **170:**971-981.

221. **Bisht H, Weisberg AS, Szajner P, Moss B.** 2009. Assembly and disassembly of the capsid-like external scaffold of immature virions during vaccinia virus morphogenesis. J Virol **83:**9140-9150.

222. **Unger B, Mercer J, Boyle KA, Traktman P.** 2013. Biogenesis of the vaccinia virus membrane: genetic and ultrastructural analysis of the contributions of the A14 and A17 proteins. J Virol **87:**1083-1097.

223. **Hyun JK, Coulibaly F, Turner AP, Baker EN, Mercer AA, Mitra AK.** 2007. The structure of a putative scaffolding protein of immature poxvirus particles as determined by electron microscopy suggests similarity with capsid proteins of large icosahedral DNA viruses. J Virol **81:**11075-11083.

224. **Bahar MW, Graham SC, Stuart DI, Grimes JM.** 2011. Insights into the evolution of a complex virus from the crystal structure of vaccinia virus D13. Structure **19:**1011-1020.

225. **Hyun JK, Accurso C, Hijnen M, Schult P, Pettikiriarachchi A, Mitra AK, Coulibaly F.** 2011. Membrane remodeling by the double-barrel scaffolding protein of poxvirus. PLoS Pathog **7:**e1002239.

226. **Sodeik B, Griffiths G, Ericsson M, Moss B, Doms RW.** 1994. Assembly of vaccinia virus: effects of rifampin on the intracellular distribution of viral protein p65. J Virol **68:**1103-1114.

227. **Mohandas AR, Dales S.** 1995. Involvement of spicules in the formation of vaccinia virus envelopes elucidated by a conditional lethal mutant. Virology **214:**494-502.

228. **Rodriguez D, Rodriguez JR, Esteban M.** 1993. The vaccinia virus 14-kilodalton fusion protein forms a stable complex with the processed protein encoded by the vaccinia virus A17L gene. J Virol **67:**3435-3440.

229. **Takahashi T, Oie M, Ichihashi Y.** 1994. N-terminal amino acid sequences of vaccinia virus structural proteins. Virology **202:**844-852.

230. **Betakova T, Wolffe EJ, Moss B.** 1999. Regulation of vaccinia virus morphogenesis: phosphorylation of the A14L and A17L membrane proteins and C-terminal truncation of the A17L protein are dependent on the F10L kinase. J Virol **73:**3534-3543.

231. **Yeh WW, Moss B, Wolffe EJ.** 2000. The vaccinia virus A9L gene encodes a membrane protein required for an early step in virion morphogenesis. J Virol **74:**9701-9711.

232. **Elofsson A, von Heijne G.** 2007. Membrane protein structure: prediction versus reality. Annu Rev Biochem **76:**125-140.

233. **Laudon H, Hansson EM, Melen K, Bergman A, Farmery MR, Winblad B, Lendahl U, von Heijne G, Naslund J.** 2005. A nine-transmembrane domain topology for presenilin 1. J Biol Chem **280:**35352-35360.

234. **Pan CJ, Lei KJ, Annabi B, Hemrika W, Chou JY.** 1998. Transmembrane topology of glucose-6-phosphatase. J Biol Chem **273:**6144-6148.

235. **Lorenz H, Hailey DW, Wunder C, Lippincott-Schwartz J.** 2006. The fluorescence protease protection (FPP) assay to determine protein localization and membrane topology. Nat Protoc **1:**276-279.

236. **Wright LP, Court H, Mor A, Ahearn IM, Casey PJ, Philips MR.** 2009. Topology of mammalian isoprenylcysteine carboxyl methyltransferase determined in live cells with a fluorescent probe. Mol Cell Biol **29:**1826-1833.

237. **Remy I, Michnick SW.** 2006. A highly sensitive protein-protein interaction assay based on Gaussia luciferase. Nat Methods **3:**977-979.

238. **Li HY, Zheng XM, Che MX, Hu HY.** 2012. A redox-sensitive luciferase assay for determining the localization and topology of endoplasmic reticulum proteins. PLoS One **7:**e35628.

239. **Magliery TJ, Wilson CG, Pan W, Mishler D, Ghosh I, Hamilton AD, Regan L.** 2005. Detecting protein-protein interactions with a green fluorescent protein fragment reassembly trap: scope and mechanism. J Am Chem Soc **127:**146-157.

240. **Cabantous S, Terwilliger TC, Waldo GS.** 2005. Protein tagging and detection with engineered self-assembling fragments of green fluorescent protein. Nat Biotechnol **23:**102-107.

241. **van Dooren GG, Tomova C, Agrawal S, Humbel BM, Striepen B.** 2008. Toxoplasma gondii Tic20 is essential for apicoplast protein import. Proc Natl Acad Sci U S A **105:**13574-13579.

242. **Sommer MS, Daum B, Gross LE, Weis BL, Mirus O, Abram L, Maier UG, Kuhlbrandt W, Schleiff E.** 2011. Chloroplast Omp85 proteins change orientation during evolution. Proc Natl Acad Sci U S A **108:**13841-13846.

243. **Kulzer S, Petersen W, Baser A, Mandel K, Przyborski JM.** 2013. Use of self-assembling GFP to determine protein topology and compartmentalisation

in the Plasmodium falciparum-infected erythrocyte. Mol Biochem Parasitol **187:**87-90.

244. **Toddo S, Soderstrom B, Palombo I, von Heijne G, Norholm MH, Daley DO.** 2012. Application of split-green fluorescent protein for topology mapping membrane proteins in Escherichia coli. Protein Sci **21:**1571-1576.

245. **Kaddoum L, Magdeleine E, Waldo GS, Joly E, Cabantous S.** 2010. One-step split GFP staining for sensitive protein detection and localization in mammalian cells. Biotechniques **49:**727-728, 730, 732 passim.

246. **Cabantous S, Nguyen HB, Pedelacq JD, Koraichi F, Chaudhary A, Ganguly K, Lockard MA, Favre G, Terwilliger TC, Waldo GS.** 2013. A new protein-protein interaction sensor based on tripartite split-GFP association. Sci Rep **3:**2854.

247. **Brach T, Soyk S, Muller C, Hinz G, Hell R, Brandizzi F, Meyer AJ.** 2009. Non-invasive topology analysis of membrane proteins in the secretory pathway. Plant J **57:**534-541.

248. **Lee H, Min J, von Heijne G, Kim H.** 2012. Glycosylatable GFP as a compartment-specific membrane topology reporter. Biochem Biophys Res Commun **427:**780-784.

249. **Earl PL, Cooper N, Wyatt LS, Moss B, Carroll MW.** 2001. Preparation of cell cultures and vaccinia virus stocks. Curr Protoc Mol Biol **Chapter 16:**Unit16 16.

250. **Chakrabarti S, Sisler JR, Moss B.** 1997. Compact, synthetic, vaccinia virus early/late promoter for protein expression. BioTechniques **23:**1094-1097.

251. **Cochran MA, Mackett M, Moss B.** 1985. Eukaryotic transient expression system dependent on transcription factors and regulatory DNA sequences of vaccinia virus. Proc Natl Acad Sci USA **82:**19-23.

252. **Wilkinson B, Gilbert HF.** 2004. Protein disulfide isomerase. Biochim Biophys Acta **1699:**35-44.

253. **Paulsson KM, Jevon M, Wang JW, Li S, Wang P.** 2006. The double lysine motif of tapasin is a retrieval signal for retention of unstable MHC class I molecules in the endoplasmic reticulum. J Immunol **176:**7482-7488.

254. **Teng MS, Stephens R, Du Pasquier L, Freeman T, Lindquist JA, Trowsdale J.** 2002. A human TAPBP (TAPASIN)-related gene, TAPBP-R. Eur J Immunol **32:**1059-1068.

255. **Condit RC, Moussatche N, Traktman P.** 2006. In a nutshell: structure and assembly of the vaccinia virion. Adv Virus Res **66:**31-124.

256. **Yoder JD, Chen TS, Gagnier CR, Vemulapalli S, Maier CS, Hruby DE.** 2006. Pox proteomics: mass spectrometry analysis and identification of Vaccinia virion proteins. Virol J **3:**10.

257. **Chung CS, Chen CH, Ho MY, Huang CY, Liao CL, Chang W.** 2006. Vaccinia virus proteome: Identification of proteins in vaccinia virus intracellular mature virion particles. J Virol **80:**2127-2140.

258. **Resch W, Hixson KK, Moore RJ, Lipton MS, Moss B.** 2007. Protein composition of the vaccinia virus mature virion. Virology **358:**233-247.

259. **Ngo T, Mirzakhanyan Y, Moussatche N, Gershon PD.** 2016. Primary structures of the virion proteins of vaccinia virus at increased resolution. J Virol **90:**9905-9919.

260. **Nichols RJ, Stanitsa E, Unger B, Traktman P.** 2008. The vaccinia virus gene I2L encodes a membrane protein with an essential role in virion entry. J Virol **82:**10247-10261.

261. **Cotter CA, Earl PL, Wyatt LS, Moss B.** 2017. Preparation of Cell Cultures and Vaccinia Virus Stocks. Curr Protoc Mol Biol **117:**16 16 11-16 16 18.

262. **Yang X, Boehm JS, Yang X, Salehi-Ashtiani K, Hao T, Shen Y, Lubonja R, Thomas SR, Alkan O, Bhimdi T, Green TM, Johannessen CM, Silver SJ, Nguyen C, Murray RR, Hieronymus H, Balcha D, Fan C, Lin C, Ghamsari L, Vidal M, Hahn WC, Hill DE, Root DE.** 2011. A public genome-scale lentiviral expression library of human ORFs. Nat Methods **8:**659-661.

263. **Nelson GE, Sisler JR, Chandran D, Moss B.** 2008. Vaccinia virus entry/fusion complex subunit A28 is a target of neutralizing and protective antibodies. Virology **380:**394-401.

264. **Szajner P, Weisberg AS, Moss B.** 2004. Physical and functional interactions between vaccinia virus F10 protein kinase and virion assembly proteins A30 and G7. J Virol **78:**266-274.

265. **Szajner P, Jaffe H, Weisberg AS, Moss B.** 2003. Vaccinia virus G7L protein Interacts with the A30L protein and is required for association of viral membranes with dense viroplasm to form immature virions. J Virol **77:**3418-3429.

266. **da Fonseca FG, Wolffe EJ, Weisberg A, Moss B.** 2000. Characterization of the vaccinia virus H3L envelope protein: topology and posttranslational membrane insertion via the C-terminal hydrophobic tail. J Virol **74:**7508-7517.

267. **Kane EM, Shuman S.** 1993. Vaccinia virus morphogenesis is blocked by a temperature-sensitive mutation in the I7 gene that encodes a virion component. J Virol **67:**2689-2698.

268. **Lustig S, Fogg C, Whitbeck JC, Eisenberg RJ, Cohen GH, Moss B.** 2005. Combinations of polyclonal or monoclonal antibodies to proteins of the outer membranes of the two infectious forms of vaccinia virus protect mice against a lethal respiratory challenge. J Virol **79:**13454-13462.

269. **Davies DH, Wyatt LS, Newman FK, Earl PL, Chun S, Hernandez JE, Molina DM, Hirst S, Moss B, Frey SE, Felgner PL.** 2008. Antibody profiling by proteome microarray reveals the immunogenicity of the attenuated smallpox vaccine modified vaccinia virus ankara is comparable to that of Dryvax. J Virol **82:**652-663.

270. **Meng X, Zhong Y, Embry A, Yan B, Lu S, Zhong G, Xiang Y.** 2011. Generation and characterization of a large panel of murine monoclonal antibodies against vaccinia virus. Virology **409:**271-279.

271. **Vanderplasschen A, Hollinshead M, Smith GL.** 1998. Intracellular and extracellular vaccinia virions enter cells by different mechanisms. J Gen Virol **79 (Pt 4):**877-887.

272. **Payne LG.** 1979. Identification of the vaccinia hemagglutinin polypeptide from a cell system yielding large amounts of extracellular enveloped virus. J Virol **31:**147-155.

273. **Isaacs SN, Wolffe EJ, Payne LG, Moss B.** 1992. Characterization of a vaccinia virus-encoded 42-kilodalton class I membrane glycoprotein component of the extracellular virus envelope. J Virol **66:**7217-7224.

274. **Lawrence J, Steward F.** 2010. Purification of viruses by centrifugation, p 166-181, MANUAL of AQUATIC VIRAL ECOLOGY.

275. **Senkevich TG, Wyatt LS, Weisberg AS, Koonin EV, Moss B.** 2008. A conserved poxvirus NlpC/P60 superfamily protein contributes to vaccinia virus virulence in mice but not to replication in cell culture. Virology **374:**506-514.

276. **Holzer G, Falkner FG.** 1997. Construction of a vaccinia virus deficient in the essential DNA repair enzyme uracil DNA glycosylase by a complementing cell line. J Virol **71:**4997-5002.

277. **Warren RD, Cotter C, Moss B.** 2012. Reverse genetic analysis of poxvirus intermediate transcription factors. J Virol **86:**9514-9519.

278. **Ericsson M, Cudmore S, Shuman S, Condit RC, Griffiths G, Locker JK.** 1995. Characterization of ts 16, a temperature-sensitive mutant of vaccinia virus. J Virol **69:**7072-7086.

279. **Wolffe EJ, Vijaya S, Moss B.** 1995. A myristylated membrane protein encoded by the vaccinia virus L1R open reading frame is the target of potent neutralizing monoclonal antibodies. Virology **211:**53-63.

280. **Bisht H, Brown E, Moss B.** 2010. Kinetics and intracellular location of intramolecular disulfide bond formation mediated by the cytoplasmic redox system encoded by vaccinia virus. Virology **398:**187-193.

281. **Dolan BP, Sharma AA, Gibbs JS, Cunningham TJ, Bennink JR, Yewdell JW.** 2012. MHC class I antigen processing distinguishes endogenous antigens based on their translation from cellular vs. viral mRNA. Proc Natl Acad Sci U S A **109:**7025-7030.

282. **Elde NC, Child SJ, Eickbush MT, Kitzman JO, Rogers KS, Shendure J, Geballe AP, Malik HS.** 2012. Poxviruses deploy genomic accordions to adapt rapidly against host antiviral defenses. Cell **150:**831-841.

283. **Kyte J, Doolittle RF.** 1982. A simple method for displaying the hydropathic character of a protein. J Mol Biol **157:**105-132.

284. **Wallin E, von Heijne G.** 1998. Genome-wide analysis of integral membrane proteins from eubacterial, archaean, and eukaryotic organisms. Protein Sci **7:**1029-1038.

285. **Lorenz H, Hailey DW, Lippincott-Schwartz J.** 2006. Fluorescence protease protection of GFP chimeras to reveal protein topology and subcellular localization. Nat Methods **3:**205-210.

286. **Webster A, Hay RT, Kemp G.** 1993. The adenovirus protease is activated by a virus-coded disulphide-linked peptide. Cell **72:**97-104.

287. **Ding J, McGrath WJ, Sweet RM, Mangel WF.** 1996. Crystal structure of the human adenovirus proteinase with its 11 amino acid cofactor. EMBO J **15:**1778-1783.

288. **Greber UF, Webster P, Weber J, Helenius A.** 1996. The role of the adenovirus protease on virus entry into cells. EMBO J **15:**1766-1777.

289. **Satheshkumar PS, Anton LC, Sanz P, Moss B.** 2009. Inhibition of the ubiquitin-proteasome system prevents vaccinia virus DNA replication and expression of intermediate and late genes. J Virol **83:**2469-2479.

290. **Ravid T, Hochstrasser M.** 2008. Diversity of degradation signals in the ubiquitin-proteasome system. Nat Rev Mol Cell Biol **9:**679-690.

291. **Luttge BG, Moyer RW.** 2005. Suppressors of a host range mutation in the rabbitpox virus serpin SPI-1 map to proteins essential for viral DNA replication. J Virol **79:**9168-9179.

292. **Erlandson KJ, Cotter CA, Charity JC, Martens C, Fischer ER, Ricklefs SM, Porcella SF, Moss B.** 2014. Duplication of the A17L Locus of Vaccinia Virus Provides an Alternate Route to Rifampin Resistance. J Virol **88:**11576-11585.